INTERDISCIPLINARY CONTRIBUTIONS TO SPATIAL AND TEMPORAL ANALYSES FOR LAND COVER CHANGE

By

MATT MARSIK

A DISSERTATION PRESENTED TO THE GRADUATE SCHOOL
OF THE UNIVERSITY OF FLORIDA IN PARTIAL FULFILLMENT
OF THE REQUIREMENTS FOR THE DEGREE OF
DOCTOR OF PHILOSOPHY

UNIVERSITY OF FLORIDA

2008

To the memory of Carolyn Sue Marsik and Fredrick Henry Studenka

ACKNOWLEDGMENTS

First, I would like to thank my committee. I am grateful to Peter Waylen for giving me the opportunity to pursue my master's and doctorate degrees with his guidance and supervision. I thank Jane Southworth for her encouragement and guidance to incorporate remote sensing and land cover change into my research repertoire. Tim Fik provided stimulating and challenging discussions about advanced statistics, most of which I generally understood at the time. I thank Graeme Cumming for always challenging me to expand my conceptual and theoretical bounds, even though my head hurt afterwards.

As for those people who directly and indirectly supported me, I first thank Jim Sloan for introducing me to GIS and making me do it the "right way." I thank David Coley and Forrest Stevens for being the people I could actually ask for research and technical help and advice. Folks in LUECI include Lin Cassidy, Andrea Chavez, Amy Daniels, Andrea Gaughan, Daniel Godwin, Jackie Hall, Joel Hartter, Luke Rostant, Gaby Stocks, Tracy Van Holt, Jaime Waggnor, and Miriam Wyman. I also thank the myriad professors that supported me during my university education. I thank those students who endured my GIS classes over the four years I taught. I profusely thank Julia Williams and Desiree Price for all their administrative help in making my graduate experience easier. A large debt of gratitude goes to Dr. Corene Matyas for allowing access to her super-computer, the Weather Machine. I especially thank Dr Cesar Caviedes for his friendship, guidance, advice, support, and watchful eye during my graduate career.

I am grateful for general, and at times, specific, social interfacing with Jose Torres, David Coley, Jim Penn, Jim Sloan, Matt Langholtz, Brian Becker, Brian Condon, Norman Breuer, Adam and Melania Szylagi, Valerio Gomes, Amy Duchelle, Jon Colburn, and Alfredo Rios. From the Department of Geography I am grateful to know Andrea Wolf, Anna Szyniszewska, Carlos Cañas, Kofi Abu-Brempong, Keith Yearwood, Jim Rasmussen, Kwadwo Owusu, Phillip

Morris, and Cerian Gibbes. Along these same lines, I am grateful to have fallen in with and had the chance to play Frisbee with Greg Parent, Lisa Seales, Maria DiGiano, Jon Engels, Miriam Wyman, Forrest Stevens, Alex Cheeseman, Joel Hartter, Kelly Biedenweg, Rachel Hartter, JG Collomb, and the random people who showed up to join in the game. I also thank the Latino community I had a chance to know over the past couple of years.

I thank my colleague Marvin Quesada for collaborating on Costa Rican hydrology and climatology over eight years, providing a place to stay during my travels, taking me on some pretty great tours of Costa Rica, and being a good friend. During my time in Costa Rica Trino Barrantes and Ana Cecilia Jimenez- Barrantes and their family were always gracious to take me in and treat me as one of their own; for that no amount of words and gratitude are sufficient.

Funding for research conducted in Bolivia was provided by the Working Forests in the Tropics Program at the University of Florida supported by the National Science Foundation (DGE-0221599) for field work during summer 2007, and by a two-year research assistantship from the National Science Foundation Human and Social Dynamics program (#0527511) awarded to the University of Florida through the Department of Sociology. Angelica Almeyda, Chris Baraloto, Grenville Barnes, Kelly Biedenweg, Eben Broadbent, I. Foster Brown, Liliana Cabrerra, Lin Cassidy, Andrea Chavez, Jaime Chavez, Graeme Cumming, Frank Paul de la Barra, Monica de Los Rios, Amy Duchelle, Hugo Dueñas Linares, Florida Ferreira, Carlos Varelio Gomes, Dean Kenji Vaca, Erika Llanos, Elsa Mendoza, Stephen Perz, Karla Rocha, Cara Rockwell, Daniel Rojas, Julio Rojas, Allie Shenkin, and Jackie Vadjunec helped support and encourage me during my time in Bolivia.

I thank my family for fully supporting me during my graduate career even though, at times, they didn’t know where I was at during my field studies. I am just glad I finished my PhD before my kid-sister finished her undergraduate degree.

The final thanks, gratitude and support go to Kelly Biedenweg, for being my “sunshine” during the past two years. Also, earnest earns a spot for being a good cat.

TABLE OF CONTENTS

page

LIST OF TABLES

LIST OF FIGURES

Abstract of Dissertation Presented to the Graduate School
of the University of Florida in Partial Fulfillment of the
Requirements for the Degree of Doctor of Philosophy

INTEDISCIPLINARY CONTRIBUTIONS TO SPATIAL AND TEMPORAL ANALYSES FOR LAND COVER CHANGE

By

Matt Marsik

December 2008

Chair: Peter Waylen
Cochair: Jane Southworth
Major: Geography

Land cover change drives global change through interactions with climate, ecosystem processes, biogeochemical cycles, biodiversity, and human activities. By understanding the linkages between the patterns and causes of land cover change, we can predict possible outcomes and offer alternatives to ameliorate potential negative effects. Methods that link and analyze spatial and temporal patterns of land cover improve the understanding of the complexity and dynamics of land cover change in various geographic locations. I present intedisciplinary methods and accompanying theory from landscape ecology, remote sensing and hydrologic modeling for analyzing impacts and characteristics of the spatial and temporal changes of land cover.

Development of new multiscalar analytical methods to analyze observed patterns captured by remotely sensed data can yield appropriate temporal and spatial scale domains important for the applied study of linking landscape and ecological patterns and processes. The incorporation and scaling of spatial, temporal and spectral information into land cover change analyses and greatly improves the amount of information obtained facilitating linkages between landscape pattern and process. Combining techniques from remote sensing and landscape ecology allows

the observation of land cover and the analysis of changing patterns and rates of the spatial structure in northern Bolivia. The combined simulation modeling and statistical analysis to investigate changing discharge contributions to the Rio Grande de Tarcoles an integrated approach to assess the impacts of land cover change within a coupled hydro-climatic system. Despite confounding results of determining whether climate variability or anthropogenic causes created the observed change in river discharge, the combined approach highlights the complexity of the hydro-climatic system and investigates, simultaneously, the various aspects of the spatial and temporal heterogeneity of a complex watershed.

The goal is to combine the strengths of each discipline to form intedisciplinary tenants for spatial-temporal analyses for land cover change. A intedisciplinary approach to land cover change would comprise pattern-process linkages across multiple scales with the spatial analysis of historic regional and global remotely sensed data with the detailed description of ecosystem sub-processes.

CHAPTER 1
INTRODUCTION

I present intedisciplinary methods and accompanying theory from landscape ecology, remote sensing and hydrologic modeling to characterize spatial and temporal changes in land cover and their consequent impacts. The research is presented as three separate studies in publication format for submission to academic journals. The first study (Chapter 2) develops an approach for scaling of space and time as applied to satellite images, which form the core data source for land cover change studies. The second study (Chapter 3) investigates spatial and temporal rates and patterns of land cover change and fragmentation in the face of population increase and road development and expansion in Pando, the northernmost department in Bolivia. The final study, (Chapter 4) focuses on the potential interplay between land cover change and climate variability and their impact on river discharge. These studies are topically diverse and are unified by the investigation of methods to determine the spatial and temporal characteristics of land cover change. With a background in physical geography and guiding theory from land change science these studies incorporate concepts from landscape ecology, remote sensing, and hillslope hydrology and modeling to identify spatial and temporal methods capable of enhancing the understanding of land cover change and its advance as a science.

Land Cover Change

Land cover exerts a fundamental impact on, and links many parts of, human and physical environments and changes in land cover are regarded as the single most important process of global change affecting ecological systems (Vitousek 1994). Observed land cover patterns represent the net result of individual, communal or societal decision-making processes regarding the relative returns to land use (Currie 1981) set within a local, regional or national context. Human activity by way of individual or societal needs or wants drives present land cover change

(Ojima et al. 1994) and these purposes define land use – the intent and underlying manner in which the biophysical attributes of the land are manipulated (Lambin and Geist 2006) – which purports land cover change.

Land cover change can drive global change through interactions with climate, ecosystem processes, biogeochemical cycles, biodiversity, and human activities (Turner et al. 1995). Important natural resources of climate, soils, vegetation, water resources and biodiversity (E.F.Lambin et al. 1999) reflect human history and are linked with economic development, population growth, and technology. Global effects include the conversion of potentially productive land with diminished capacity to support crops, forests and people, and the irreplaceable loss of species and the emission of chemically active and heat-trapping gases to the atmosphere (Ojima et al. 1994). Potential deleterious local and regional effects of deforestation to pastures, for example, include erosion of soils, reduced rainfall, reduced capacity of soils to hold water, increased frequency and severity of floods, and siltation of dams (Houghton 1994). Land cover change has been linked to changes in flood and drought frequency (Nepstad et al. 2001) and impacts on water quality (Rogers 1994). Forest clearing affects local and regional hydrology through reduced infiltration and evapotranspiration, and changes to river and groundwater regimes (Giambelluca 2002; Bonell 1998; Bruijnzeel 2004). These myriad effects of land cover change at the human-environment interface necessitate the quantification of and cataloging of land cover change at multiple scales.

Gutman (2004) has proposed the development of a multidisciplinary land change science, which draws on the diverse disciplines of geography, remote sensing, GIScience, and various other social and ecological sciences. To further cultivate the development of this young science, land change theory requires the application of a diverse array of techniques of analyses and

models (Rindfuss et al. 2004). The ultimate and broad objective of land cover change is to improve understanding, and to accrue knowledge of regionally based, interactive changes between land uses and covers (Turner et al. 1995). Thus we can gain an understanding of the nature of human decisions that alter land cover at regional scales, where policy interventions are possible and effective (E.F.Lambin et al. 1999).

Linking Pattern and Process to Understand Land Cover Change

Development of a land change science (Woodcock and Ozdogan 2004) relies on the understanding of linkages between patterns and processes. The hierarchical examination of levels in a system as the outcomes of a collection of results from smaller, underlying processes or behaviors (Levin 1992) comprises the main goal of pattern-process linkages. Remote sensing and spatial statistics, along with other types of spatial analyses (Schroder and Seppelt 2006), can describe spatial distributions, at multiple scales using multiple data sources and indicate the controls and constraints that determine their nature.

Methods of spatial and temporal analysis of land cover change can help better link observed pattern with the underlying processes of formation. However, there is certain inherent complexity in distinguishing processes of formation, either anthropogenic or climate driven (Rindfuss et al. 2004). Lambin and Geist (2006) note that the complexity of land cover change embodies multiple scales and rates of modifications. We have regional change in land cover conditions caused by climate variability overlying localized human-induced land cover modifications. They note that “[m]ultiple spatial and temporal scales of change, with interactions between climate-driven and anthropogenic changes, are a significant source of complexity in the assessment of land cover change” (Lambin and Geist 2006). Analyzing both space and time together in the study of land cover change can help ameliorate this dual complexity.

Interdisciplinary spatial-temporal analysis methods are necessary to tackle the complexities associated with land cover change (Rindfuss et al. 2004).

Scale

The definitions and concepts of scale and scaling are well known and have be reported in the literature time again (Gibson et al. 2000; Marceau 1999; Meentemeyer 1989; Turner et al. 1989). Currently no unified theory or science of scale and scaling exists. Possible steps to identify and remediate scale effects are: (1) to recognize scale dependency in observed phenomena, (2) to predict and control for scale effects using spatially explicit methods, (3) explicitly state the scale or scales of analysis, and (4) to make use of a solid unified theoretical framework, such as hierarchy theory (Allen and Starr 1982; O'Neill et al. 1989) to derive and test hypotheses, and generalize analysis results. Hierarchical structuring (O'Neill et al. 1989) simply means that, at a given level of resolution, a system is composed of interacting components (i.e., lower-level entities) and is itself a component of a larger system (i.e., higher level entity). This concept emphasizes that the behavior of a system is limited (1) by the potential behaviors of its lower level components (i.e., biotic potential) and (2) by the environmental constraints (e.g. abiotic and biotic environmental limits) imposed by higher levels.

Remotely sensed data can fit nicely into this concept of hierarchically organized structures as the pixel is the minimum mapping unit and can be easily aggregated upward in a nested fashion from its base resolution. Remote sensing offers great potential for scaling (Woodcock and Strahler 1987; Quattrochi and Goodchild 1997; Stewart et al. 1998; Marceau and Hay 1999) as it provides the required data for upscaling and downscaling physical models, provides the possibility of conducting empirical studies to understand the behavior of variables when changing scales, and to derive the appropriate rules for scaling. Interdisciplinary methods for spatial-temporal analyses of land cover change are inherently multiscalar with the combination

of many pattern forming processes occurring at many scales. By considering landscapes and land cover change hierarchically organized, multilevel analysis techniques can be applied that are potentially able to resolve critical landscape thresholds, domains of scale, and correctly linked data between scales and landscape components.

Intedisciplinary Approaches to Spatial-Temporal Analysis

Landscape ecology has a history of space-time studies (Turner et al. 1989; Turner 2005; Turner 1990) used primarily to deduce dominant processes of formation from observed patterns. Patterns observed from remotely sensed data provide the foundation upon which simulation modeling, ideally empirically driven, verified, and executed at multiple scales, facilitates the identification of ecological processes responsible for generating the patterns (Levin 1992). Bellehumeur and Legendre (1998) suggest careful planning of sampling design coupled with pattern detection techniques (e.g. spatial correlograms, geostatistical analyses and frequency analysis) applied at multiple scales to an ecological community or landscape to help detect key scales of spatial variation. With a strong foundation in explanation of spatial patterns and the effects of changing scale on key pattern forming processes (Turner 1990), the integration of multi-temporal levels is recognized and are incorporated into sampling designs and analyses (Southworth et al. 2006).

To better understand pattern-process interdependencies, we need to determine important scales of landscape heterogeneity, human activities, and ecosystem processes that most effectively explain heterogeneous spatial patterns. The first study (Chapter 2) found at smaller spatial scales the spatial variance was greater than temporal variations in the landscape, that temporal variance increased with increasing spatial scales, and landscapes show inherent temporal variation without spatial changes in landscape pattern. The development of new methods, as occurs in this study, specifically of multiscalar analysis as applied to observed

patterns captured by remotely sensed data, can yield appropriate temporal and spatial scale domains important for the applied study of linking landscape and ecological patterns and processes. The incorporation and scaling of spatial, temporal and spectral information into land cover change analyses greatly improves the amount of information obtained.

Remote sensing and associated analytical methods provide the capacity to analyze space and time together (Mertens and Lambin 2000; Gutman 2004; Lambin and Geist 2006). Calculation of land cover trajectories (Petit and Lambin 2001; Mertens and Lambin 2000; Southworth et al. 2002) creates temporal change classes (i.e., categories between two or more dates), and the resulting image shows the spatial distribution of these changes. This approach has permitted the development of a multivariate spatial models to determine the probability of change in land cover (Mertens and Lambin 2000), enhanced model predictions of the expansion of disturbed and anthropogenic land cover at the expense of naturally vegetated land covers (Petit et al. 2001), and detected reforestation patterns in western Honduras (Southworth et al. 2002).

The second study (Chapter 3) presents an integrated set of tools for the spatial and temporal rates and patterns of land cover change and landscape level fragmentation. The multiscalar analysis of land cover fragmentation at the regional extent (65,000 km^2) and with increasing distances (1-15 km) along a major access road and from a major population center provides a comprehensive spatial and temporal view of land cover change with regard to population increases and road improvements. These spatial-temporal patterns coupled with socio-economic data in a modeling framework may permit the identification of social actors and drivers of land cover change.

Hydrologic models often relegate land cover change to a position secondary to description of watershed processes. Land cover is usually explicitly represented (Wu et al. 2007; Marsik and Waylen 2006; Marshall and Randhir 2008) and derived from satellite images or existing GIS data. Specific data describing changes in surface roughness, which affect overland flow velocities, or canopy cover, which controls the partition of precipitation into interception and throughfall, are not commonly measured. Rarer still are the observations and analyses of temporal changes in important hydrologic variables resulting from land cover change. Instead many detailed hydrologic studies (Elsenbeer et al. 1992; Elsenbeer et al. 1999; Western et al. 1999; Western et al. 2001; Western et al. 2004) focus on the spatial distributions of hydrologically important variables (i.e., soil moisture, hydraulic conductivity, and other soil hydraulic properties), which occur in small, experimental watersheds, usually with very little change in land cover and over relatively short time frames.

The third study (Chapter 4) investigates the potential roles of non-linear hydrologic responses to changes in land use and land cover, and climate variability within two adjacent sub-basins in the Central Valley, Costa Rica. A semi-distributed hydrologic model, SWAT, incorporating historic land cover changes delineated is coupled with statistical analysis of precipitation variability to better understand possible causes of a change noted in the mid-1970s of the relative contributions of the Rios Virilla and Grande de San Ramón, the principle tributaries of the Rio Grande de Tarcóles. This research illustrates that changes in land cover, contemporary to changes in climate variability may further amplify or dampen the observed response of river discharge.

Importance of Study

Together these studies contribute to contemporary methods to analyze spatial and temporal rates and patterns of land cover change based on techniques used in landscape ecology, remote

sensing, and hillslope hydrology. Current research agendas for land cover change science are based upon methods from multiple disciplines such as geography, remote sensing, sociology, anthropology, and GIScience (Rindfuss et al. 2004; Gutman 2004), which serve to analyze the biophysical and environmental dimensions of land cover change. The analyses presented in these studies offer one geographic perspective on an interdisciplinary approach and draw on strengths of spatial analyses used in multiple sub-disciplines of physical geography. Linking pattern-forming processes is one outcome of using these types of spatial analyses for land cover change studies.

CHAPTER 2
LINKING SPATIAL AND TEMPORAL VARIATION AT MULTIPLE SCALES IN A HETEROGENEOUS LANDSCAPE

Introduction

The global impacts of the earth's human population are reflected in extensive changes in the spatial patterns of land cover and land use (O'Neill et al. 1996). Interacting anthropogenic, ecological and land-surface processes occur in landscapes at multiple scales. If we are to understand and manage the causes and consequences of anthropogenic effects on landscapes, it is imperative that we develop approaches to understanding spatial and temporal variation, the processes that produce the patterns that we observe, and the ways in which pattern-process relationships change with scale. Remote sensing has traditionally been considered an ideal tool for providing data to describe landscape patterns and dynamics. However, our understanding of the scale dependency of landscape pattern-process interactions is limited (Moody and Woodcock 1995). Understanding scaling effects is critical to our ability to better understand, model and/or predict landscape dynamics, and specifically for understanding the roles of spatial and temporal heterogeneity and the hierarchical arrangement of landscape elements (Qi and Wu 1996).

Most natural systems across the world exhibit some form of spatial structure. As stated by Wu et al. (2000), "Spatial heterogeneity is the most fundamental characteristic of all landscapes and scale multiplicity is inherent in spatial heterogeneity. Thus, multiscale analysis is imperative for understanding the structure, function and dynamics of landscapes." Studies of spatial structure occur across a suite of disciplines, and many different approaches and methodologies for the analysis of spatial pattern have been developed (Dale et al. 2002). It is valuable in such studies to characterize heterogeneity and to assess the ways in which it changes in both space and time (O'Neill et al. 1996). Due in part to the demands of data collection, both landscape ecology and remote sensing studies typically focus on either spatial or temporal

variation. The central goal of this study is to conduct a geographical analysis of landscape change in North-Central Florida in a way that directly addresses variation in both space and time by integrating landscape ecology, remote sensing, and GIS technologies. In this way we hope to link form, both spatially and temporally, to function. As stated in Goodchild (2004), geographic information science (GIScience) is an emphasis on form with the inclusion of process to bolster our understanding, which is what we attempt to do in this research using an integration of GIScience and landscape ecology.

Landscape studies that are intended to determine pattern-process interactions often occur at a single scale, which dictates the relationships that are found and the patterns of spatiotemporal heterogeneity that are seen (Habeeb et al. 2005). In order to understand pattern-process interdependencies, we need to find the scales of landscape heterogeneity, human activities, and ecosystem processes that most effectively explain variation in spatial patterns. In other words, spatial and temporal scales of observation must match those of ecological patterns and processes (Marceau 1999). The question of scale has been a central topic in remote sensing since the earliest days of non-military research, and in geography for even longer (Gehlke and Biel 1934). Openshaw (1977; 1978; 1984) suggested an approach in which the determination of an optimal spatial resolution is a required early step in any spatial analysis. This protocol is supported by some very recent works (Wu and David 2002), although there is also an increasing realization that a multi-scale understanding is important. In the remote sensing arena, Cohen and Justice (1999) hypothesize "that there is a fundamental grain size of each landscape (or biome) above which error rates accelerate when modeling NPP; test of hypothesis using field data, Landsat ETM+, and geostatistical models," implying that the "fundamental grain size" must be determined.

Much attention has been paid to the questions of scale in ecology (Peterson and Parker 1998), environmental science, land-cover/land-use change (Evans et al. 2001) remote sensing and GIS (Quattrochi and Goodchild 1997), hydrology (Droogers and Kite 2002), and geology and geomorphology, even to the point that a book chapter (O'Neill and King 1998) was titled "…Why are there so many books on scale?" Despite this intellectual activity, the role of scale in remote sensing studies is still poorly understood, in both subjective and objective contexts; our scale of measurement influences our perceptions of the world, while landscape processes vary in magnitude and rate across a range of scales. The development of scaling relationships typically involves the repeated measurement of a quantity of interest at different dimensions, whether length, space, mass, or time. For example, the loglinear body mass-metabolic rate relationship is a classical scaling relationship that is widely cited in ecology. Many past studies of landscapes have examined how changes in spatial scale (predominantly in grain) can impact measures of habitat configuration and composition (Wu and David 2002). Fewer studies have addressed the role of changing temporal scale in landscape analyses, although there has been substantial research within the fields of geography, landscape ecology, and remote sensing on temporal variation in ecosystems and anthropogenic influences on landscapes.

Many statistical techniques have been developed for the scaling analysis of remotely sensed imagery. A seminal paper by Woodcock and Strahler (1987) proposed a local variance technique to determine the appropriate resolution (i.e., cell size) of a remotely sensed image to view the spatial structure of the landscape. They used the mean value of the standard deviation calculated with a 3 x 3 window around each pixel, excluding the edge pixels of the image. The local variance measures denote, within the 3 x 3 window, the similarity or spatial dependence of pixel values on the center pixel under investigation. Woodcock and Strahler (1987) extended

their method by progressively degrading the image resolution to measure local variation within the image at multiple resolutions. This degradation or coarsening of resolution led to multiple representations of the same landscape, with fewer pixels in the coarser resolution images. Measures of local variance at multiple resolutions were then plotted as local variance versus image resolution to determine the scales at which the dominant landscape patterns were occurring. The calculation of the local variance for an image described the size of discrete landscape objects (e.g. forest stands or pastures) within the image and could be used to select a scale at which to analyze these objects.

Other researchers have utilized this scaling approach in a variety of applications. For instance, Coops and Catling (1997) applied a modified local variance technique to videographic imagery of individual tree canopies. The mean value of the standard deviation of each spectral channel was calculated at increasingly large pixel windows (i.e., 3 x 3, 5 x 5.... 49 x 49), yielding local variance values for each pixel. They found low within-window variance at a window size significantly smaller than individual tree canopies in the scene. Local variance increased to a maximum as window size increased to the canopy size (around 20 m), and constant local variance resulted within the window as the window size increased beyond the size of the individual tree crowns.

Coops and Culvenor (2000) applied their modified local variance or texture variance technique to determine if minimized values of local variance (with window sizes of 5 x 5, 20 x 20, 30 x 30, and 80 x 80 pixels) resulted from regular spatial distribution of high-resolution tree canopy structures within a simulated forest environment. Conversely, maximum variance would result from clumped or aggregated tree canopies. As the percentage of canopy cover increased,

the texture variance decreased, with a plateau at the maximum local variance regardless of the inclusion of additional tree canopy objects to a simulated forest scene.

Our research expands on some of these ideas in the context of GIScience, as driven by scientific and technological motivations, to develop a multiscale approach to investigate the related patterns of spatial and temporal scales concurrently (Walsh and Crews-Meyer 2002). Of particular interest is the question of whether unified comparisons of spatial and temporal variation across a range of different scales yield any general patterns or scaling relationships (Woodcock and Strahler 1987; Wu et al. 2000). In this sense the development of the technique presented here employs commonly used geographic technologies (remote sensing, variance analysis, regression analysis, custom application development for randomizing null landscape models, etc.) to facilitate analysis of seemingly disparate issues of temporal and spatial scaling. Our conceptual study lends itself to furthering GIScience in that the development of new methods, specifically of multiscale analysis, can yield appropriate temporal and spatial scale domains important for the applied study of the patterns and processes of landscape analyses.

Study Area

Our study area is in north central and northeast Florida, and southern Georgia on the U.S. Atlantic coastal plain. The area is defined by Landsat WRS 2 path 17, and row 39 (Figure 2-1) with bounding latitude and longitude coordinates of approximately 31° 13' N, 83° 10' W (northwest corner), and 29° 20' N, 81° 41' W (southeast corner). The entire scene footprint covers an area of about 34,000 km^2. The study area is useful for addressing scaling questions for several reasons. First, the Coastal Plain of the southeastern United States east of the Mississippi River (Figure 2-1 inset) is large (nearly 600,000 km^2), covering a land area 2.5 times the size of the United Kingdom. Second, despite its size, it is also of relatively low relief, reducing the importance of gross topography (but not fine-scale topography) as a factor structuring the

landscape, and has a generally uniform and moderate subtropical climate. Elevation across the study landscape ranges from near sea level to a high point of 63 m in the north. The topography is flat to very gently rolling, with slopes > 5% rare. Third, the Coastal Plain has a large and rapidly growing human population with a long history of habitation and rapid land-use change, and a very high diversity of natural ecosystems and endemic biodiversity, controlled mainly by the subtle variations in topography, geology and soils (Myers 1990). This diverse and heterogeneous landscape consists of a mixture of natural and plantation forests, urban centers, urban and rural residential areas, and commercial and small-scale agricultural operations. The dominant upland forests are pine flatwoods, with mixed hardwoods and pines at intermediate moisture levels, leading to bottomland hardwood or mixed cypress forests near streams and rivers.

Only 1.5% of the historical area of the upland *Pinus palustris* (longleaf pine) forest remains after clearing during the past 150 years, although this ecosystem once covered 25 million ha (Myers 1990; Ware et al. 1989). Widely spaced trees and frequent, low-intensity ground fires characterized the original forests. Most of the "natural" forests in the region today are mixed pine stands that have regenerated under a variety of fire regimes after being used for cattle grazing. Most of the flatwoods in Florida were converted to plantations of the native slash pine (*Pinus elliottii*), starting in the 1950's. The total area in plantations has been roughly constant for the past 20 years, while the total area of forest in the region has declined. The hydrologically isolated cypress wetlands that dot the landscape are largely unmanaged, although most have had their larger trees harvested at some time in the past century. This diversity of land cover types is spatially heterogeneous and patch sizes of the various vegetation classes vary across a wide range of scales. The temporal scales of management and land-cover change are

also variable depending on the size of forest stands, areas of rapid urbanization, and kinds of agricultural operations.

Methods

The data consisted of Landsat TM/ETM+ scenes from the USGS EROS Data Center with level-1G preprocessing. The data used here comprise six cloud-free images acquired on January 16, 1985 (TM); February 12, 1989 (TM); January 20, 1992 (TM); January 17, 1997 (TM); January 4, 2001 (ETM+); and February 11, 2003 (ETM+).

We used NDVI (Normalized Difference Vegetation Index) as the quantity of interest throughout this research. NDVI represents a continuous variable related to productivity of land cover or vegetation biomass, which varies both in space and time. The Normalized Difference Vegetation Index (NDVI) is based upon the observation that healthy leaves reflect near-infrared light while absorbing red light that provides the bulk of energy for photosynthesis. The NDVI provides an assessment of vegetative canopy cover characteristics, and is strongly correlated with the fraction of photosynthetically active radiation intercepted by the canopy (Jensen 2005).

NDVI (Equation 2-1) is calculated where NIRBand4 is the digital number (DN) that describes reflectance in near-infrared wavelengths, and REDBand3, reflectance in red wavelengths for Landsat TM/ETM+ imagery.

$$NDVI = \frac{NIR_{(Band\,4)} - RED_{(Band\,3)}}{NIR_{(Band\,4)} + RED_{(Band\,3)}} \tag{2-1}$$

NDVI values were calculated for every image for the entire spatial extent of each Landsat scene (Figure 2-2).

The use of a continuous variable such as NDVI contrasts with more traditional classification schemes, where each pixel (or spatial unit) is represented by a single categorical value (Lambin 1999). In general, the incorporation of both spatial and spectral information into

land-cover change analyses greatly improves the amount of information that is obtained (Figure 2-2) (Southworth et al. 2004a). For example, Lambin and Strahler (1994) found that changes in the spatial extent are more likely to reveal longer-lasting and longer-term land-cover changes, while spectral differences are more sensitive to shorter-term fluctuations e.g., inter-annual variability in climatic conditions.

The image dates represent the winter phenological season (January and February) within six weeks of each other to keep the biomass amount consistent enough not to yield extreme inter-annual differences in NDVI. Since NDVI values were needed for the entire study area, we worked only with cloud-free images that fell within a six-week window during the winter season. The image dates selected avoid extreme climatologic years of drought or excess precipitation as indicated by the El Niño Southern Oscillation (ENSO) index according to the Center of Ocean-Atmospheric Prediction Studies (COAPS) (http://www.coaps.fsu.edu/research/jma_index1.shtml). Avoidance of extreme climate years prevents climatic variability influences in NDVI values for vegetation between each image date.

Local Variance Analysis

We used the modified local variance or texture variance approach (Coops and Catling 1997; Coops and Culvenor 2000). However, instead of degrading the original resolution of the images through averaging cell values, we used the neighboring pixel values at a given window size to calculate the variance about a pixel value (Figures 2-2 and 2-3). Using the moving window maintains the spatial integrity of the landscape without changing the NDVI values, while providing a measure of neighborhood variance. This approach may be superior to resolution coarsening (Woodcock and Strahler 1987) which alters the original NDVI values and degrades variance measures.

Data Analysis

All image processing was performed in ERDAS Imagine 8.5. Image preprocessing required geometric correction to the UTM Zone 17 NAD1983 coordinate system. NDVI values were calculated for all image dates used. Image subtraction was performed between the 2001 image date and the remaining five image dates (Figure 2-2). The spatial variance was calculated for the 2001 image date using the six window sizes. The temporal variance was calculated for the image subtraction products (Figure 2-3). The spatial and temporal variance image products were combined into one image for each image subtraction pair, in which a sub-sample of every twentieth column and row were output to an ASCII text file for regression analysis in SPSS version 10 (Figures 2-4 and 2-5).

Image to GPS control point geometric correction was performed for a September 1997 base image, which, although not used in this analysis, served as the base image for geometric registration for all other image dates. Thirty to forty control points, collected using a Magellan handheld GPS with an accuracy of 7-10 meters, were used for the geometric correction of the September 1997 base image. A second order polynomial algorithm was used with nearest neighbor resampling to a cell size of 30 meters and an RSME of +/- 0.5 pixel or 15 meters. Image to image correction was performed for the remaining image dates. No radiometric correction/calibration was performed before NDVI calculation because of NDVI is a normalized ratio.

The January 4, 2001 image date served as the base image standard for the calculation of spatial variance, as it was the latest image date with complete cloud-free coverage for the entire scene (since the research began we obtained a 2003 image which was then added to the analysis). To analyze spatial variance, a moving window was passed over the entire NDVI image, pixel by pixel. The variance that was calculated within the window was assigned to the focal (central)

pixel (Figure 2-2b, Figure 2-3). In different runs, we varied the size of the moving window to include 3 x 3, 10 x 10, 25 x 25, 50 x 50, 100 x 100, or 250 x 250 pixels. These window extents represented observations of landscape patterns across a range of scales. The spatial analysis of variance using a moving window resulted in 30 image products (spatial variance for 5 dates x 6 window extents).

Each of the five remaining NDVI image dates in the time series was subtracted from the 2001 NDVI image to produce an image subtraction product (Figure 2-3). Five subtraction images were generated. These represented the changes in landscape patterns over time. The NDVI image subtraction products served as input for the calculation of temporal variance (Figure 2-2c). As for the calculation of spatial variance, a moving window was applied to the five NDVI subtraction image products and the temporal variance within the window was assigned to the focal (central) pixel. Pixels thus contained a measure of the change in spatial variance through time. The calculation of temporal variance for each of the five image date pairs at each of the six window sizes yielded 30 temporal variance images that were paired with the previously generated spatial variance images.

For input into regression analysis, the spatial and temporal variance data values were exported to ASCII text format. We reduced the size of the data set because of the large number (greater than 80 million) of pixel values that resulted from stacking each pair of temporal and spatial variance images. NDVI values at every twentieth row and column were exported from ERDAS into ASCII text format for regression analysis in SPSS (Figure 2-4).

This approach allowed for a more manageable regression analysis for each image date pair in the statistics package SPSS 10. Linear regression without any data transformation was run on the image products for each of the window sizes at each of five time intervals using the spatial

variance values as the dependent variable and the temporal variance values as the independent variable (Figure 2-4). Regression parameters were compared across image dates with each respective parameter plotted against the log (base 10) of window area. In other words, we examined how the relationship between spatial and temporal variance varies across multiple scales of analysis in the same landscape. Transforming areas using logarithms allowed for easier visualization of the regression results (the area within the window varies from 8100 m^2 for the 3 x 3 pixel window to 56.25 x 10^6 m^2 for the 250 x 250 pixel window).

The moving window approach to scaling results in a varying sample size for the calculation of variance. In order to check that our results were not merely an artifact of the sampling procedure, we created a null variance model (Figure 2-2d, Figure 2-5). NDVI values from the 2001 and 1997 image dates were used to create a neutral landscape in which the NDVI values from each of the original images were randomly rearranged about the landscape.

To generate the neutral landscape, we converted the 2001 and 1997 NDVI images from ERDAS native image format to ASCII text format. The ASCII values were read into a VB randomizer program, which calculated a frequency histogram with 2000 bins, to create output NDVI values with a numerical precision (though not necessarily accuracy) of three decimal places. Absolute and relative frequency histograms were calculated from the sampled frequency histogram. For each original input NDVI value, random numbers were generated and were compared to the values of the relative frequency histogram to determine the spatial location of the output NDVI values. If the random number was less than the relative frequency at a certain bin number then the random number was placed in that bin, becoming the new output NDVI value. The new output NDVI values were written to a new ASCII text file, which was then reconstituted into the ERDAS native image format for the variance calculations. This

randomization was performed for both the 2001 and 1997 image dates. The spatial and temporal variances at each moving window size were calculated for the 2001 and 1997 random images as described above. A linear regression was conducted following the same format as described above for the original NDVI spatial and temporal variance images (Figure 2-5). The hypothesis tested by this analysis was that if the results from the analysis of actual landscapes were an artifact of our sampling procedure, they should follow the same form as the results from the neutral model.

Results and Discussion

The results showed interesting patterns in the relationship between spatial and temporal variation. The strength of the relationship between spatial variance and temporal variance, as measured using the adjusted R^2 value, was highest at a window size of 10 x 10 pixels or 300 x 300 m^2 (Figure 2-6). Beyond this window size, the relationship between spatial and temporal variance is less similar than expected by chance; i.e., spatial variance explains less temporal variance than is expected by chance. There were also two clusters of responses in the temporal dimension. The longer time scales (9-16 yr windows) were generally more strongly related to spatial variation than were the shorter time scales, except for the smallest window size.

The R^2 values for the null model are high because the randomization (in space) of NDVI results in more equal variances from window to window when the window size is larger than 3 x 3. The expectation for randomly distributed (in space) data is that the variance of a sub-sample of the entire image (e.g. 10 x 10 cells or larger) will equal the variance of the entire image. Thus the spatial and temporal variances are necessarily much more strongly related to one another than those of the real landscape (Figure 2-6).

The results for the slope and intercept relationships (Figures 2-7 and 2-8) revealed that the magnitude of the relationship between spatial variance and temporal variance was highest at

a window size of 50 x 50 pixels (1500 x 1500 m^2) for slope (Figure 2-7), and 100 x 100 pixels (3000 x 3000 m^2) for the intercept (Figure 2-8).

The ratio of temporal variance to spatial variance (indicated by the slope) increased as we increased the spatial scale of analysis, meaning that at smaller spatial scales, the level of spatial variation was greater than that of temporal variation in the landscape. This result is consistent with Lambin and Strahler's (1994) observation that longer-term land-cover changes tend to occur over larger spatial extents. Conversely, at increasing spatial scales we found increased temporal variance. Hence, at increasing scales, the difference between actual and random data increased with an increasing decoupling of spatial and temporal variation (coupling peaks at a 10 x 10 pixel window size, Figure 2-6). So, spatial variation explained less and less temporal variation (compared to the null model) as the spatial scale of analysis increased.

A non-zero intercept of the regression line relating spatial to temporal variation indicates that even when the land cover does not change spatially, there is an inherent amount of temporal variation, perhaps the consequence of climate variation (Figure 2-8). This suggestion is supported further because slope increases with increasing spatial window (Figure 2-7), up to a plateau at 100 x 100 and above, but is lower with higher temporal windows. The inherent temporal variation is larger in larger areas (possibly because larger areas include a higher diversity of vegetation with more variable responses to climate fluctuation), but is damped when integrated over longer time spans.

The results show that an interesting relationship may exist between spatial and temporal variation in this landscape. Although the mechanisms behind the patterns that we have described are unclear, and will take further research to fully understand, the finding that spatial and temporal variance are correlated at certain scales but less so at others is intriguing. We can

imagine instances in which spatial and temporal variation could interact with one another to drive changes in landscapes. For example, frequent fires are characteristic of many landscapes, including our study area. Differences in the rate of accumulation of flammable plant matter through space will affect the frequency of fires, and hence temporal variation in primary production. Areas in which fuel accumulates evenly through space will experience hot, homogeneous and less frequent fires that return succession to an early stage throughout the area. By contrast, areas in which fuel accumulates unevenly may experience cooler, heterogeneous and more frequent fires, resulting in a mosaic of patches of vegetation at differing successional stages. Another process is the planting, growth, and harvest of large tracts of tree plantations that dominate the study landscape. The spatial scale that explains most of the temporal variance (10^5 to 10^6 m^2) includes the range of management unit sizes used by forest-products companies, and the most influential temporal scale (9-16 years) is the closest to the 20-25 year plantation harvest cycle.

This kind of mechanism implies that there is a strong possibility that positive and negative feedbacks can occur between spatial and temporal variation. Disturbances that are facilitated by heterogeneity may create further heterogeneity, leading to further disturbance, and so on. The end consequence of such a feedback would be extreme anisotropy in landscapes, possibly originating from quite small initial differences. Another possibility would be dampening, in which spatial variation in landscapes is reduced by the slow rate of change in more heterogeneous areas. Dampening would lead to greater homogeneity in landscapes than the dominant processes themselves would imply. We would expect such dynamics to be strongly non-linear and highly scale-dependent. Unfortunately, demonstrating causal interactions between spatial and temporal variation will be difficult; the standard, correlative approaches that are

typically used to analyze remotely sensed data are generally inadequate for causal analysis. Rigorous tests of causation will require simulation modeling and ideally, experimental manipulations (if possible).

Conclusions and Recommendations

An important contribution that our approach offers is a framework in which landscape variation through space and time can be considered together, rather than individually. This is useful for problems where we know that both spatial and temporal variation are likely to be important but there has been no quantitative way of considering the two together. In addition, our approach has the potential to help link pattern to process and to highlight the spatiotemporal grain(s) at which dominant processes occur in a given landscape. Previous researchers have addressed spatial variance in some detail, and most studies in the field of remote sensing concern changes over space or time, but few researchers have managed to link the two in a quantitative framework. One preliminary attempt to do so incorporated trajectories of land cover change (based on multiple dates of satellite imagery land cover classifications) into a landscape fragmentation analysis (Nagendra et al. 2003; Southworth et al. 2002). Similarly, Mertens and Lambin (2000) attempted to model land cover change using landscape trajectories, again incorporating time into the analysis. Other researchers in remote sensing are also starting to incorporate such methods into their research (Munroe et al. 2004). However, these studies use land cover classifications, a discrete data source, and so lose much of the inherent variability within the dataset prior to analysis. While some researchers are trying to overcome this limitation by working more with continuous data (Southworth et al. 2004a) such research is still in its infancy.

Research assessing spatial variance is much more common in the field of remote sensing than that assessing temporal variance. The scaling relationships of spatial patterns have received

some attention (Wu and David 2002), primarily through studies looking at how spatial grain and extent impact landscape metrics. Wu et al. (2000) found that in order to adequately quantify spatial heterogeneity, response curves (i.e., of metrics to changing scale) were necessary, as opposed to the more widely used single-scale measures. O'Neill et al. (1996) in a study for the southeastern U.S., developed a method using pattern state space and a distance metric that measured the overall differences between landscapes or changes through time. Lambin (1997), in a study of landscape disturbance in Africa, found that spatial heterogeneity was a key variable of interest; landscapes with either very high or very low levels of disturbance were characterized by low spatial heterogeneity, while areas of moderate disturbance were very heterogeneous. However, as our results would suggest, this relationship varied with the scale of the analysis. In a study using local spatial variance measures of simulated high resolution imagery to predict the spatial patterns of forest stands, Coops and Culvener (2000) found a technique using local variance and spatial pattern statistics to be successful. Their results suggested that for their study the relationship between spatial patterns of objects and variance is strongest at window sizes between 20-30 m, which matches the resolution of SPOT and Landsat TM data.

Ecology has a longer history than remote sensing of addressing both spatial and temporal patterns in plant and animal populations. In particular, attempts to explain spatiotemporal variation in community structure have yielded a range of statistical approaches that could conceivably be applied to remotely sensed data. For example, a common approach in the analysis of community patterns is to partition variance in community composition between environmental (spatial) factors and temporal factors (Williams 1982; Rundle and Jackson 1996; Ault and Johnson 1998; Legendre and Legendre 1998; Herbert and Gelwick 2003). Once the computational difficulties of working with very large matrices have been overcome, approaches

such as Redundancy Analysis (RDA) and Principal Coordinates of Neighborhood Matrices (PCNM) (Borcard and Legendre 2002; Legendre and Gallagher 2001) have considerable potential for application to remotely sensed data. Another new but promising approach in ecology uses Markov Chain models to assess spatio-temporal relationships (Hill et al. 2002), extending some of the trajectory analyses described above. The primary challenges in applying methods from community and landscape ecology to land cover data sets are computational rather than conceptual, and hence should be relatively easy to overcome as computing technology continues to improve.

Wu et al. (2000) found that scaling analysis of variance can be a powerful method for describing and detecting the dominant patterns within a given landscape. They proposed that the scientific community should address three related groups of questions: (1) how does changing the scale of observation or analysis impact the results, and does it do so in a predictable way; (2) are the systems hierarchically or multi-scaled structures, and how do we relate these to the resultant pattern and process in a landscape; and (3) what scaling laws exist in heterogeneous landscapes? Wu et al. (2000) concluded that while these research questions are critical to the development of landscape ecology, they are also among the most challenging to address. The approach that we have outlined offers one way in which we can start to use remotely sensed data to identify key scales in landscapes and to look for interactions between spatial and temporal patterns at different scales. While our study was limited in scale, with no sub-pixel or finer scale spatial variation being included below a 3x3 pixel area (Butler et al. 2004; Malanson et al. 2002) remote sensing data can be used to track variation at both finer and coarser scales. Many remote sensing studies lack transferability across space and time of established relationships; it remains to be seen whether our approach is more generalizable to other landscapes and across remote

sensing platforms. Although the full integration of spatial and temporal data across multiple scales will ultimately require a more mechanistic approach, the results that we have presented offer a novel and interesting way in which to start investigating some of the questions that are most critical for the further theoretical development and unification of remote sensing, GIS approaches, and landscape ecology.

Finally, this study is focused on the linkages between landscape ecology and GIScience and remote sensing applications, and used data from remote sensing coupled with development of a multiscale spatiotemporal variance analysis approach to address a fundamental question in landscape ecology. All three "disciplines" were necessary to conduct the study, but one could argue that the substantive questions came from landscape ecology while remote sensing and GIScience provided the materials and methods. The methods developed and employed here, addressing form and function within a landscape across multiple spatial and temporal scales, ultimately heeds the call of the GIScience research agenda in terms of better representing landscape dynamics in association with a closer coupling of analysis and the conceptualization of process (Goodchild 2004). This confluence of landscape ecology and GIScience is inevitable—many multiscale techniques, as employed here, are commonplace for analyzing pattern and process issues relating to scale. Where else will we obtain sufficient information about landscape dynamics, and where else will we develop methods to answer the questions?

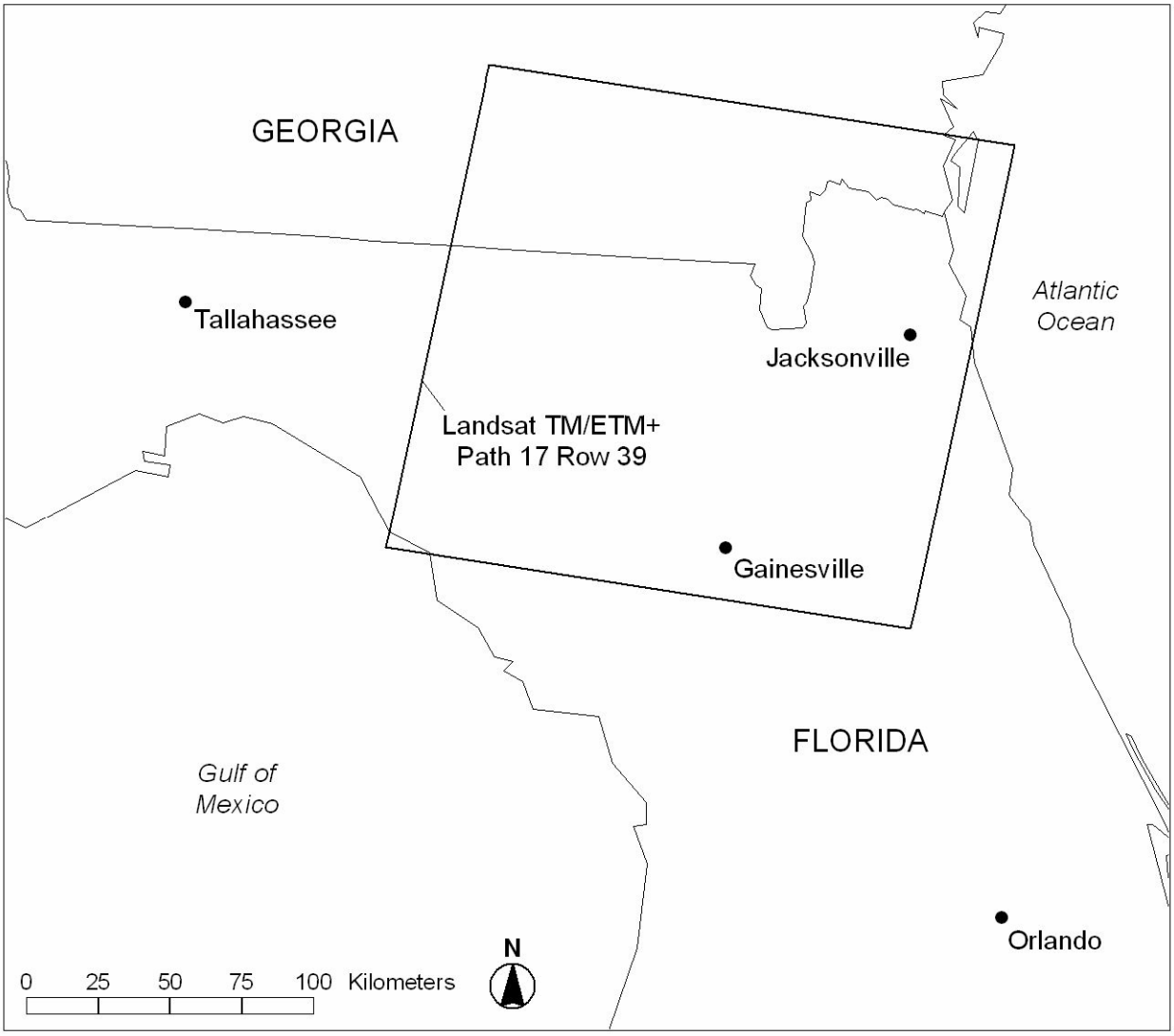

Figure 2-1. Study area of the southeastern coastal plain, with focus region and location of Landsat TM image footprint.

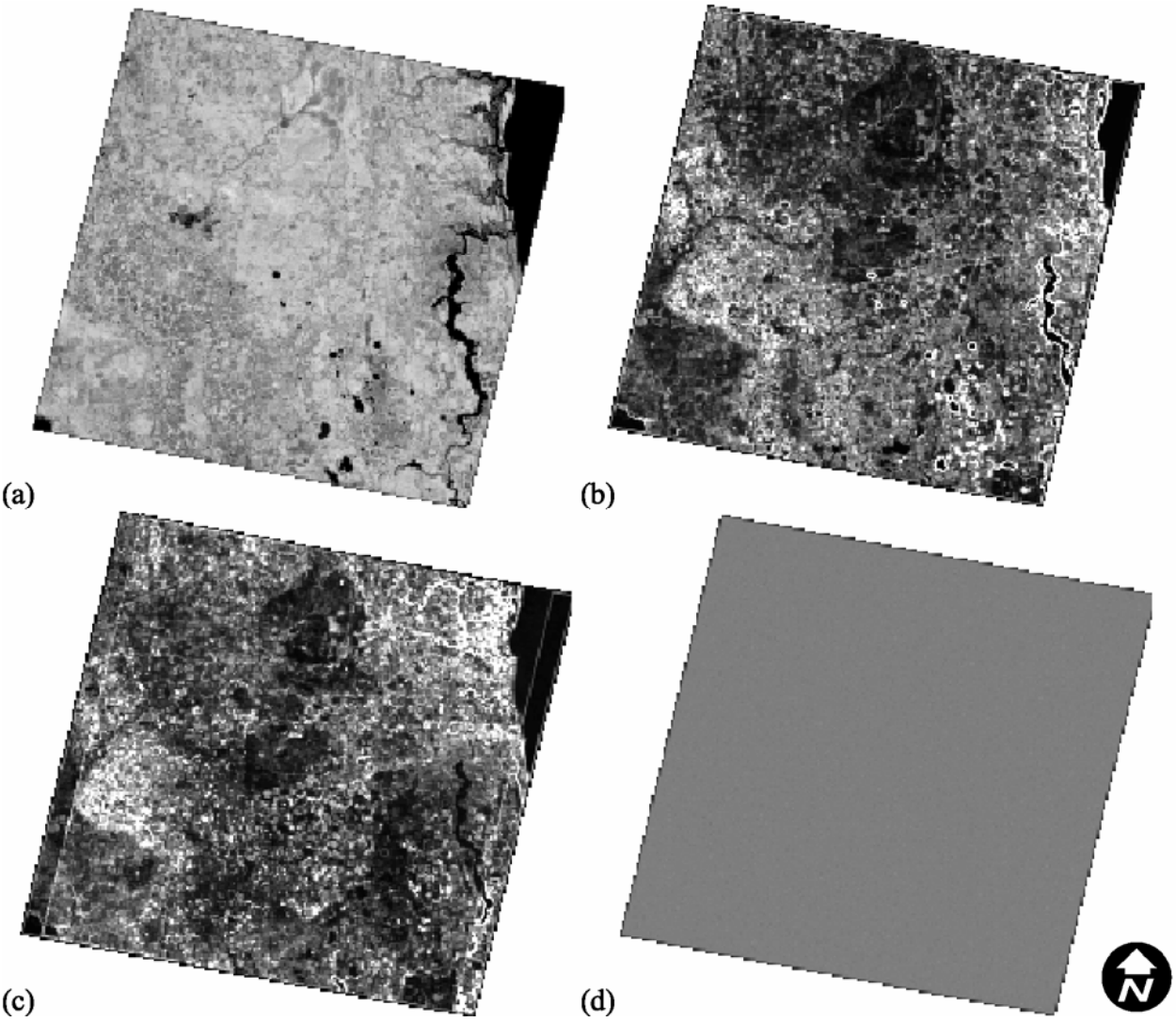

Figure 2-2. Landsat TM Image NDVI products created for each image date, each filter size, and each pair of dates, here using the example for (a) January 1997 NDVI Image, (b) January 2001 spatial variance of NDVI Image with a 10 x 10 filter, (c) January 1997 temporal variance NDVI, and (d) January 1997 Null Model NDVI.

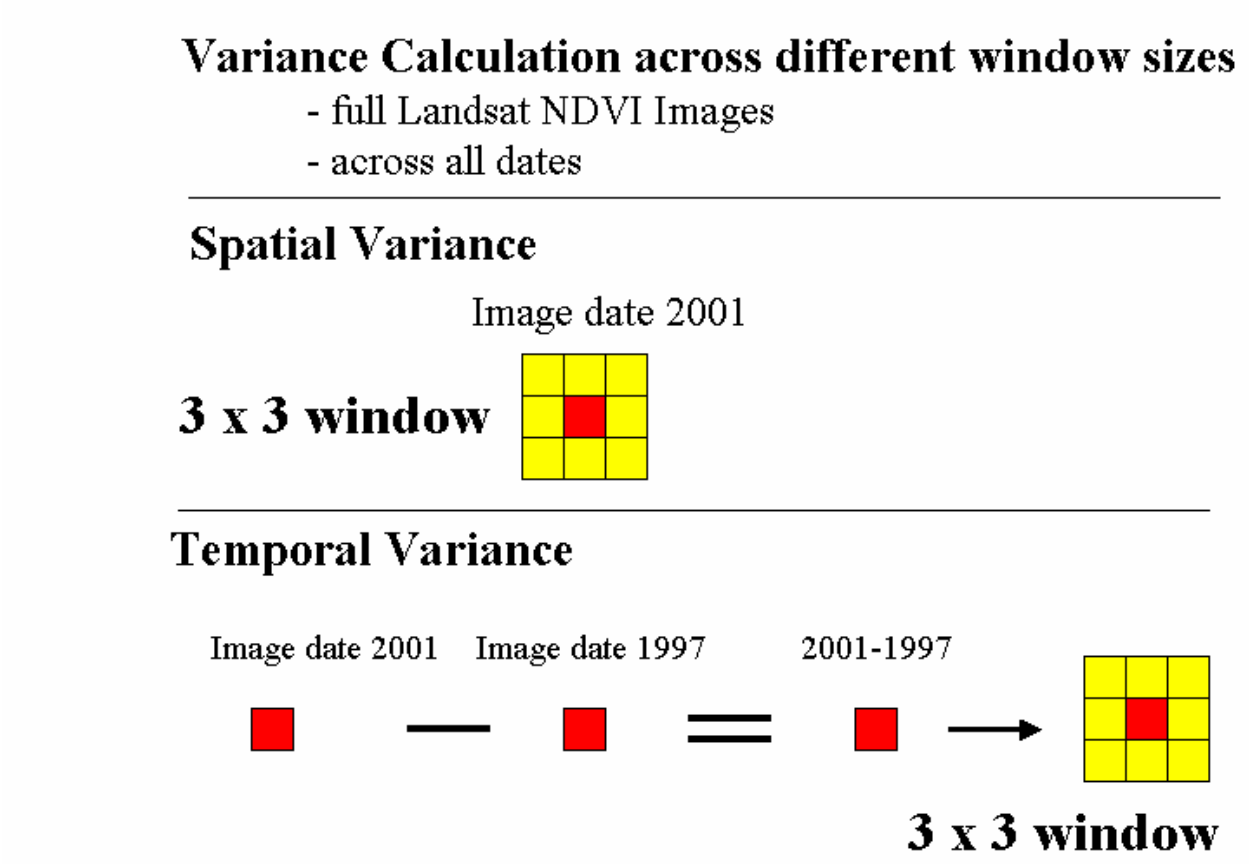

Figure 2-3. Illustration of the spatial and temporal variance calculations.

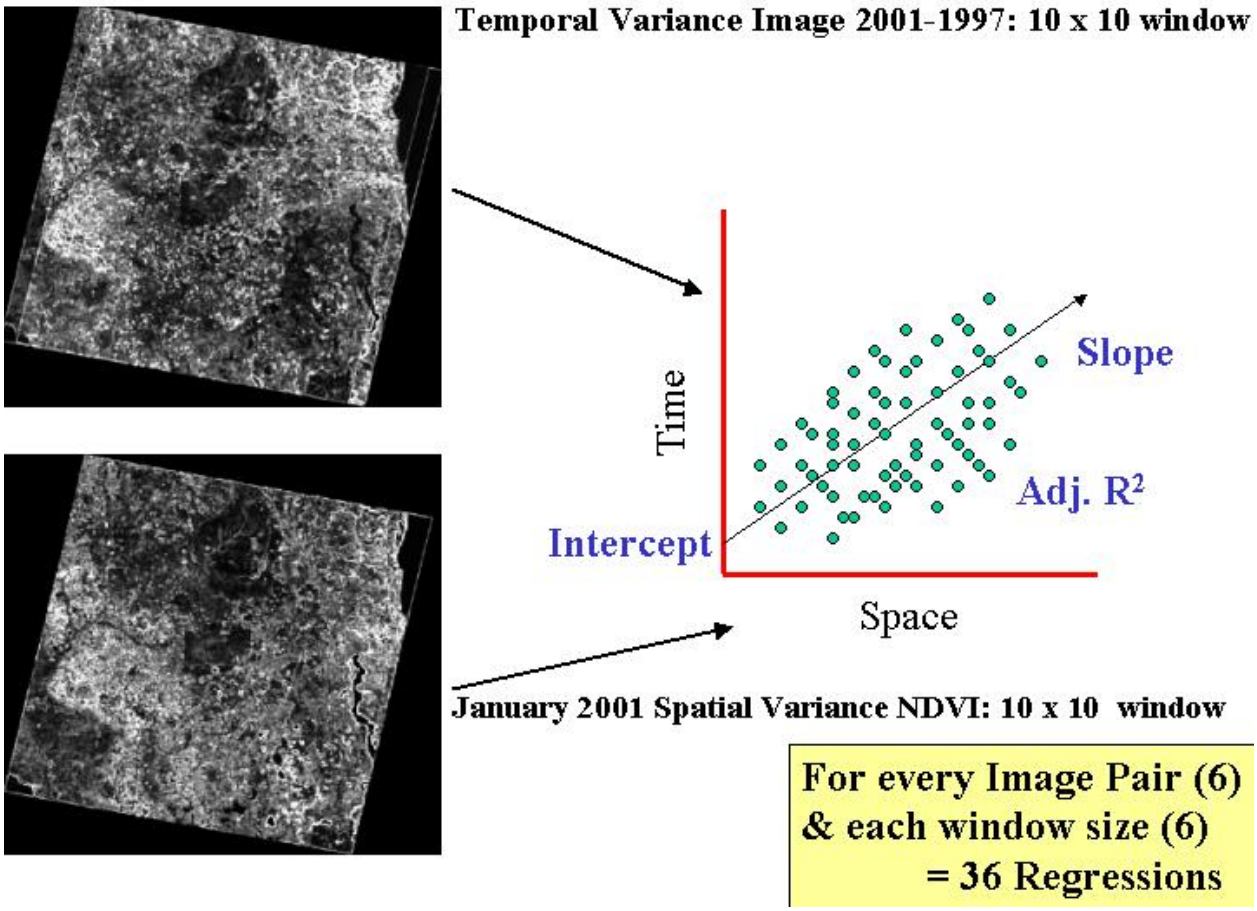

Figure 2-4. Regression models used in analysis.

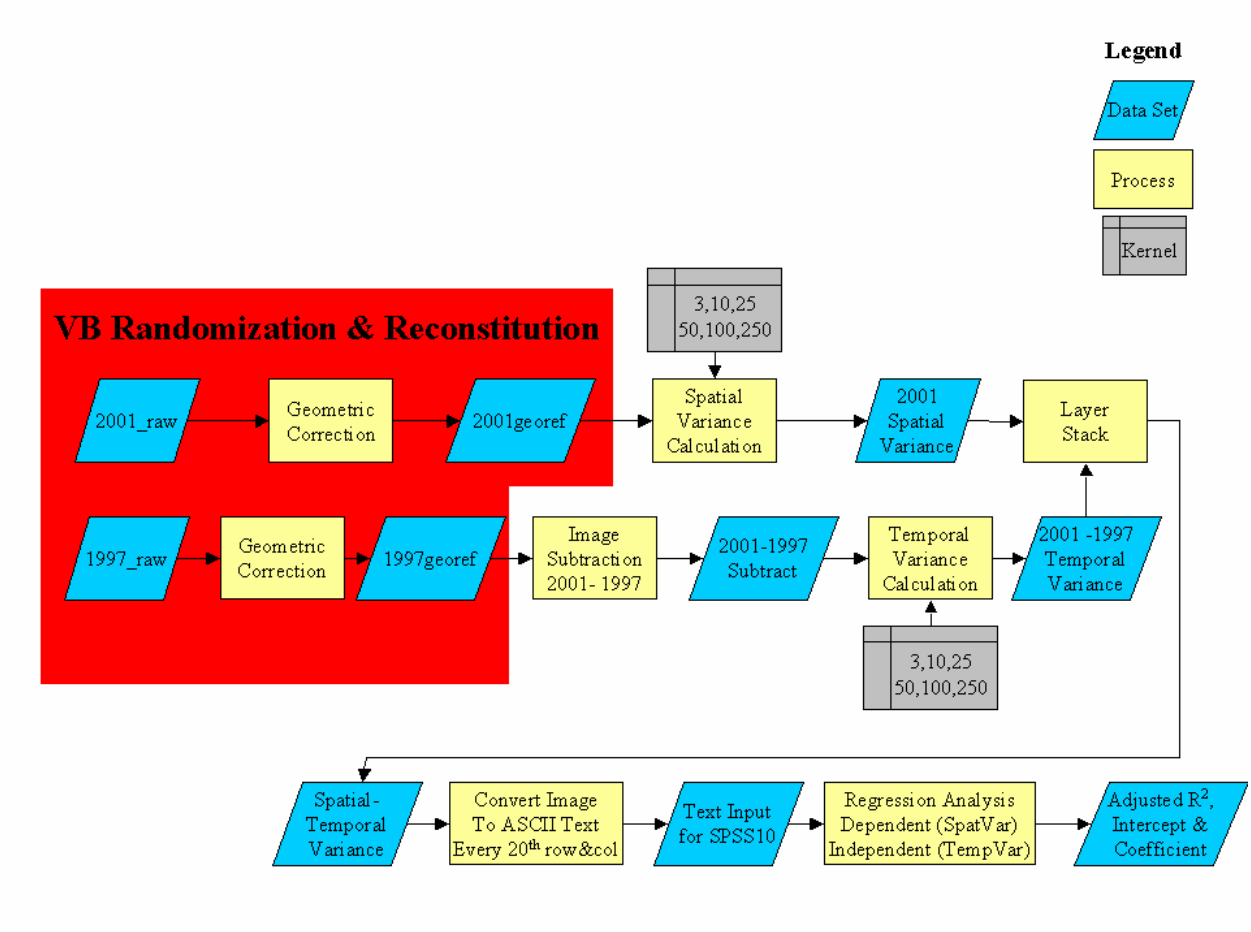

Figure 2-5. Flowchart of analysis methods and null model creation.

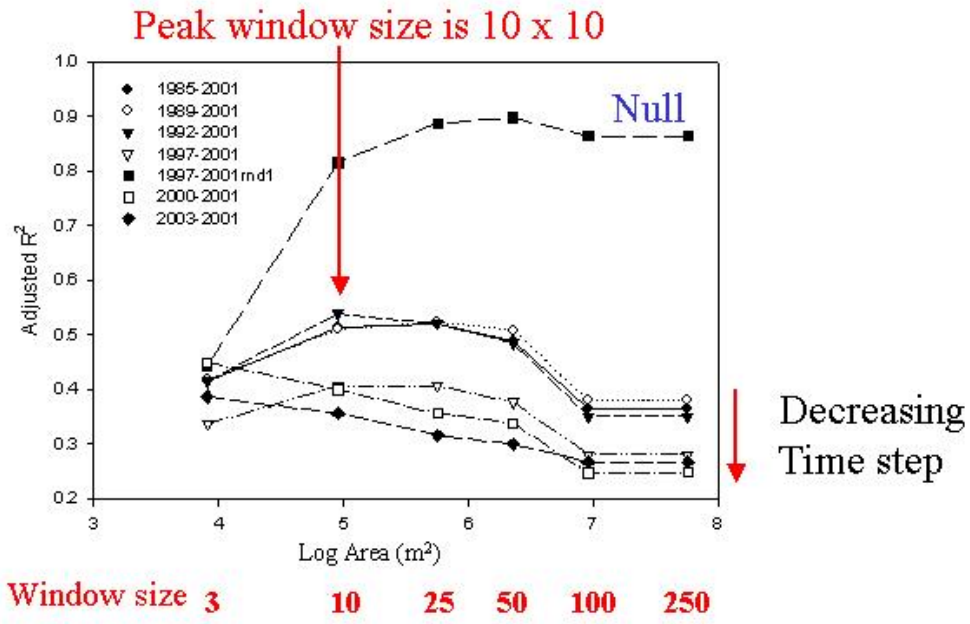

Figure 2-6. Adjusted R^2 relationships between spatial versus temporal variance, across the different time-steps and window size and area.

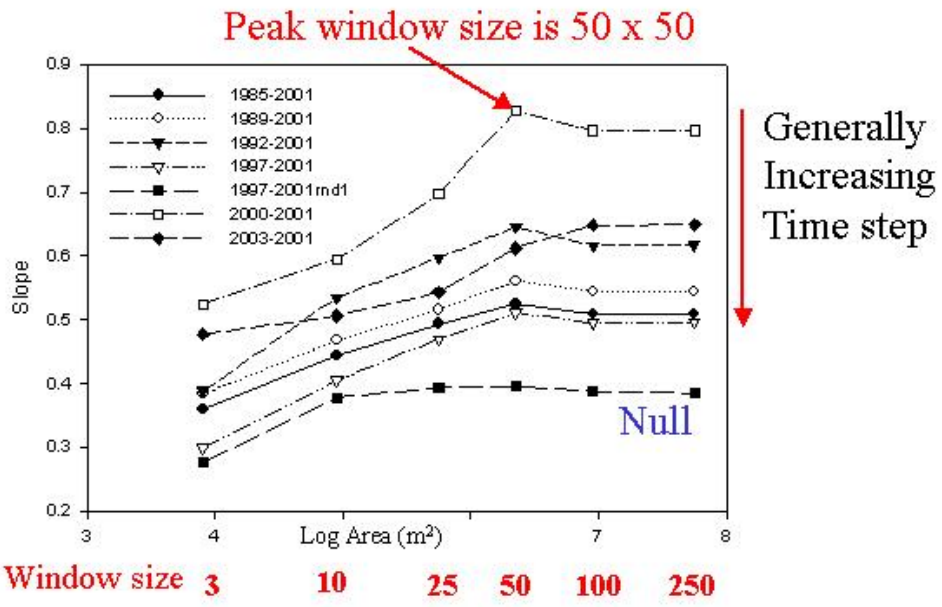

Figure 2-7. Slope relationships between spatial versus temporal variance, across the different time-steps and window size and area.

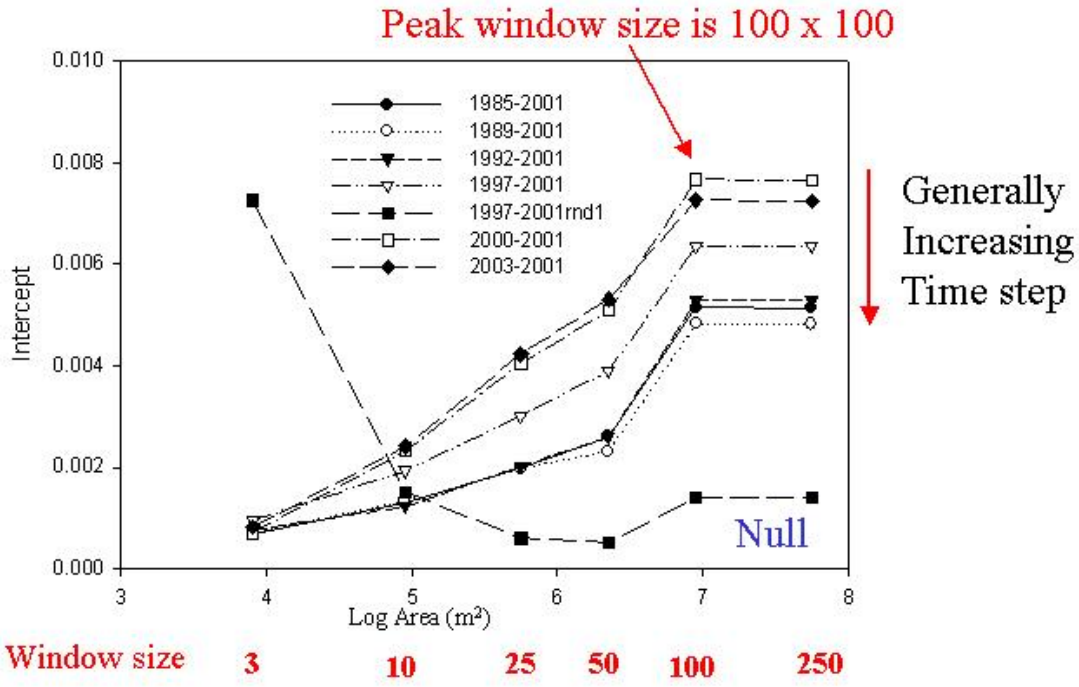

Figure 2-8. Intercept relationships between spatial versus temporal variance, across the different time-steps and window size and area.

CHAPTER 3
RATES AND PATTERNS OF LAND COVER CHANGE AND FRAGMENTATION IN PANDO, NORTHERN BOLIVIA FROM 1986 TO 2005

Introduction

Mertens and Lambin (2000) contend that land use change is necessarily a complex and often multidirectional process of biophysical and socioeconomic interactions. While land-use change is a fundamentally local process, it is nested in a structure of hierarchical decision-making (Moran et al. 1998). Observed land cover patterns are the net result of individual decision-making processes regarding the relative returns to land use (Currie 1981) set within the regional or national context. Hence, land cover, along with pattern analysis and social science measures, can be used to indicate the changing patterns in land use (i.e., to link land cover to land use). Patterns of land cover change in most tropical countries relate significantly to anthropogenic impacts and are extremely complex, with changes occurring across multiple spatial and temporal scales (Woods and Skole 1998; Duncan et al. 1999).

Land cover change is regarded as the single most important variable of global change affecting ecological systems (Vitousek 1994) with an impact on the environment that is at least as large as that associated with climate change (Skole et al. 1994; Chen 2002). Several factors need to be addressed while monitoring land cover change: what kinds of alterations are taking place? Where do they occur? What are the rates of change? What are the patterns of change? What other factors influence each of the above? Much attention has been paid to the issues of human-induced land cover change within the last few decades as evidenced by such multi-disciplinary, multi-national programs as NASA's Land Cover Land Use Change (LCLUC) programs (http://lcluc.gsfc.nasa.gov/) or the International Geosphere Biosphere Programmes (http://www.igbp.kva.se/cgi-bin/php/frameset.php).

According to the Land-Use and Land-Cover Change Science/Research Plan of the International Geosphere-Biosphere Programme (IGBP), to explain land-cover change, particularly tropical deforestation, we must consider the likely determinants of land use. Such factors include: population size or density, technology, level of affluence, political structures, economic factors such as systems of exchange or ownership, and attitudes and values (Turner et al. 1995). Thus, land-cover change is in great part the realization of changing patterns in land use. Most researchers break up the determinants of land use into two broad categories: proximate and ultimate driving forces. At a regional or landscape level, causal mechanisms include broader economic forces (price policies, wage trends), and intersectoral linkages, such as factor markets and trade (Moran et al. 1998; Coxhead et al. 2001). At this landscape scale, one can answer questions appropriate to this level of analysis, such as: Does infrastructure development cause deforestation? Do markets cause deforestation?

A second level of analysis has been called the proximate causes of land-cover change (Turner et al. 1995). Other researchers have called this level the “enabling environment” (Coxhead et al. 2001) or “direct causes” (Panayotou and Sungsuwan 1994). Land-use change is a fundamentally local process, but it is nested in a structure of hierarchical decision-making (Moran et al. 1998). At the local level, one can consider such factors as changes in population density, technical innovation, or changes in agricultural production systems (e.g., switching from a subsistence crop to a cash crop). Incentives formed at the landscape level, such as policy changes, are realized by human decision-making at the local level. For example, in Bolivia INRA and the Forest Law allow a specific amount of forest cleared per head of cattle (about 5 ha).

Remote Sensing for Change Detection

Remote sensing is an attractive source of land cover data as it provides a representation of the Earth's surface that is spatially continuous and highly consistent. Such data are available at a range of spatial and temporal scales. Remote sensing data collected for the same season during a year over many years provides a temporal sequence of information as to the changes and evolution of land cover on a landscape or a region. Much information about land cover types and changes has been derived from satellite images, specifically the Landsat platform, in the past 30 years. Analyzing changes in spatial pattern in land cover over time may allow for the identification of biophysical processes driving changes in land cover (Brown et al. 2000). These spatio-temporal patterns coupled with socio-economic data in a modeling framework may permit the identification of social actors and drivers of land cover change for a particular area. Thematic mapping from remotely sensed data is based typically on an image classification; and while a thematic map provides unquestioned simplification of reality, it is only one model or representation of the depicted theme (Woodcock and Gopal 2000).

While most classification strategies have focused on the use of spectral dimension, the spatial domain (as represented by the spatial organization or pattern of the data) also contains important information that to date has not been utilized well within land cover and classification methodologies (Cihlar 2000). Land cover fragmentation analyses are used frequently to help interpret the impact of land cover changes within a landscape, by calculating for each land cover class a range of metrics to describe fragmentation and spatial distribution, often from satellite based land cover classifications. Analyzing changes in spatial pattern over time will facilitate the identification of the social and biophysical processes driving these changes (Brown et al. 2000). A discrete classification is generally used for this purpose, to partition a landscape into

homogeneous units with distinct boundaries, so that interpreting numbers that refer to the geometry and arrangement of these discrete units is conceptually simple (Pearson 2002).

It is an exciting time for the use of remote sensing for monitoring global land cover change. A multitude of new satellite platforms have been launched within the past decade and more recently, offering a variety of data products with varying spatial, temporal, and spectral resolutions. A variety of derived data products (e.g. variance and local spatial autocorrelation indices as measures of image texture) from satellite images are available along with improved methods for image classification accounting for these and additional ancillary data products. The use of images from multiple satellite platforms allows for improved identification of patterns and hotspots of land cover change.

Previous Work in the Amazon

The Amazon basin has seen accelerated rates of deforestation since the 1970s (Laurance et al. 2004). Business-as-usual estimates predict that forest cover will be reduced to 53% of its original area by 2050 with large agricultural and timber industries as the primary beneficiaries (Soares et al. 2006). Current development of the Amazon by deforestation predicts increased fire frequency, and modified regional climate (Laurance et al. 2004; Nepstad et al. 2001; Soares et al. 2006)**.** The Amazon forest provides ecosystem services for carbon sequestration in biomass and soils from the global atmosphere, regulation of the water balance and flow of the entire Amazon river system, the modulation of regional climate and air patterns over much of South America and the potential prevention of the spread of vector- and water borne diseases (Foley et al. 2007). Enhanced drying of the forest floor, increased fire frequency and lowered productivity are examples of collateral damage incurred by surrounding forests through canopy damage due to deforestation and selective logging (Foley et al. 2007; Nepstad et al. 2001; Alencar et al. 2004).

Much previous work on deforestation and land cover change has been highlighted by research occurring in the Brazilian Amazon. Such studies have been the proxy for global deforestation rates and have garnered much attention to the processes of deforestation (Roberts et al. 2003; Nepstad et al. 2001; Laurance et al. 2004; Moran 1993; Lu et al. 2007). Given the longevity of NASA's Landsat program coupled with newer satellite platforms (e.g. MODIS and ASTER) remote sensing affords a reasonably economic and attractive source of data for the monitoring and assessment of deforestation in the Amazon basin. The latest, most reliable annual rate of deforestation in the legal Brazilian Amazon was calculated at 27,379 km^2 yr^{-1} for 2004 (INPE 2008) with unofficial annual rates of 18759 km^2 yr^{-1}, 14039 km^2 yr^{-1}, and 11224 km^2 yr^{-1}, respectively, for 2005, 2006, and 2007. Many other studies have more focused local investigations of deforestation and forest fragmentation in various parts of the Brazilian Amazon where deforestation hotspots occur. (Roberts et al. 2003) summarize early research results from the Large Scale Biosphere Atmosphere experiment in Amazonia of projects using remote sensing for monitoring of the regional ecosystem functioning of the area. Land cover mapping along with forest degradation were two of many applications of remote sensing for monitoring the land cover/land use change occurring in the Brazilian Amazon. Although much attention of the scientific community on deforestation is directed to the Brazilian Amazon, some studies document land cover changes in the countries that comprise the Amazon Basin (Oliveira et al. 2007; Armenteras et al. 2006; Etter et al. 2006; Naughton-Treves 2004; Imbernon and Branthomme 2001).

Tropical deforestation can be couched in terms of Von Thünen bid-rent theory where land is allocated to the highest value (Walker 2004; Kaimowitz et al. 1998). In the case of deforestation in frontier zones of tropical countries, ease of accessibility factors into the land

rent; therefore forested land nearest to population centers and roads is most likely to be deforested sooner than remote areas. In addition to industrial agriculture, cattle ranching and colonization projects (Steininger et al. 2001), roads and construction of new roads have been reported as proximate cause for forest clearing and widespread deforestation, especially in frontier areas of tropical countries where governments encourage new colonization projects (Arima et al. 2005). New roads offer market access for timber and agricultural products from previously remote areas and roads lower transportation costs for internal migration, land access and land clearing for subsistence farming (Chomitz and Gray 1996). Road construction into forested areas increases incentives to log these areas and allows access to forest resources, which increases the probability for deforestation nelson and (Nelson and Hellerstein 1997). Forest conversion along road corridors results in habitat fragmentation and exposes the forest to various forms of degradation (Chomitz and Gray 1996). Locations nearer to existing deforestation tend to be deforested (Mertens and Lambin 2000) and forest fragments are more accessible thus susceptible to new deforestation than larger, contiguous areas of forest (Kaimowitz et al. 1998; Mertens and Lambin 2000). These impacts of roads on forest integrity and health are important to consider here given the multitude of infrastructure projects underway in Brazil (Fearnside 2002) and Peru in the southwestern Amazon (Perz et al. 2008), which will directly impact northern Bolivia.

The southwestern Amazon is slowly receiving increased attention from the scientific community (Oliveira et al. 2007; Asner et al. 2005; Naughton-Treves 2004). Deforestation around and extending from Puerto Maldonado, the capital of Madre de Dios, Peru accounted for 23% of total forest damage (deforestation and forest disturbance) incurred in the Peruvian Amazon between 1999 and 2005 (Oliveira et al. 2007). Asner et al. (2005) found an average of

76 km^2 yr^{-1} of selective logging and 564 km^2 yr^{-1} of deforestation in Acre, Brazil between 1999 and 2002. Contrastingly, deforestation in the Amazonian lowlands of Tambopata, Peru proceeded at the net annual rate of 0.1% (Naughton-Treves 2004). These examples scratch the surface; however, more attention is needed on land cover change in this region given the vast area, large number of people, and settlement and road improvement projects encouraged by respective national governments.

As the northern-most department in Bolivia, Pando is coming into the scientific spotlight with the recent paving of the Interoceanic highway in nearby Brazil (Hamilton 2006). Pando is the only Bolivian department that is entirely within the Amazon and holds the most intact forest. There has been limited research in quantitatively inventorying the amounts of forest loss in Pando both at the department and municipal levels. Few department wide studies have been conducted with results accessible outside Bolivia; the most notable is the Zonificacion Agroecológica y Socioeconómica y Perfil Ambiental del Departamento de Pando (Agro-ecological and Socioeconomic Zoning and Environmental Profile of the Department of Pando) conducted in 1997 (ZONISIG 1997). This current research comprises a multi-date, and multi-scene high spatial resolution regional investigation of deforestation in Pando, Bolivia between 1986 and 2005 using Landsat TM and ETM+ images acquired every five years. The objective of this study is to determine the extent, rates and patterns of land cover change and associated forest/non-forest trajectory classes for Pando, Bolivia from 1986 to 2005.

Study Area

Pando is the northern most department of Bolivia, with an area of 63,872 km^2 that represents 5.8% of the total area of Bolivia. Pando contains five provinces comprised of fifteen municipalities with the capital, Cobija, located on the border with Acre, Brazil. With an elevation range between 90 to 289 meters Pando is considered tropical lowlands. Approximately 98%

forest cover that remains is comprised of evergreen forests broadly classified into two types of upland forest and floodplain forests with minor amounts of open savanna with tree islands (Mostacedo et al. 2006). The climate of Pando is classified as warm-humid tropical and tropical wet and dry climate (Köppen *Aw*) with a pronounced dry period from May to September and a rainy season from November to March, during which the north-south migration of Intertropical Convergence Zone produces heavy rains due to low air pressure and extremely unstable atmospheric conditions. From 1944 to 1990 average monthly temperatures were reported from 23.6 to 26.4°C with an annual average of 25.4°C. For the same time period the annual average precipitation 1,834 mm (ZONISIG 1997).

From the 1992 census the total population in Cobija was about 11,000 of the 38,000 persons residing in Pando. The most recent census placed the 2001 populations at slightly more than 22,000 and 52,500 for Cobija and Pando, respectively, with the 2005 estimated populations at almost 32,000 and 67,000 (Instituto Nacional de Estadísta de Bolivia, www.ine.gov.bo). Rural economic activities consist of Brazil nut harvesting, timber extraction, and cattle ranching while some gold mining occurs within river alluvial bars (ZONISIG 1997). Petroleum has been discovered in southern Pando, but is not extracted. Commercial and retail activities, especially in Cobija, along with communications and road construction are other leading economic activities (ZONISIG 1997). Two major road corridors dissect Pando with the central west to east Cobija-Porvenir-El Sena-Puerto Copacabana-Riberalta (in the neighboring department of Beni) road, and the north-south Porvenir-San Silvestre-Chive road along the western edge of Pando (Figure 3-1). The main access into the interior of Pando is by paved road from Cobija to Porvenir, and then by dirt road from Porvenir through Puerto Rico to El Sena and on to Riberalta in the neighboring department of Beni (Figure 3-1).

In contrast to the widespread deforestation and larger patches in Acre, Brazil, the deforestation landscape in Pando is relatively recent (i.e., in past few decades). Spatially extensive deforestation, extending up to 2 kilometers, occurs on privately owned lands adjacent to the roads, close to the main population center of Cobija. After about 20 kilometers along the roads to Sena and to Extrema, these large non-forest areas become less pronounced on the landscape and deforestation becomes patchy and more linear along the road less than 0.5 kilometers into the forest.

In Pando under the Ley Forestal or National Forestry Law of Bolivia (República de Bolivia 1996), landholders are permitted to clear one hectare of land per year for chacos.) Clearing occurs through traditional slash-and-burn methods. The cleared land is in chaco for one year after which it is generally maintained for agriculture for another year or so before left fallow. In a few cases, fallows are converted to pasture. The maintenance of pasture is cyclical with active burning every year near the end of the dry season in September (later in the year than most images obtained for this study). Annual burning is used to remove stumps and felled trees over time.

Methods

Image Selection and Preprocessing

Landsat 4 and 5 TM and 7 ETM+ images (Appendix A) were acquired for 1986, 1991, 1996, 2000 and 2005 during the dry season (May to October) totaling 40 images for the area. This seasonal time period permits image acquisition with relatively minimal cloud cover and haze from smoke from the burning of pastures and recently cleared forests. Due to some clouds a few images were acquired outside of this time period. Best efforts were made to minimize intra- and inter-annual precipitation differences between images although incomplete and often non-overlapping annual and monthly records made this process challenging.

The images were corrected for atmospheric and seasonal differences following (Green et al. 1999; Green et al. 2001) and were georeferenced to less than 0.5 pixels or 15 meters using the University of Maryland Global Land Cover Facility Geocover 2000 images, which make up part of the analysis. The images were mosaicked to generate a seamless coverage of the area for each date. Clouds, shadows and water were removed from each individual image and from the mosaics using a PCA image differencing and thresholding method (Varlyguin et al. 2001). The masks were combined together from individual dates and applied to the mosaics in preparation for classification.

Next, secondary image products were derived to assist with the image classification. The tasseled cap indices (Kauth et al. 1976), a mid-infrared index (Boyd and Petitcolin 2004) and a 3 by 3 moving window calculation of the variance of each pixel for bands 4, 5 and 7 (as a measure of image texture) were generated for each mosaic. The Kauth-Thomas transformation bands, particularly the greenness band along with the mid-infrared bands, are useful for discriminating forest structure from other types of vegetation and the brightness band is useful in identifying non-forest areas. Texture is useful for classification of forest versus non-forests (Boyd and Danson 2005) and useful in aiding classification of forests where selective logging has occurred (Chan et al. 2003) resulting in small cleared patches in a complex forest matrix.

Image Classification

Image classification using decision trees handle non-parametric data at different spatial, spectral and temporal resolutions, generate easily interpretable and explicit classification rules, and produce an importance score for each variable (Breiman 1984). Given the vast geographic extent of the study region and its complex ecosystems and eco-regions, a rule-based or decision tree classification (Breiman 1984) was chosen over traditional unsupervised and supervised techniques. The visible and thermal bands contained striping, which proved to be difficult to

remove, thus limiting the available information for a traditional classification. The rule based classification approach provided flexibility to eliminate these bands, using only the near- and mid-infrared bands along with secondary derived products.

From an initial field visit to Pando in May 2006 coupled with visual interpretation of the 2005 mosaic, known locations of forest, pasture and bare-built were identified and used as training samples for the creation of the decision rules. Three initial classes were created for forest, pasture, and bare/built. Pasture and bare/built were aggregated to create the non-forest class. The pixel values of these areas were extracted from the mosaics of the infrared bands 4, 5, and 7; the Kauth-Thomas brightness, greenness, and wetness images; and a 3x3 windowed calculation of image variance for each of the infrared bands.

The data mining software Compumine (www.compumine.com) was used to create the decision rules for each mosaic. Similar to logistic regression, Compumine predicts user specified classes based on the recursive portioning of continuous input data resulting in a decision tree based on variable importance in the model. The variable importance is a relative measure of how much each of the variables used in the model contributes to reducing the prediction error of the model. A split sample validation was used for the training sample points whereby 85% were used to train or create the decision tree and 15% were used to test the tree. This process was repeated for each mosaic date.

Performance assessment statistics of accuracy, precision, and recall are provided for the resulting decision rules and accompanying tree models. Accuracy is the number of correctly predicted test examples divided by the total number of test examples reported as a percentage. Precision (Equation 3-1), reported between 0 and 1, is the measure of accuracy that a specific

class has been predicted where *tp* and *fp* are the number of true positive and false positive predictions for the considered class.

$$precision = \frac{tp}{tp + fp} \tag{3-1}$$

Recall (Equation 3-2) measures the ability to select instances of a certain class from a data set where *tp* and *fn* are the numbers of true positive and false negative predictions for the considered class. The total number of test examples of the considered class is *tp* + *fn*.

$$recall = \frac{tp}{tp + fn} \tag{3-2}$$

The resulting classified images were subset to the extent of Pando that coincided within the mosaic extent. That is, due to the selection of the Landsat image path and rows for the creation of the mosaics and due to the major road corridors through Pando which omitted the northeastern municipality of Federico Roman, the spatial extent of Pando described here is smaller than that of the department of Pando.

Change Detection

Since deforestation is categorical change (Woodcock and Ozdogan 2004) change trajectories were chosen as the best means to analyze temporal changes in forest cover and to calculate the rates of deforestation (Southworth et al. 2004a; Petit et al. 2001). Image change trajectories are defined as sequences of successive changes in land cover types providing information changes between two or more time periods of an area or region. That is, the number of change categories (Equation 3-3) is defined as m_t, the number of change trajectories, m_c the number of land cover classes defined, and the superscript *t* as the number of images (Petit et al. 2001).

$$m_t = m_c^t \tag{3-3}$$

Change trajectories were calculated between the five dates of classified mosaics resulting in four date pairs for 1986-1991, 1991-1996, 1996-2000, and 2000-2005. Four trajectory classes of stable forest (F-F), deforestation (F-NF), reforestation (NF-F), and stable non-forest (NF-NF) are possible from this type of analysis. These simple two-date pairs were selected for ease of analysis as calculating a trajectory image using all five dates for the classification would result in 32 change trajectory classes, which would be difficult to interpret. The calculation of trajectory images for pairs of images also allows for the calculation of rates of conversion for deforestation and reforestation between the two dates, thus making the results comparable to other studies of the region.

Classification Accuracy

Classification accuracy was assessed using Kappa coefficient and overall percent accuracy for each class and for the overall classification. Field observations about the land cover type at locations close to transportation corridors (i.e., roads and rivers) around the study area were collected in 2006 and 2007. The 2006 points were collected around four communities in Acre, Brazil and seven communities in Pando. These points were aggregated to a FNF classification from a finer level of classification and 30 points were selected for each forest and non forest class. The data collected in 2007 were based on a stratified random sample of 300 points within 1.5 kilometers of the Cobija-Sena road corridor for each cover type derived from a preliminary FNF classification using the 2005 mosaic. Of these 300 points, at least ten percent were selected to be visited within the field based on accessibility. One hundred and fifty points were collected during the 2007 field season; all were used for accuracy assessment of the 2005 FNF classification.

Since field data do not exist for the 2000 FNF classified mosaic, temporally and spatially corresponding ASTER images (Appendix B) were used as an independent data source for

additional accuracy assessment. The classification accuracy of 2000-2005 FNF trajectory image was assessed also using ASTER images from 2000 and 2005. Since ASTER has a higher spatial resolution than Landsat, making it easier to discern forest from non forest, it is appropriate for use as an accuracy assessment data set. The ASTER images were acquired from the USGS GLOVIS archive and not all of the study extent was covered by one year; therefore 2001 and 2006 images were included with the 2000 and 2005 ASTER images, respectively resulting in 31 and 35 images used for each date. A stratified random sampling design of 100,000 points was generated within the overlapping extent of the ASTER images and classification mosaics. Great care was taken to ensure the accuracy sampling points were well within the FNF and trajectory patches by buffering each patch edge by 60 meters to compensate for edge effects between forest and non-forest patches and differences in resolution between ASTER and Landsat. From these mass points 150 for each class (300 for the FNF classification and 600 points for the four class 2000-2005 trajectory image) were randomly selected as testing points. The points were assigned a class of forest or non-forest based on visual comparison of the points to their corresponding location on the ASTER images.

In this way, the test points derived from the ASTER data along with sampling points from the 2006 and 2007 field seasons provide sufficient information to test the 2000 and 2005 classifications along with the 2000-2005 trajectory image. No historical data exist to test the remaining FNF classifications or the trajectory images.

Fragmentation Analysis

A fragmentation analysis was performed on the FNF trajectory images at the Pando extent and at road buffer distances of 1, 3, 5, 8, 10, and 15 km using APACK (Mladenoff and DeZonia 2000). The buffer distances correspond to influences of roads on the forest structure for ‘near’: with 1 and 3 km corresponding to along-the-road development, intermediate distances (5 and 8

km) and remote distances at which 10 and 15 km represent influences from secondary roads or no road influence. Given the duplication of information using multiple landscape metrics measuring essentially the same aspect of a landscape (Gustafson 1998; Riitters et al. 1995) basic measures of mean patch size (MPS) and corrected perimeter-area ratio (PARC), along with fractal dimension (FRAC) (Loehle and Li 1996), and an aggregation index (AI) (He et al. 2002) were used to quantify the spatial configurations of the forest/non-forest in the land cover change trajectory images. These metrics capture the essential information about the landscape structure to assist in describing the spatial patterns of land cover change in the study area at all spatial extents. A Kruskall-Wallis test (Appendix C) was applied to MPS and PARC metrics calculated for the four FNF trajectory image dates (1986-1991, 1991-1996, 1996-2000, and 2000-2005) to determine if any of the date pairs were statistically significant from one another.

Results

Decision Tree Model Accuracies

The overall accuracy for the classification rules (Table 3-1) were quite high ranging from 98% (1996) to 99.8% (2005), and these were corroborated by the high values of total area under the curve. The number of rules used in each classification ranged from six for the 1986 classification to sixteen for the 1996 classification. At the class level the precision, comparison of the true and false positives, ranged from 0.923 (the lowest in the 1996 classification for bare-built) to 1.000. Recall, comparing true positives against false negatives, also measured high ranging from 0.93 (also in 1996) to 1.0. Overall, the classification rules distinguished the classes well. The precision and recall for the 1996 mosaic showed the most confusion between predicting true positives and false negatives for the pasture and bare-built classes. This is reflected in the overall accuracy being the lowest in the sets of classification rules and is also addressed by grouping these classes together to represent ‘non-forest’.

Classification and Trajectory Accuracies

An overall accuracy of 87.85% and an overall Kappa of 0.6762 (Table 3-2) was reported for the 2005 FNF image based on the field samples. Accuracy assessment based on samples from the 2005-2006 ASTER images showed 97.96% overall accuracy and an overall Kappa of 0.9592. Although the producers accuracy for forest based on the field samples was 100%, the users accuracy for forest was low compared to the ASTER assessment of the same classification. The overall accuracy of the 2000 FNF classification compared to the 2000-2001 ASTER images was 96.96% with an overall Kappa of 0.9592. Based on the ASTER comparison with the 2000 and 2005 FNF classifications at the class level the producers and users accuracies and Kappa are comparable in magnitude. The overall accuracy and Kappa for the 2000-2005 FNF trajectory image are 82.01% and 0.7592, respectively. The NF-F transition class has the lowest users accuracy compared to the remaining three change classes, with the F-F class having the highest users accuracy. Stable non-forest has the lowest producers accuracy and the NF-F class has the highest producers accuracy, with the lowest Kappa at the class level.

Forest and Non-Forest Extents and Rates

The area of interest of Pando analyzed in this study is 5,631,414 hectares or 88.2% of the 6,384,526 hectares actually in department of Pando. The masked area makes up 3.8% or 206,346 ha of the study area. From 1986 to 2005 the extent of forest (Table 3-3) decreased very slightly from 95.96% (slightly less than 5.5 million ha) in 1986 to 94.53% (about 5.3 million ha) in 2005. The amount of non-forest quintupled from about 21,000 ha in 1986 to a little more than 100,000 ha in 2005; a change of only 1.25% increase from less than 0.5% to almost 2% in 20 years. Although the amount of non-forest has increased between 1986 and 2005, Pando still has very little non-forest.

From 1986 to 2005 stable forest (Table 3-4) decreased from 5,381,361.27 ha (99.16% of the total area) to 5,319,193.59 ha (97.91%) while stable non-forest increased slightly from 14,684.94 ha (0.27%) to 50,515.74 ha (0.93%) in 2005. The amount of deforestation doubled from about 24,500 ha (0.45%) in the first decade (1986-1996), when it was constant, to over 51,000 ha (0.95%) in the second decade (1996-2005). Deforestation rates were stable in the first decade at about 4,100 ha (0.075%) per year while they increased to almost 10,000 ha (about 0.2%) per year between 1996 and 2000 and dropped to about 8,600 ha (0.16%) per year between 2000 and 20005. Reforestation increased also, from just fewer than 7,000 ha (0.12%) in 1986 to over 22,000 ha (0.41%) in 2005 with 1,100 ha (0.02%) per year between 1986 and 1991 and a little more than 3,000 ha (between 0.06% and 0.07%) per year between 1991 and 2005.

Fragmentation Metrics: Pando and Buffer Extents

Fragmentation metrics are first discussed at the extent of Pando (Figures 3-2 and 3-3). Comparison among classes for MPS and aggregation values show a general decrease in value from stable forest to stable non-forest to patches of deforested and reforested areas except for patches of deforestation for the 1991-1996 date pair. Stable forest has the highest values for fractal dimension, but the differentiation among linearity of the other three classes is more ambiguous. The aforementioned trends break down for the PARC values, although the PARC values in conjunction with the other two shape metrics can help differentiate which "non-forest" classes have more two dimensional shapes and those that have a more linear shape.

Metrics for the road buffers are shown in Figures 3-4 through 3-7. These plots represent the four landscape metrics as a function of lateral distance (i.e., buffer distance) away from the road and in relation to increasing distance from Cobija in 50 km sections. That is, as one goes further from Cobija along the Cobija-Sena road, one would expect the various metrics to change as a function of distance, hence the sectioning of the road buffers. The Cobija-Sena road is 250

km in length and thus choosing 50 km sections was convenient for this part of the metric analysis. Lateral distance is represented by the X axis, the distance from Cobija on the Y axis and the metric value on the Z value. The plots should be read as the observer standing in the lowermost corner at a distance of one kilometer from the road and within the first 50 km section (0-50km) from Cobija, looking to the right along the Y axis. Each intersection on the data mesh represents a node for lateral distance and distance from Cobija. For example, reading the plot of MPS for stable forest in Figure 3-4a, one would observe, in general, an increase in MPS with lateral distance from the road and with increasing distance from Cobija. In section one, the first 50 km segment from Cobija, MPS values increase by an order of magnitude from a buffer distance of 1 km to 15 km from the road.

Tracking MPS through time (Figure 3-4) requires one to view the data plot vertically where MPS in 1986 is larger generally, regardless of buffer distance and distance from Cobija, than MPS in 2005. In the 200-250 km section from Cobija, MPS values appear similar for all time periods and increase with distance from the road. The plots of AI and FRAC also exhibit similar trends as the MPS plot for stable forest. Stable forest PAC values appear higher at close and far lateral distance extremes to the road and Cobija. No pronounced temporal trend is obvious. The spatial and temporal trends for the other three classes are not as neat and cannot be as easily described.

In general MPS and AI values (Figures 3-4 and 3-7) for deforested patches follows a declining trend with distance from Cobija and seem indifferent to buffer distance regardless of time; however, in the 150-200km segment from Cobija in 1991-1996 MPS values decline noticeably. FRAC values decrease in a curvilinear fashion with increased distance from Cobija and increase with lateral distance from the road (Figure 3-6). PAC values seem insensitive to

lateral distances from the road and at distance from Cobija. No distinct temporal trend is present for any of the metrics (Figure 3-5).

MPS and AI (Figures 3-4 and 3-7) for reforested patches increase with distance from Cobija except for a downturn in 150-200 km section while lateral distance seems negligible in influence. Reforested patches increase their MPS slightly through time from 1986 to 2005 except for the 1991-1996 time period that exhibits larger MPS value regardless of spatial position. At close distances to the road AI values increase considerably in the 200-250 km section following a pronounced decrease in the 150-200 km section. FRAC values generally decrease with distance from Cobija and appear to increase slightly with increasing lateral distance from the road. FRAC values less than one indicate that not enough reforestation patches were available for the metric calculation. PAC values for reforestation patches decrease from Cobija towards the 150-200 km section and then increase in the last section. Lateral distance influences cause higher PAC values closest to the road greater than 150 km from Cobija and then decrease with increased distance from the road in these sections. Again no distinct temporal trend is obvious.

For the stable non-forest patches there is a steady decline in MPS and AI values for all time periods for all 50 km sections from Cobija except for the MPS values in 200-250 km section, which show an order of magnitude increase. This section shows the lowest AI values, especially close to the road. The influence of lateral distance from the road appears negligible on MPS and AI values regardless of time and space. FRAC values decrease with distance from Cobija except at 3 and 5 km buffer distance from the road, where they remain invariant to lateral distance within 150 km of Cobija and show a clear increase through time from 1986 to 2005. PAC values increase slightly through time and decrease with distance from Cobija with a

minimum in the 150-200 km section and then increase slightly in the last section. PAC values appear to decrease with lateral distance from the road at all distances from Cobija.

Discussion

Methodological Considerations

There were many opportunities for innovation in the classification of multiple-scene Landsat mosaics for multiple time steps. This is the first time a mosaic at a large extent has created from Landsat images to cover the tri-national area of Brazil, Bolivia, and Peru. The novel combination of near and mid infrared bands, tasseled cap indices, and variance texture in a rule-based classification scheme was used as the visible bands showed heavy striping, which were difficult to resolve. Lu et al. (2004) noted that inclusion of texture data improved classification results of complex landscapes of rural settlement areas in Rhondonia. The selection of mid infrared band during data mining for the creation of the classification rules shows that the near and mid-infrared wavelengths, particularly the latter, are useful for the discrimination of forest (Boyd and Danson 2005). Although only three land cover types were classified, the decision tree classification approach has been endorsed to classify complex landscape and environments in the Amazon (Lu et al. 2004).

The overall classification accuracies were quite high despite some challenges with the mosaicking procedure, as well as spatial, temporal, and spectral resolution differences between Landsat and ASTER. Additional challenges included the potential spectral confusion between burned areas and flooded forests and non-forest areas. This was especially true in Landsat images taken in the middle of the dry season (July and August) when slash and burn begins; thus what was once vegetated (potentially classified as forest) is now burn scars (classified as non-forest). Given the considerable spectral variability of this landscape on a region scale, the rule

based classification using the infrared bands and derived image products proved robust to discriminate between the desired spectral classes for classification.

Extents and Rates of Land Cover Change in Pando

Increased attention in last 10 to 15 years has been focused on reporting the trends and rates of deforestation in Bolivian lowland forests (Table 3-5). Within this time period these forests have been listed under the World Heritage sites of most diverse remaining Amazonian forests (Killeen et al. 2007; Steininger et al. 2001) and have received attention from the Kyoto protocol for carbon storage in attempts to reduce carbon emissions and combat global warming (Killeen et al. 2007). Additionally, the department of Santa Cruz in the past two decades has experienced increased rates of deforestation due to corporate agriculture for soybean production for export to Asia (Steininger et al. 2001; Kaimowitz et al. 1999) bringing Bolivia into the deforestation spotlight.

In previous studies (Steininger et al. 2001; Killeen et al. 2007), only temporal trends of deforestation rates in Bolivia are highlighted, without much attention to the spatial patterns of land cover change, especially in Pando. Previous work on deforestation rates and extents in Bolivia was focused on the more populated areas in the lowlands of Santa Cruz, La Paz, and Cochabamba (Steininger et al. 2001; Killeen et al. 2007). Although deforestation rates for the northern departments were reported, little is known about the spatial extents and configurations of deforestation, particularly with respect to roads and population centers. There is the need of focal studies to better understand the nature and extents of deforestation in Pando.

As shown in Figure 3-5 results for the temporal rates and amounts of deforestation in Pando generally match those previously reported for Pando (Killeen et al. 2007; Wachholtz et al. 2006; Rojas et al. 2003; Steininger et al. 2001; CUMAT 1992) although there are some discrepancies in deforestation rates for certain periods. Notable exceptions include the following.

Deforestation rates from Killeen et al. (2007) for the periods 1987-1991 and 1992-2000, over- and under-estimated, respectively, ours. The annual deforestation rate reported by the Wachholtz et al. (2006) are about half of the annual rate for the 2000s. Both Rojas et al. (2003) and Steininger et al. (2001) report slightly higher (about double) rate percentages for 1993-2000, and 1984-2000.

In looking at the overall landscape, the amount of forest clearing from 1986 to 2005 in Pando is minimal, from 96% to 94.5% (an area of 886.43 km^2), and has only increased recently. The spatial locations and patterns, however, are very interesting. Analysis of deforestation extents and patterns in 50 km sections of the road corridor from Cobija to Sena (Figure 3-8) showed larger clearings for stable non-forest (i.e., pasture) along the Cobija-Porvenir road, east and west of Porvenir as evidenced by larger mean patch sizes in this section. As we go further from Porvenir, MPS for stable non-forest decreases as the lateral extent (i.e., buffer distance) decreases creating long, narrow patches along the road about one-quarter to one-third kilometer in width. The more isolated patches of transitional deforestation and reforestation tend to be the dominant pattern on the landscape in the 50 to 150 km sections, although relatively speaking they do not comprise a great area. These sections contain a number of colonist communities, in which they may have isolated patches of *chacos*, or land cleared for personal agriculture. In the last section (200 to 250 km) we see a large cluster of clearings persistent through time around the community of Conquista, which contain large clearings used for pasture thus inflating the MPS for this area, particularly close to the road (within one kilometer). Interestingly, this area has experienced considerable regrowth observed in the more recent images from 2000 and 2005.

Rapid reforestation detected with the trajectory images occurs on *chacos* after the first year of clearing before the burning season in September. Regrowth of vegetation occurs very rapidly,

even in the dry season when images were collected, and can appear as reforestation due to high reflectance in the near and mid infrared bands. This vegetation regrowth, called *barbecho*, provides a challenge to the classification process as the amount of regrowth seen in five years, the time between image acquisition, is substantial enough to alter the reflectance response to spectrally appear as forest but is structurally distinct from mature forest. In field verification proves difficult as the structure of the *barbecho* is complex with rapid growth of emergent tree species and canopy species, but the density is not sufficient to be classified as secondary forest.

Compared to other Amazonian lowland areas, the percentage of remaining forest in Pando is high and there are low rates of deforestation. Pando has considerably much higher forest cover (about 95% in 2005, Table 3-3) compared to results reported by Imbernon and Branthomme (2001) for similar areas in western Amazon - 61% and 74% remaining forest cover for Yurimaguas and Pulcallpa, Peru in 1996, and 50% and 65% forest cover remained in 1996 in Theobroma, Rhodonia and Pedro Peixoto, Acre, Brazil. Along similar trends, Etter et al. (2006) calculated 30% loss of lowland forests by 1998 for areas in the Caribbean regions of Colombia.

More on par with the rates and trends of deforestation we see in Pando are other studies in the Amazon fringe outside of the Brazilian Amazon. In the Colombian Amazon between 1985 and 2001 Armenteras et al. (2006) reported annual deforestation rates were between 0.97 to 3.73% in high population areas and less than 0.31 to 0.01% in relatively unpopulated areas of indigenous communities. Elsewhere in the southwestern Amazon, deforestation rates of 2.4% yr^{-1} (1986-91) and 1.4% yr^{-1} (1991-97) were measured within eight kilometers of the trans-Peruvian Interoceanic highway (Naughton-Treves 2004). These rates and trends are higher, except for the Armenteras et al. (2006) in unpopulated areas, than those for Pando during the similar time periods. The low deforestation rates and high percentage remaining forest are due to relative

remoteness of the area, low historic population density and growth, and restricted access into the interior of Pando.

Forest Fragmentation Patterns

Our results show that dominant patterns of land cover change in Pando follow road networks. The patterns of stable forest and non-forest metrics exhibit distinct scaling patterns along the Cobija-Sena road in perpendicular fashion along with a distinct longitudinal gradient leaving Cobija traveling towards Sena (Figure 3-8). Not surprisingly forest patches increase with size away from the road in longitudinal and perpendicular directions. Furthest along the road from Cobija forest patches become long and linear in shape with the majority of landscape being dominated by large forest patches constituting a matrix. Non forest patches or cleared areas are highly aggregated along the road between Cobija and Porvenir, and west and east of Porvenir. These pasture areas comprise large parcels of land devoid of any intact forest cover. Similarly, large non-forest (i.e., agriculture or crops) occurred along roads with the core forest remaining intact at farther from roads (Imbernon and Branthomme 2001). This is parallel to the situation seen in Pando. As distance increases along the road from Porvenir towards Puerto Rico, these consolidated patches diminish in number and size becoming long and narrow pastures of no more than one-half a kilometer in width. Further, perpendicularly from the road non-forest patches become more isolated in nature accessible only by paths and trails (Figure 3-8).

The patterns of fragmentation resulting from infrastructure development in frontier areas are linked directly to scale and the type of road building activates in the landscape (Arima et al. 2005). The fragmentation of Pando's forests along road networks and near urban areas follows similar patterns as those found in other parts of the Amazon. Oliveira Filho and Metzger (2006) reported in Mato Grosso, Brasil that independent settlements expanded in fishbone patterns and caused greater landscape fragmentation than large properties. Etter et al. (2006) identified large

proportions of agricultural and grazing lands within ten kilometers of roads and agricultural clearings in colonist areas in the Amazon and Pacific regions of Colombia. Cumming (2003) found the strongest effects of roads on mean patch sizes below 150m and forest patches decreased just 13 km from the average urban center. By comparison, within 65 km of Cobija most road effects are observed within 3 km while at greater distances, road effects decrease to less than 1 km. Additionally, spatially intact forest with large MPS is seen well under the 13 km threshold Cumming (2003) reports. In the rural areas of Pando deforestation is constrained along the road, with minimal fragmentation, and in isolated patches in a predominately forest matrix. This is similar to Imbernon and Branthomme (2001) who found relatively homogenous patches of deforestation along towns in Yuramangus, Peru and along roads in Pucullpa, Peru with patchy clearings at distance from both.

Compared to the widespread deforestation and fragmentation associated with "fishbone" patterns in Brazil (Lambin et al. 2003) Pando may be in the early stages of the evolution of deforestation and fragmentation conditions. In the rural areas of Pando outside of the Cobija and Porvenir corridor (Figure 3-8), deforestation occurs parallel to the road, but the classic "fishbone" pattern may not have evolved yet due to the lack of major secondary roads and population centers. However, the "spine" of deforestation along the road already exists near Puerto Rico and other communities. As advertised by the departmental government of Pando, paving of the Porvenir-Sena road is planned, but the timing is unknown (Figure 3-8). Other road improvement projects are underway towards Extrema and, possibly, Chive on the Madre de Dios River, and towards Bolpebra near the tri-national border with Peru and Brazil (Figure 3-1). Bridge construction was completed in May 2008 to span the Rio Orthon in Puerto Rico, about 180 km from Cobija, facilitating easier access to Sena and to Riberalta. These projects will allow

more rapid accessibility to the more remote parts of Pando. After the planned paving of the road from Porvenir to El Sena, deforestation is likely to increase given the increased access to more distant areas and communities towards El Sena. Isolated population centers of Puerto Rico, Conquista, and El Sena (Figure 3-8) may gain population serving as nodes in the transportation network. The improvement of existing secondary roads and construction of new secondary roads will increase ease of access to the interior of the large forest patches. This access potentially will allow for increased forest clearing.

Conclusions

This work highlights the patterns of land cover change in Pando, northern Bolivia as a last frontier of relatively intact forest for the lowland tropics in Bolivia. Deforestation is clustered for all years around the Cobija-Porvenir corridor with large tracts of deforested areas for pasture here. As of 2005 94% of Pando's land cover was classified as forest. The rates of deforestation from 1986 to 2005 are less than one-tenth of one percent per year, which is very small compared to Santa Cruz, one of the most deforested departments in Bolivia.

From an applied standpoint of remote sensing, this work highlights the extents and rates of land cover change in one of the important non-Brazilian Amazonian fringe areas. With much of the scientific attention focused on deforestation in the Brazilian Amazon, it is easy to overlook the surrounding countries like Bolivia that contain important diversity of flora and fauna.

As seen in previous works in the Amazon (Etter et al. 2006; Arima et al. 2005; Imbernon and Branthomme 2001), deforestation increases with increased accessibility and improved infrastructure conditions. From these results one could extrapolate that in Pando, after competition of major infrastructure improvement projects, we would expect to see increased deforestation along these transportation corridors. As byproducts of primary road improvements,

secondary roads would increases access in the forest, allowing for improved access to the forest interior facilitating more deforestation.

Future work could look at the increase in deforestation along the Cobija-Sena road as the paving of this road progresses. An agent-based modeling application including key social and economic variables would be able better explain deforestation rates patterns due to infrastructure improvements and population growth.

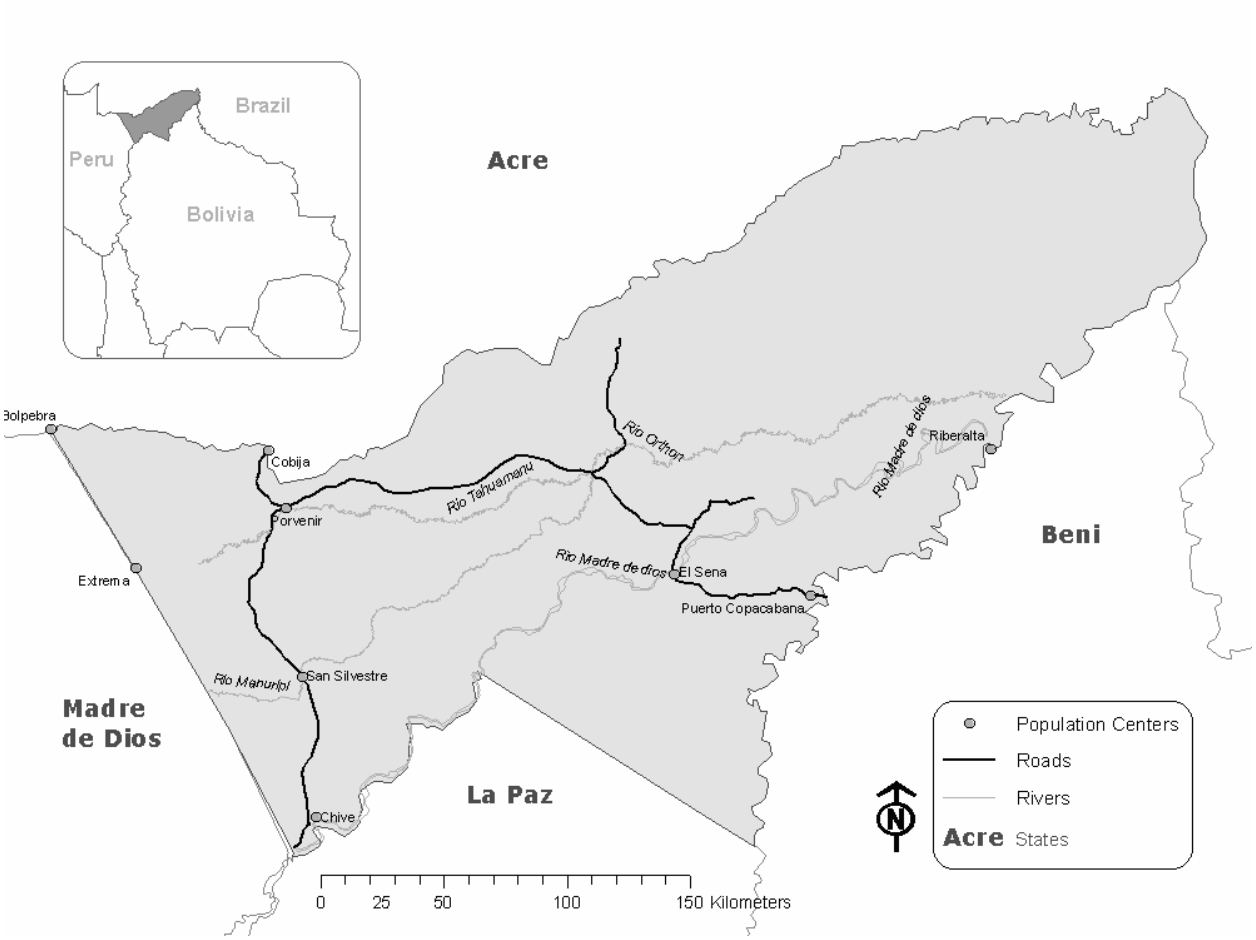

Figure 3-1. Study area, major roads, population centers, and surrounding geographies

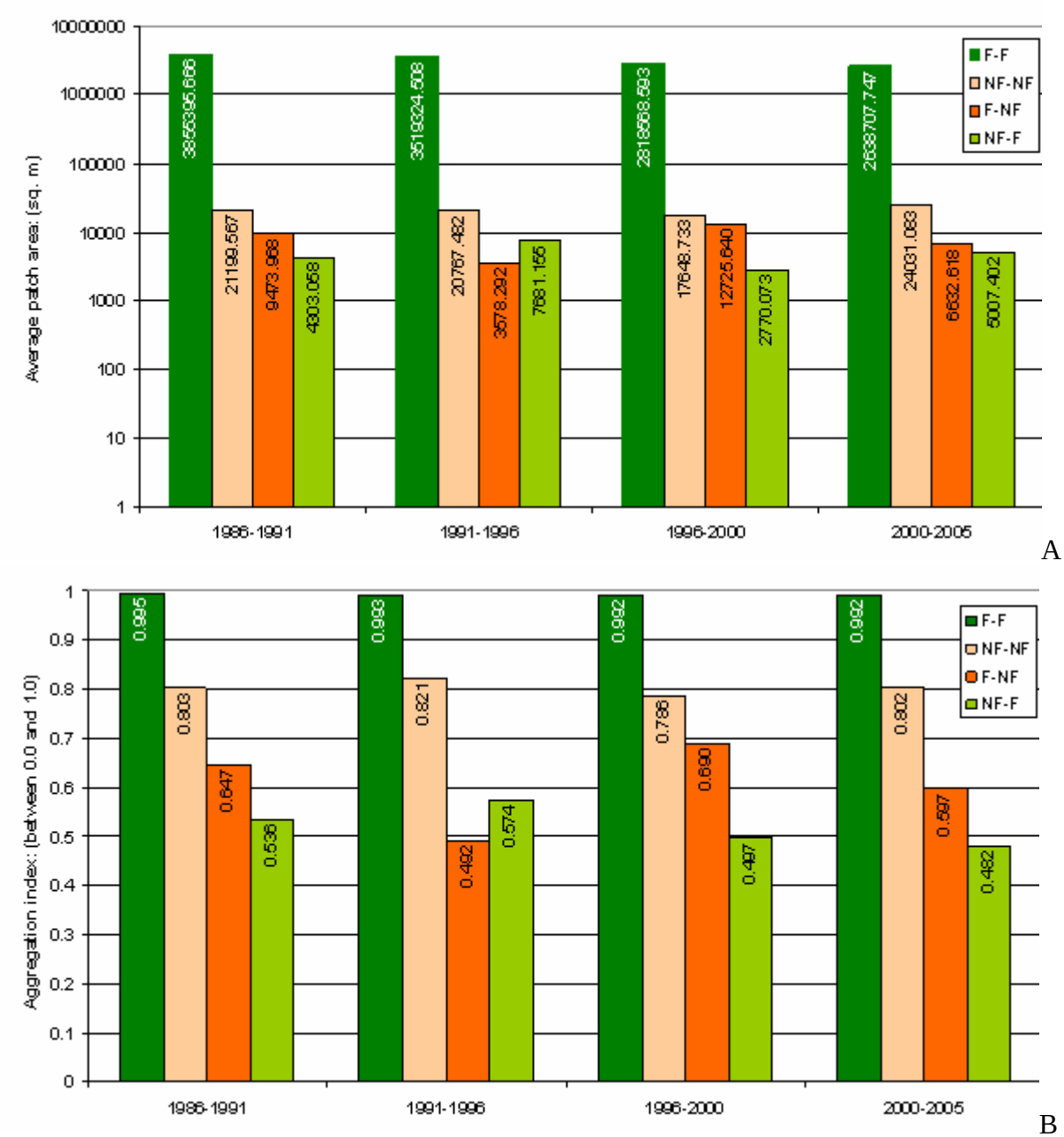

Figure 3-2. Landscape patch size metrics for trajectory images at the Pando extent. A) Mean patch size. B). Aggregation index. Classes codes are as follows: (F-F) stable forest, (F-NF) deforestation, (NF-F) reforestation, and (NF-NF) stable non-forest.

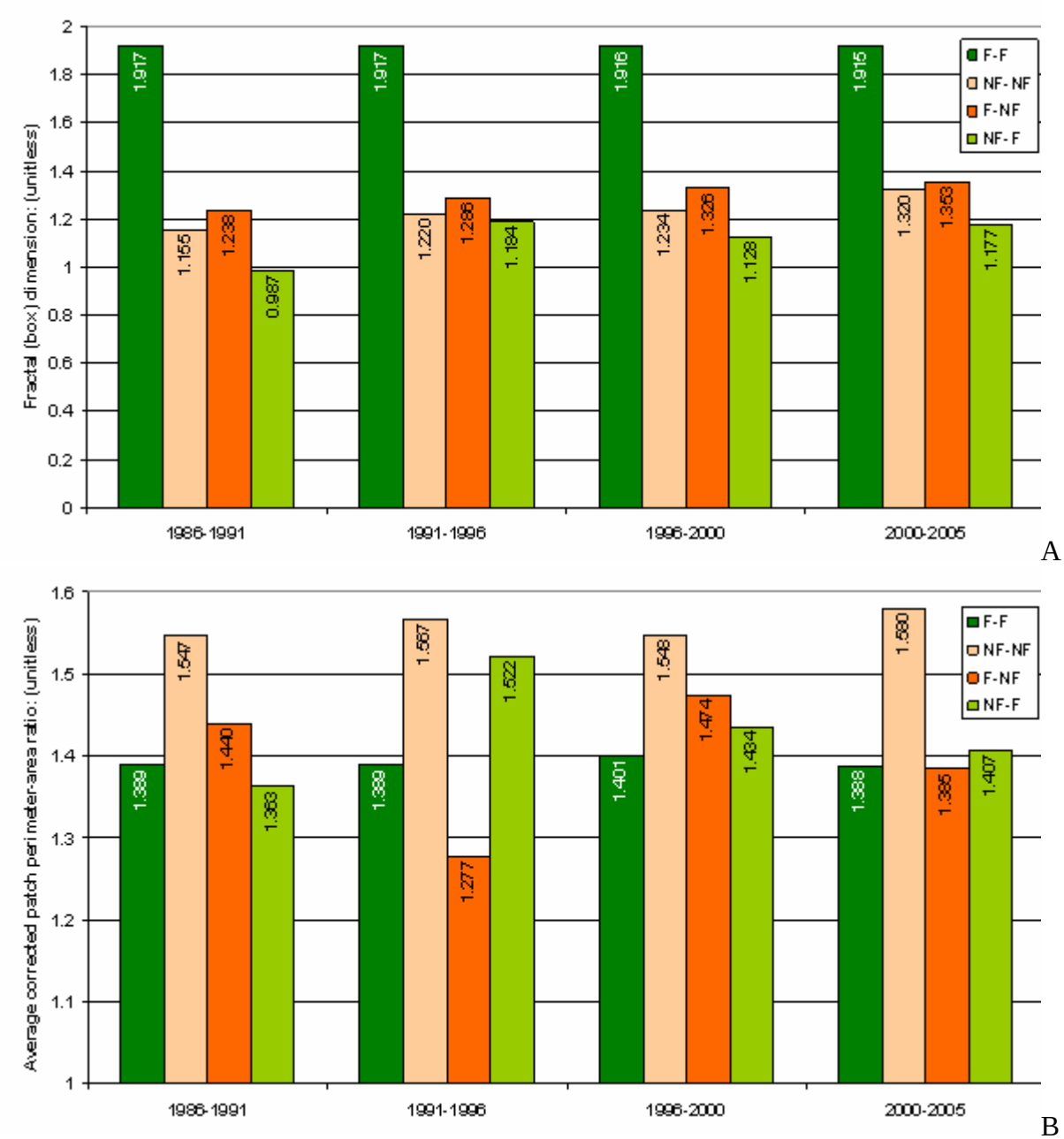

Figure 3-3. Landscape patch shape metrics for trajectory images at the Pando extent. A) Fractal dimension. B) aggregation index. Classes codes are as follows: (F-F) stable forest, (F-NF) deforestation, (NF-F) reforestation, and (NF-NF) stable non-forest.

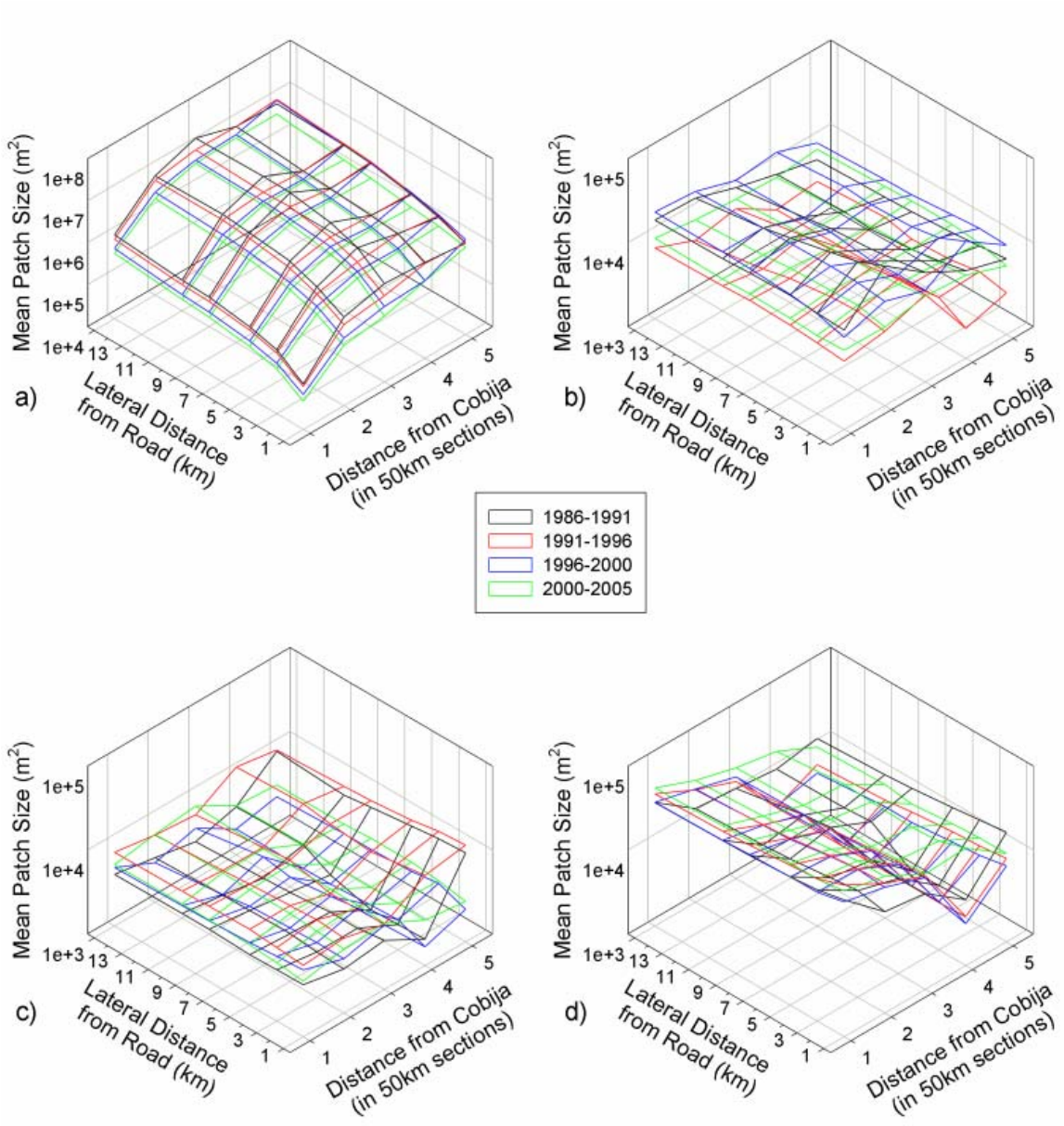

Figure 3-4. Temporal changes in mean patch size metrics for multi-distance road buffer and distance from Cobija along road. Letters refer to the following classes: a) stable forest (F-F), b) deforestation (F-NF), c) reforestation (NF-F), and d) stable non-forest (NF-NF).

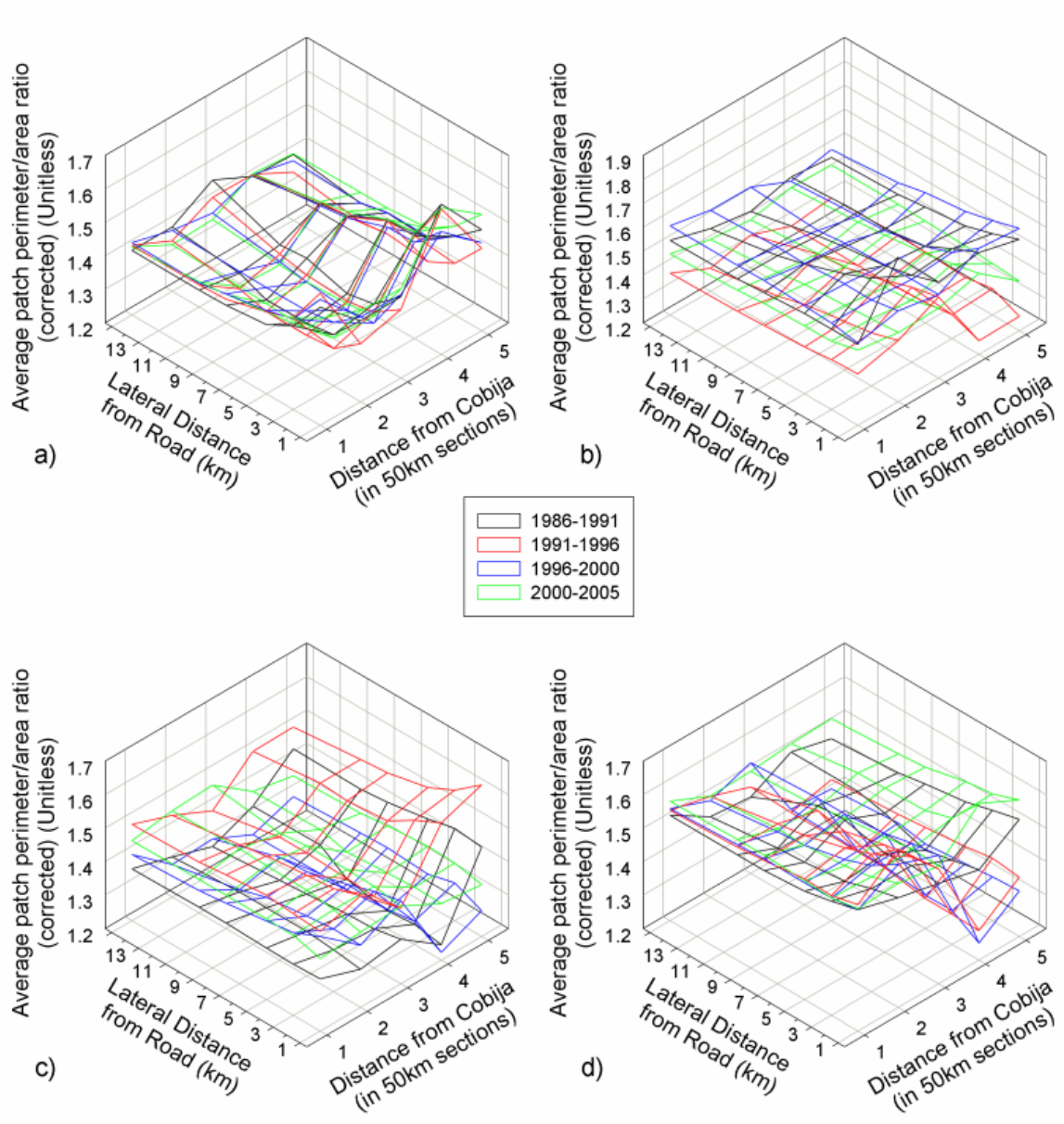

Figure 3-5. Temporal changes in corrected patch perimeter-area metrics for multi-distance road buffer and distance from Cobija along road. Letters refer to the following classes: a) stable forest (F-F), b) deforestation (F-NF), c) reforestation (NF-F), and d) stable non-forest (NF-NF).

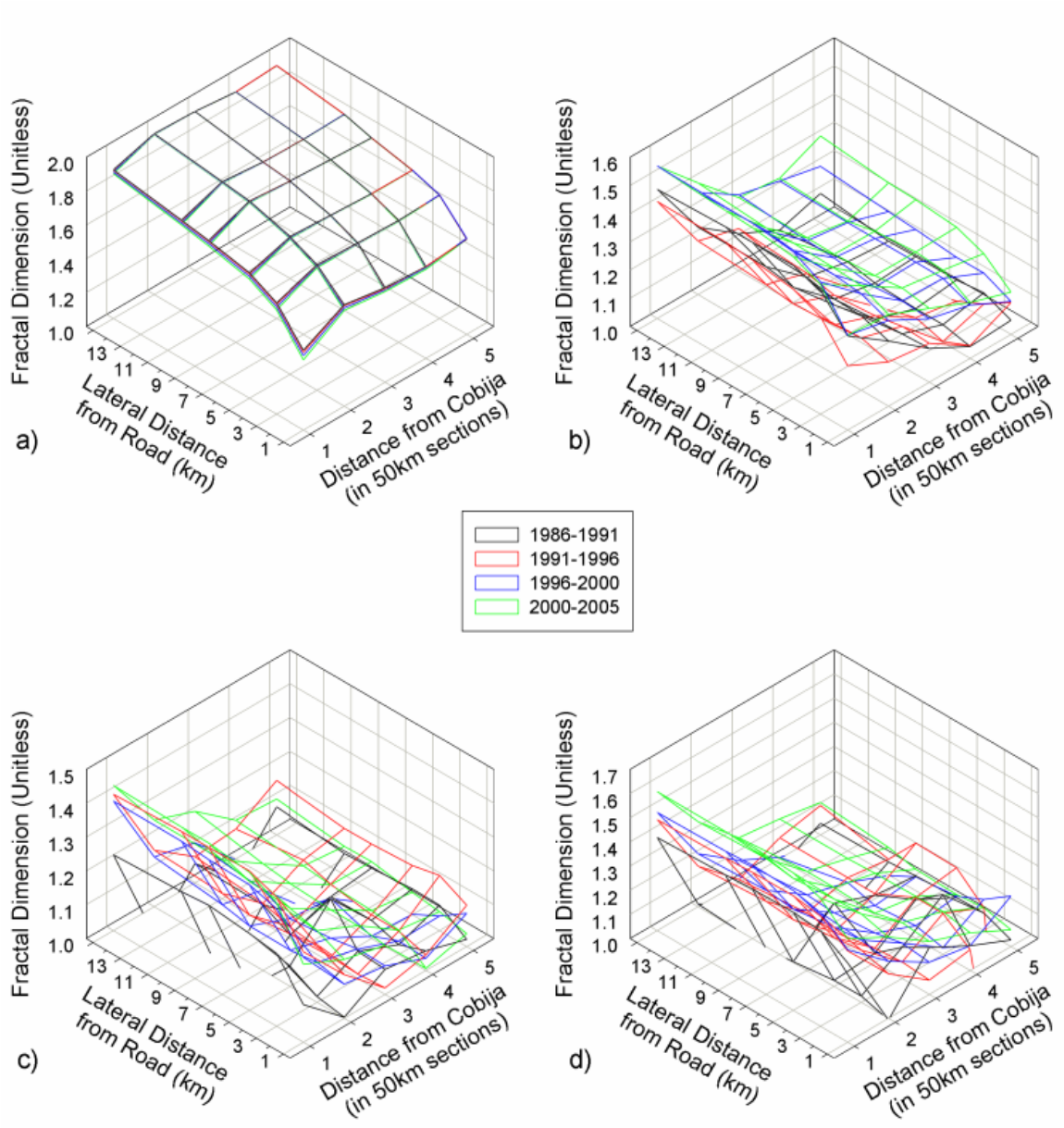

Figure 3-6. Temporal changes in fractal dimension metrics for multi-distance road buffer and distance from Cobija along road. Letters refer to the following classes: a) stable forest (F-F), b) deforestation (F-NF), c) reforestation (NF-F), and d) stable non-forest (NF-NF).

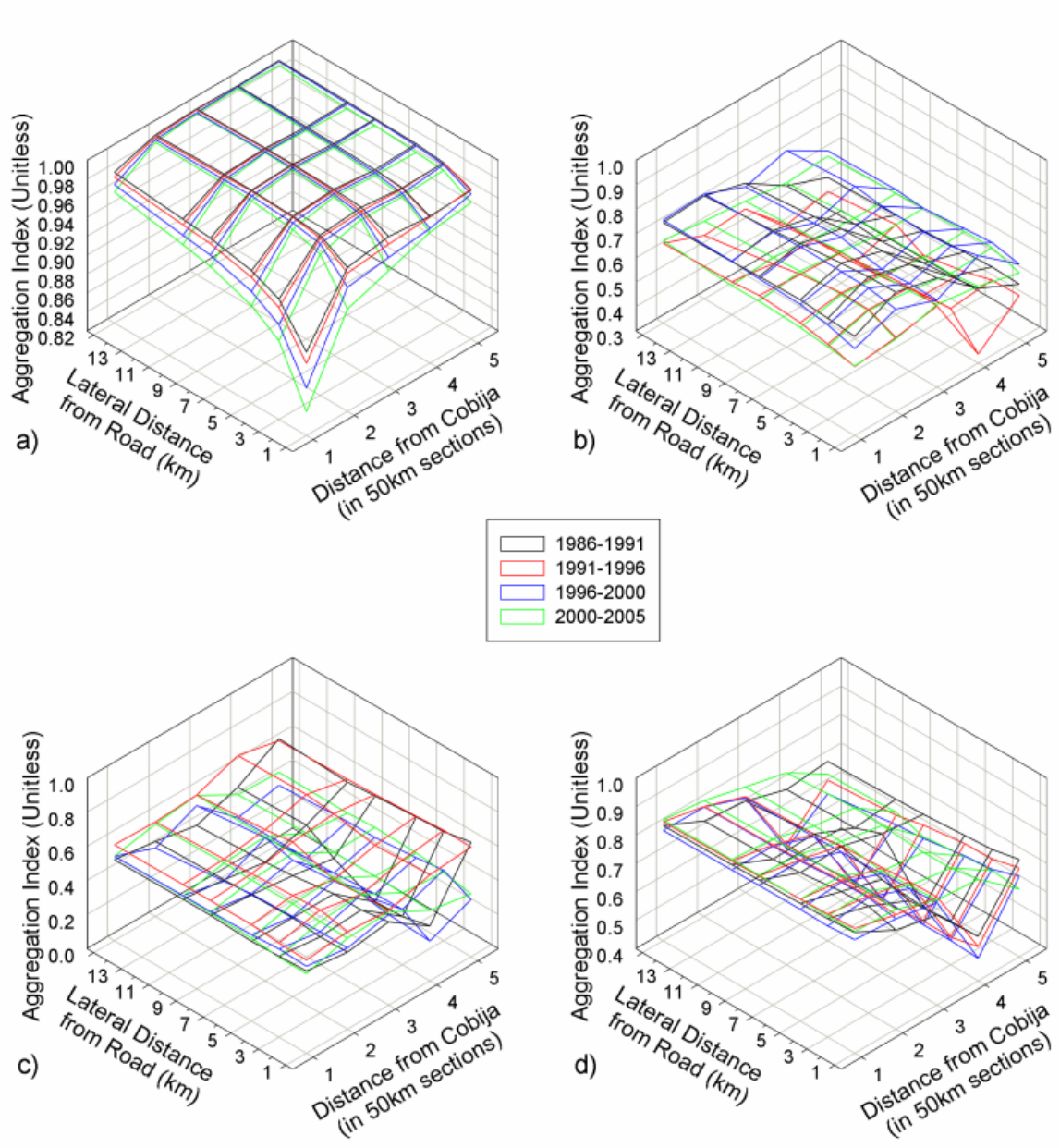

Figure 3-7. Temporal changes in aggregation index metrics for multi-distance road buffer and distance from Cobija along road. Letters refer to the following classes: a) stable forest (F-F), b) deforestation (F-NF), c) reforestation (NF-F), and d) stable non-forest (NF-NF).

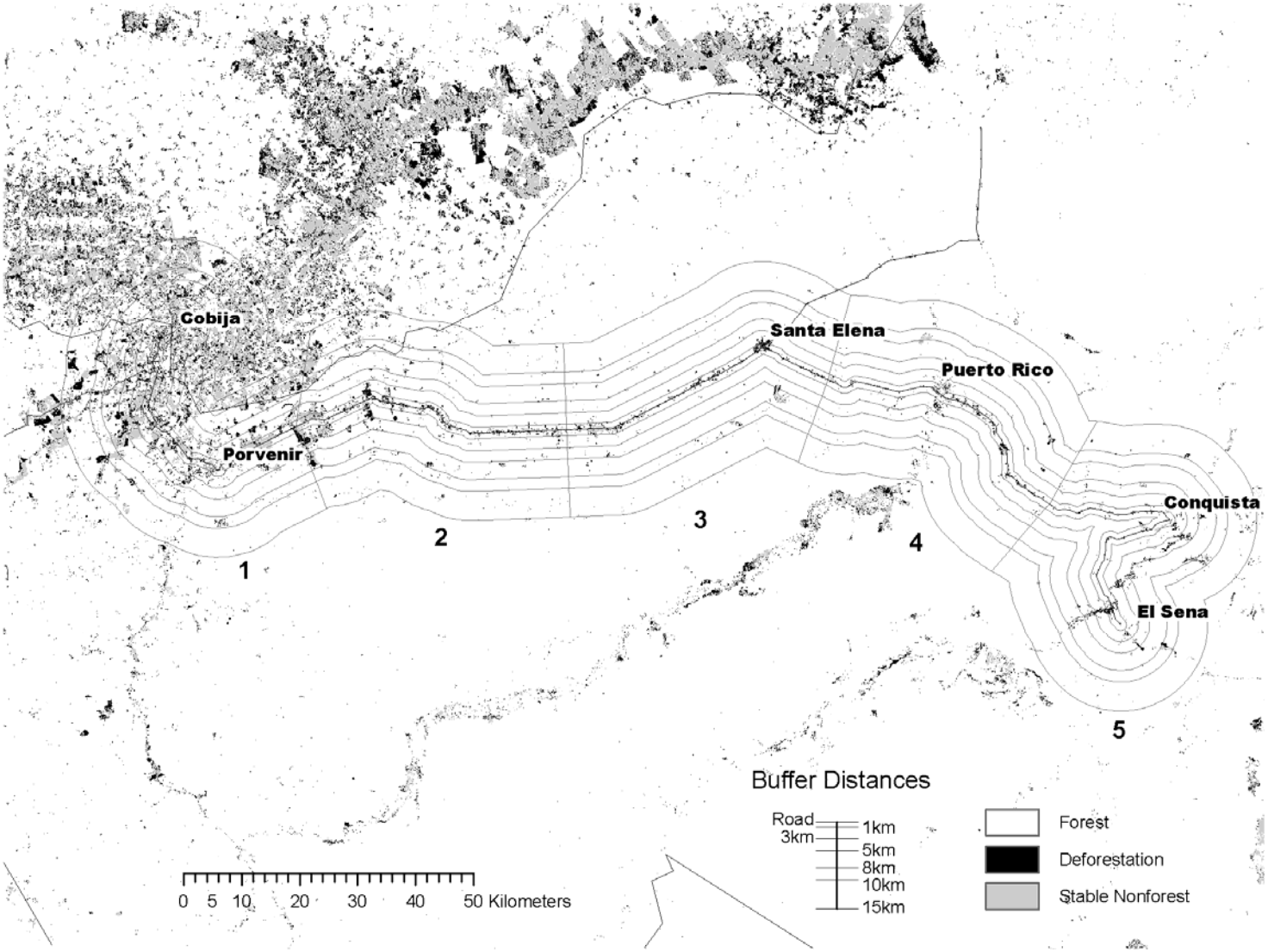

Figure 3-8. Fragmentation and deforestation by distance from road and from Cobija between 2000 and 2005. The numbers correspond to the number of 50km sections from Cobija heading towards El Sena. As represented on this map, Cobija and El Sena are exactly 250km apart, yielding five sections of 50km each.

Table 3-1. Accuracy results for classification rules developed using Compumine

Date	Number of rules	Accuracy (%)	Total AUC	Actual class	Predicted precision	Predicted recall	Predicted AUC	Predicted class 1	Predicted class 2	Predicted class 3
1986	6	99.423	1.000	1	1.000	1.000	1.000	363	0	0
				2	1.000	0.958	1.000	0	69	3
				3	0.966	1.000	1.000	0	0	85
1991	11	98.783	1.000	1	1.000	1.000	1.000	256	0	0
				2	0.925	0.980	0.999	0	49	1
				3	0.990	0.962	1.000	0	4	101
1996	16	98.067	0.999	1	0.974	0.933	0.998	112	0	8
				2	1.000	1.000	1.000	0	350	0
				3	0.923	0.970	0.998	3	0	96
2000	12	99.015	1.000	1	0.998	0.993	1.000	419	3	0
				2	0.966	0.966	0.999	1	84	2
				3	0.980	1.000	1.000	0	0	100
2005	8	99.832	0.999	1	1.000	1.000	1.000	358	0	0
				2	0.990	1.000	0.999	0	100	0
				3	1.000	0.993	0.999	0	1	135

Table 3-2. Classification accuracies for 2005 classification images and 2000-2005 trajectory image. Classes codes are as follows: (F-F) stable forest, (F-NF) deforestation, (NF-F) reforestation, and (NF-NF) stable non-forest.

Year	Overall accuracy (%)	Overall kappa	Class name	Reference totals	Classified totals	Number correct	Producers accuracy (%)	Users accuracy (%)	Kappa
2005	87.85	0.6762	F	33	55	33	100.00	60.00	0.511
			NF	148	126	126	85.14	100.00	1.000
2000	96.96	0.9392	F	145	148	142	97.93	95.95	0.921
			NF	151	148	145	96.03	97.97	0.959
2005	97.96	0.9592	F	144	148	143	99.31	96.62	0.934
			NF	150	146	145	96.67	99.32	0.986
2000-2005	82.01	0.7592	F-F	179	144	144	80.45	100.00	1.000
			F-NF	136	144	118	86.76	81.94	0.763
			NF-F	74	132	73	98.65	55.30	0.486
			NF-NF	178	147	130	73.03	88.44	0.831

Table 3-3. Absolute values and percentages of forest and non-forest in Pando

		Hectares	Area (Sq. km.)	Area (%)
1986	Forest	5,405,403	54,054.029	95.96
	Non-Forest	21,338	213.380	0.38
1991	Forest	5,387,568	53,875.679	95.64
	Non-Forest	39,167	391.667	0.70
1996	Forest	5,384,200	53,842.001	95.58
	Non-Forest	42,912	429.116	0.76
2000	Forest	5,353,909	53,539.088	95.04
	Non-Forest	72,832	728.321	1.29
2005	Forest	5,325,250	53,252.504	94.53
	Non-Forest	101,861	1,018.613	1.81

Table 3-4. Percentages of forest and non-forest, and rates of deforestation and reforestation for Pando. Classes codes are as follows: (F-F) stable forest, (F-NF) deforestation, (NF-F) reforestation, and (NF-NF) stable non-forest.

Date pair	F-F(%)	F-NF(%)	NF-F(%)	NF-NF(%)	F-NF rate(%)	NF-F rate(%)
1986-1991	95.52	0.43	0.12	0.26	0.07	0.02
1991-1996	95.21	0.44	0.37	0.33	0.07	0.06
1996-2000	94.71	0.87	0.34	0.42	0.17	0.06
2000-2005	94.13	0.91	0.40	0.90	0.15	0.07
1986-2005	94.42	1.54	0.11	0.27	0.08	0.02

Table 3-5. Rates of deforestation and extents of forest and non-forest from other research conducted in Pando, Bolivia

Source	Data source	Date of forest cover estimate	Forest cover (ha)	Non-forest cover (ha)	Total area (ha)	Total forest cleared (ha)	Deforestation rate (ha yr-1)	Deforestation rate (% yr-1)
CUMUT (1992)	Unknown	pre-1985		160,000				
		1985-1990	6,311,000		6,471,000		4,900	0.08
Steininger et al. (2001)	Landsat MSS and TM	1984-1987	5,707,000	191,800	6,133,100	61,500	6,745	0.11
		1992-1994	5,509,800	389,000	6,133,100	135,700		
Rojas et al. (2003)	Landsat ETM+	1993-2000			5,370,825	49,352	6,169	0.11
Superintendencia Forestal (2006)	MODIS MOD13Q1	2004				27,056		0.9
		2005				29,420		
Killeen et al. (2007)	Landsat TM and ETM+	<1976					700	
		1976-1986					1,200	
		1987-1991					9,600	
		1992-2000					3,000	
		2001-2004	5,877,000				8,800	0.15
Current study	Landsat TM and ETM+	1986-1991	5,381,361	14,685	5,396,046	24,475	4,079	0.07
		1991-1996	5,363,451	18,336	5,381,786	24,567	4,095	0.07
		1996-2000	5,335,268	23,826	5,359,094	49,006	9,801	0.17
		2000-2005	5,303,011	50,516	5,353,527	51,334	8,556	0.15

CHAPTER 4
CHANGING DISCHARGE CONTRIBUTIONS TO THE RÍO GRANDE DE TÁRCOLES

Introduction

Water quantity issues are of increasing global concern. Many countries in Central America rely on hydroelectric power generation and on surface water withdrawals for agricultural and water supply. Costa Rica generates more than 80% of its national power from hydroelectricity and constructed more than 30 dams in the 1990s (Anderson et al. 2006). Decreased flow from major tributaries would imperil reliable power generation, diminish surficial and groundwater storage accumulated during the rainy season and create water quality issues for municipal and agricultural sectors. In the Río Grande de Tárcoles groundwater comprises 6% of total water used for industrial and urban purposes, and provides 60% of all water for agricultural irrigation (Blomquist et al. 2005). As such reduced water supply coupled with anthropogenic alteration of the surface hydrologic cycle has critical implications for water availability. The conceptual framework of this research is that altered vegetated and urban land cover conditions modify hillslope hydrology and produce the non-linear watershed responses, impacting water supply.

Tropical Hillslope Hydrology: Undisturbed Conditions

A watersheds' hydrological response to rainfall depends on the interplay between climatic, geological and land use/land cover. Additional important characteristics include the hydraulic conductivity of the soil at different depths, rainfall intensity and duration, and slope morphology (Dunne 1978). Generally speaking, infiltration capacities of undisturbed forest soils are sufficient to accommodate most rainfall intensities (Bruijnzeel 1990). Overland flow in the tropics seems spatially restricted to areas of less permeable soils, on steeper slopes, and at or near soil saturation (Bonell 1998). The three flow pathways of runoff generation; infiltration excess

Hortonian overland flow (HOF), saturation excess overland flow (SOF), and subsurface flow (SSF), have all been observed in undisturbed forests.

HOF (Horton 1933) is critical in humid areas with disturbed soils and vegetation, but is restricted temporally and spatially within a watershed. Overland flow is unlikely on mid- to upper-slopes unless a shallow impeding layer is present (Bruijnzeel 1990), occurring only on lower floodplain areas as SOF (Nortcliff and Thornes 1981). Regardless of position and land cover, during high intensity precipitation rapid runoff (HOF) likely dominates the hydrological response of a watershed. SOF generally prevails in flat bottom valleys with gentle, thinly soiled, slopes (Dunne 1978) and occurs with no obvious topographic or landscape control (Elsenbeer and Cassel 1991). SSF can contribute significantly to storm flow through unsaturated ground on deeply incised convex hillslopes with well drained, deep, and highly permeable soils (Dunne 1978). It is propagated in undisturbed forests by macro-pores and soil pipes on slopes (Bruijnzeel 2004) with high field saturated hydraulic conductivities. SSF may also prevail mainly at depth (Nortcliff and Thornes 1981) and through hollows below perched water tables (Dykes and Thornes 2000).

Tropical Hillslope Hydrology: Altered Conditions

Conversion of tropical forest may produce permanent changes in the hydrologic response of a stream (Bruijnzeel 2004) resulting from soil compaction, soil crusting and removal of organic forest litter, which, when coupled with high rainfall intensities, favors HOF in the long term (Bonell and Balek 1993). Several reviews (Bruijnzeel 1990; Bruijnzeel 2004; Bonell 1998; Bosch and Hewlett 1982) exist of the hydrologic responses to land cover change in small watersheds. Bosch and Hewlett (1982) examining experiments in 94 catchment ranging from 1 to 2500 hectares, concluded that increased water yield resulted from reduced vegetation. Similar conclusions are drawn from a review of paired catchment studies (Bonell 1998) and indicated

that more than a 20% loss of forest cover is required to appreciably increase total annual water yield. Increases in water yield are conditioned upon the spatial and temporal variability of rainfall and degree of surface disturbance.

Low saturated hydraulic conductivities associated with consolidated surfaces contribute disproportionately to storm flow responses via HOF during events of small rainfall totals and low intensities. Reduced surficial saturated hydraulic conductivity produces a greater likelihood of HOF, while reductions in subsurface saturated hydraulic conductivity may increase the frequency of non-Hortonian overland flow mechanisms (Ziegler et al. 2004). Elsenbeer (2001) posits that human disturbance diminishes subsurface saturated hydraulic conductivity, thereby disrupting subsurface hydrological pathways and enhancing the generation of non-Hortonian (i.e., return flow) overland flow on fragmented hillslopes (Ziegler et al. 2004). Land cover disturbances can further alter runoff in a non-linear manner through processes such as infiltration and evaporation.

Mesoscale Watershed Studies

Fewer land cover change studies have been conducted in mesoscale watersheds (Bonell 1999; Bruijnzeel 2004). To disentangle the effects of changing land cover and climate forcing, statistical and hydrologic modeling methods are required (Refsgaard et al. 1989). Lorup et al. (1998), employing this combination, detected no change in annual runoff in six semi-arid watersheds (200-1000 km^2) in Zimbabwe, even though population density and urban areas increased. A 78% increase in runoff observed in the Comet River watershed (16,440 km^2) Central Queensland, Australia, (Siriwardena et al. 2006) following forest clearing and conversion to grasses and cropland was attributed partially to an 8.4% increase in rainfall. Applications of an annual water balance model and a simple conceptual daily rainfall-runoff model suggested that showed forest clearing increased runoff by 58% and 40%, respectively. Despite a decrease in

forest cover of 80% to 30% from 1957 to 1995 in the 12,100km^2 Nam Pong watershed in northeast Thailand, Wilk et al. (2001) observed no statistically significant differences in precipitation, discharge and evapotranspiration. However, despite no significant changes in precipitation, Costa et al. (2003) linked significant changes in mean annual and high-flow season discharge on the Tocantins River to a 20% increase in agricultural lands from 1960 to 1995.

Only two dynamic simulation hydrologic modeling studies (Colby 2001) and (van Loon and Troch 2002) have been carried out in Costa Rica. and neither used a physically-based, spatially explicit hydrologic model to assess the impacts of changing land cover. Krishnaswamy et al. (2001) used dynamic linear regression modeling investigated land cover and hydro-climatic effects on stream flow in the Terraba watershed (4767 km^2), primarily focused on sediment production. In this region of intense human alteration and high climate variability further research is needed on climate and land cover impacts on surface hydrology.

Research Justification

The balance of contributions of the two major tributaries, Rios Grande de San Ramón and Virilla, to the Río Grande de Tárcoles, Costa Rica appears to have changed around 1975. The change could result from the non-linearity of basin runoff responses to land cover change, a change of climate forcing, or both. An applied, multifaceted approach of simulation modeling and statistical analysis is employed to investigate these potential causes for the observed changes in discharge.

- **Objective 1:** Determine the significance of changes in discharges and precipitation.
- **Objective 2:** Construct a hydrologic model for the two sub basins for long term simulations of potential non-linear responses of discharge contribution conditioned on dominant land cover conditions.
- **Objective 3:** Assess the potential of climate variability as cause of discharge changes.

- **Hypothesis 1:** Precipitation input to the Rio Virilla sub basin has increased after 1975 forcing a greater contribution to discharge in the Rio Grande de Tarcóles.
- **Hypothesis 2:** Differences in the proportions of vegetated versus urban land covers caused the sub basins to act as non-linear amplifiers of precipitation, through differences in soil moisture and evapotranspiration fluxes.
- **Hypothesis 3:** Differential spatial responses to precipitation influenced by El Niño Southern Oscillation (ENSO) and Atlantic sea surface temperatures result in distinct discharge responses even though the basins are adjacent.

Study Site

The Rio Grande de Tárcoles watershed (1745 km^2) (Figure 4-1) lies in Costa Rica's central tectonic depression flanked to the north by the northwest-southeast trending Cordillera Central and to the south by the Cordillera Talamanca. The watershed encompasses much of the valley and contains most of the metropolitan population of Costa Rica. Two major sub-basins, the Rio Grande de San Ramón (916 km^2) and the Rio Virilla (829 km^2), comprise the Tárcoles watershed. The area is topographically varied and rugged, with steep slopes geomorphologically dominated by ancient volcanic pyroclastic flows and lacustrine depositions. Alfisols, entisols, inceptisoles, ultisols, and vertisols are the primary soil orders in the watershed (Centro Científico Tropical (CCT) 1989) constituted primarily of volcanically-derived clays. Land cover differences between the Grande de San Ramon and Virilla are marked. The former is dominantly forested, pastoral and agricultural lands (approximately 98%) with less than 2% urban areas (Ministerio de Agricultura y Ganadería (MAG) 1992). By contrast the Gran Metropolitan urban area of Costa Rica occupies about 15% of the Rio Virilla sub-basin and agriculture is the dominate vegetated land cover class (about 33%).

Due to Costa Rica's location between the Caribbean and the Pacific, precipitation generating mechanisms are complex (Waylen et al. 1998). The northeast trade winds bring ample precipitation to the Caribbean coast, leaving the Pacific side in rain shadow during the dry season

(November-April) except for the southeastern corner of the Rio Virilla sub-basin, which is exposed to a wind gap in the Cordillera Central. As the Inter-Tropical Convergence Zone (ITCZ) of the Eastern Pacific (Hastenrath 2002) migrates northward through the boreal summer, convective precipitation falls over much of the Pacific coast and montane areas from May to November. Low flows during the dry season are sustained by depletion of groundwater and soil water storage from the previous rainy season. Precipitation at the onset of wet season begins to replenish the stores. July and August witness the veranillos, a temporary dry period caused by intensification of Northeast trade winds This seasonal reduction is a prominent feature of the precipitation climatology throughout Central America (Magana et al. 1999). During the post-veranillos months of September and October soil moisture stores are saturated or near saturated producing high runoff regardless of precipitation totals and intensity. The southward migration of the ITCZ heralds the dry season in November, initiating the release of groundwater stores and

Methods

SWAT Model

The Soil and Water Assessment Tool (SWAT) (Arnold et al. 1998; Arnold and Fohrer 2005) is a semi-distributed, process based, computer hydrologic model that simulates the land based hydrologic cycle using a water balance. Complex, mesoscale watersheds are partitioned into hydrologic response units (HRUs) comprised of unique land cover and soil combinations. Hydro-climatic inputs drive the relative importance of each hydrologic components in SWAT. After canopy storage and interception are simulated excess precipitation is (1) passed to the land surface to be infiltrated with the potential for redistribution within the soil, (2) moved out of a HRU by subsurface lateral flow, or (3) moved over the land surface as surface runoff. Flood water accumulations are calculated for main channels and routed, preserving channel mass flow, through the stream network and reservoirs, ponds or lakes to the watershed outlet. SWAT has

been primarily applied in the United States and Europe with few applications in tropical countries (e.g. Kenya and India) (Arnold and Fohrer 2005).

Data

Daily discharge data were obtained from the Costa Rican Institute of Electricity for five gauging locations within the watershed. The length of record for the gauges on the Rio Poas at Tacares, the Rio Virilla at San Miguel and the Rio Tarcoles at Balsa spanned 1964 to 1986. Daily discharge data for the Tarcoles and Virilla were aggregated to monthly and annual time scales, and estimates of monthly discharge for the Rio Grande de San Ramón, which is currently ungauged, obtained by subtracting the discharge of the Virilla (immediately above the confluence) from that of the Tarcoles (below confluence). Data from the remaining gauges were aggregated similarly and employed as inputs for the sensitivity analysis and autocalibration in the SWAT model.

Precipitation data were obtained from the Costa Rican Institute of Electricity and the Ministry of Environment and Energy (1988). Sixty seven stations had periods of monthly totals from 1960 to 1986, of varying lengths, of these only three report complete records. Nine stations had daily records of varying lengths (1964 - 1986). Missing daily and monthly precipitation data were filled used inverse distance weighted spatial interpolation to produce a temporally continuous record. From the interpolated monthly records, seasonal and annual time series were generated for each station. For input into the SWAT model, two random sampling designs, one for the input precipitation and the other for the stochastic weather generation, were generated based on the daily interpolations. Two sets of 30 random points, 15 in each subbasin to ensure adequate spatial representation of precipitation, were generated and the daily precipitation data extracted at each point location.

The NCEP/NCAR reanalysis program (Kalnay et al. 1996) provided surface atmospheric data at both 2 x 2 degree and 2.5 x 2.5 degree resolution and daily time steps from 1964 to 1986. Relative humidity, minimum and maximum temperatures, and insolation were extracted from global datasets and potential evapotranspiration estimates were conditioned upon mean surface temperatures and average wind speeds calculated from the U and V vector wind data.

Expanded soil properties of percentages of silt and clay, profile depth, texture, and organic content from Vasquez (1980) were related to the a GIS soils layer at 1:200,000 based on the great group classification (Centro Científico Tropical (CCT) 1989), while median bulk densities were based on soil order (Alvarado and Forsythe 2005). Additional hydraulic soil parameters of available water content, field capacity and saturated hydraulic conductivity were calculated for each great group using the pedotransfer program Rosetta (Schaap et al. 2001)

Land cover data were generated from Landsat images from 1975 (MSS 3) and 1986 (TM 4). Image preprocessing included georeferencing the MSS image to the TM image and radiometrically calibrating both images. Both images were classified using the RuleGen (Loh and Shih 1997) decision tree classifier creating five classes for forest, developed, grassland, cropland, and shrubland. Derived products included in the decision tree classification included tasseled cap transformation and local Moran's I at a spatial lag of 3 pixels. Elevation, slope, and cloud and shadow masks were also included in the classification. Classified images were resampled to 57x57 meters resolution and Manning's n values assigned to each land cover class following Bedient and Huber (1988).

HydroShed (Lehner et al. 2006) furnished elevation data at 15 arc seconds (approximately 92 x 92 meters) and yielded slope data for use in ArcSWAT Data were processed further using the ArcSWAT watershed delineation module to enforce the observed stream drainage network,

digitized from 1:50,000 scale topographic maps, onto the elevation data. In this way the delineated streams closely followed actual stream courses, resulting in better accuracy of flow length and slope. Stream channel dimensions were calculated using ArcSWAT and Manning's n roughness values were assigned following Bedient and Huber (1988).

Statistical Analysis: Change detection

The significance ($\alpha = 0.05$) of changes in annual runoff contributions from each sub-basin before and after 1975 were determined using a hypergeometric distribution (Equation 4-1), which defines the probability of drawing a sample, n, (without replacement) containing *x* successes, from a finite population, *N*, consisting of *R* successes.

$$f(x) = \frac{\binom{R}{x}\binom{N-R}{n-x}}{\binom{N}{n}} \qquad (4\text{-}1)$$

In this case *x* is the number of above (below) long-run median annual runoff (or precipitation) values before and after 1975.

Monthly flow volumes from the Rio Virilla are expressed as percentages of the combined volume observed in the Rio Grande de Tárcoles each year. Simple linear regression fit to the time series for each monthly plot indicate the presence of statistically significant trends($\alpha = 0.05$) in percentage contribution of the Rio Virilla. Comparable monthly precipitation inputs to each sub-basin are estimated via four methods; Arithmetic mean, Theissen polygons, Inverse distance weighted and Spline interpolation (Dingman 2002), employing a custom application in ArcGIS©.

Double mass curves of sub-basin input and runoff derived from each method were compared for each sub-basin and time scale using the Kolmogorov-Smirnov goodness of fit

statistic. No significant differences (alpha = 0.20) were detected between the methods at the annual and seasonal time scales, while the Arithmetic mean/Theissen polygon combination and the Inverse distance weighted/Spline combination curves tested similar at monthly scales. A representative precipitation input to each sub-basin was therefore derived as the average of the estimates from each method. Deviations of annual and monthly inputs (sub-basin volumes) from their respective long-run medians for the Virilla and Grande de San Ramón were analyzed in a similar fashion to flows.

Statistical Analysis: Climate Variability

Monthly precipitation totals from 1959-1986 were aggregated into five seasons (JFMA, MJ, JA, SO, and ND) at all stations and expressed as standard normal deviates. These were then categorized according to the joint states (above/below median) of sea surface temperatures (SSTs) in the equatorial Pacific (ITCZ) and tropical Atlantic (Northeast trades). Composite maps of seasonal standard deviates in each of the four possible combinations of oceanic states indicate the seasonally varying importance of the Pacific and Atlantic SSTs, and their interaction, on precipitation. Spatial interpolation of composite deviates across the basins reveal any geographic patterns of such influences and any changes (Waylen and Quesada 2002).

SWAT Model Construction

Following data preprocessing, SWAT model construction proceeded using the ArcSWAT (Winchell et al. 2007) interface for ArcGIS. The interface provides for watershed delineation with outlet and stream definition; creation of hydrologic response units (HRUs); input of climatic variables; writing of input files and running of the model. Hydrologic response units define unique combinations of land cover, soils and slope, which act as the spatial control in the conversion of effective precipitation into runoff. For each land cover condition in 1975 and 1986,

61 HRUs were delineated. In addition to model construction and execution, ArcSWAT provides tools for calibration, sensitivity and uncertainty analyses.

Daily precipitation and discharge records were split into three periods for calibration, validation and simulation dependent upon the land cover conditions under which the model was executed. Under the 1975 land cover, calibration was from 1964-1970, validation, 1971-1975, and simulation, 1976-1986. Under the 1986 land cover, SWAT was calibrated from 1976-1981, validated 1982-1986, and the simulation was from 1964-1975. The first year of calibration was omitted during the evaluation of the model performance. During each calibration and validation period simulated monthly runoff was compared to observed and linear regression used to assess initial model fit with an R^2 threshold of 0.60-0.80 (Neitsch et al. 2002). More quantitative measures of OLS bisector slope (Isobe et al. 1990) and Nash-Sutcliffe efficiency metric (Nash and Sutcliffe 1970) were calculated subsequently.

The SWAT model possesses a built-in sensitivity analysis routine (Green and van Griensven 2008) employing a Latin-hypercube combined with a one-factor-at-a-time sampling. Each parameter selected following Neitsch et al. (2002), the range of parameter values and the method by which the parameter is adjusted during the sensitivity analysis are listed in Table 4-1. Given the large number of model parameters potentially adjusted during calibration, sensitivity analysis was used to identify those parameters most likely to improve model performance during automatic calibration. One thousand combinations of values of the 11 parameters were run for the respective calibration periods under each land cover condition and the model parameters ranked by sensitivity. The three least sensitive were omitted from the subsequent autocalibration.

SWAT employs the PARASOL (Parameter Solution method) autocalibration method (Green and van Griensven 2008; van Griensven and Meixner 2004) coupled with uncertainty

analysis of model parameters to improve overall model fit. PARASOL is based on the Shuffled Complex Evolution Algorithm (SCE), a global search algorithm that minimizes the sum of squares residuals between observed and simulated runoff, based on multiple model parameters and is run and evaluated following the manual calibration and sensitivity analyses. Initial autocalibration produced unreasonable results as parameters controlling runoff were preferentially selected for adjustment and unlikely ranges, consequently, only parameters controlling subsurface and groundwater flow were selected in the autocalibration step. The Virilla seemed particularly sensitive during manual calibration; therefore autocalibration was dominantly focused on improving the modeled runoffs with a more feasible set of model parameters.

SWAT also contains SUNGLASSES (Sources of Uncertainty Global Assessment using Split Samples) (van Griensven and Meixner 2004) as a means of assessing uncertainty in the model output attributable to model formulation rather than parameter uncertainty. In order to better evaluate model predictive power and prediction errors, SUNGLASSES examines the validation parameter set separate from the calibration set (van Griensven and Meixner 2004). Global optimization criterion (Chi-squared, $\alpha = 0.05$) assesses the fit between the observed and simulated runoffs. The procedure was replicated 2000 times for the simulation periods for both subbasins and land cover conditions.

Once acceptable calibration and validation results were obtained, SWAT was rerun under both land cover conditions for the simulation periods in the sub-basins thereby creating four scenarios based on combinations of pre- and post-1975 precipitation, coupled with the two different land cover conditions (Figure 4-2). Scenarios 1 and 4 actually occurred, while 2 and 3

assist in identifying the relative dominance of precipitation regime and land cover over runoff. Differences in runoff from each scenario provide the basis for the e following hypotheses.

- **H0:** Precipitation and land cover do not influence runoff (scenarios 1 and 4 not different)
- **HA1:** Land cover changed so runoff changed (scenarios 1 and 3, and 2 and 4, different)
- **HA2:** Precipitation changed so runoff changed (scenarios 1 and 2, and 3 and 4, different)

The greatest differences in simulated runoffs might be expected between scenarios 1 and 4 due to combined changes in precipitation regime and hydrologic processes affected by land cover. Large differences under the other hypotheses would implicate one particular variable as the cause of the change in runoff. Further quantitative determination of the relative importance of these controls is provided by the application of the Mann-Whitney U test of medians to the mean monthly runoff values under each scenario.

Results

Statistical Analysis

Time series (Figure 4-3) of sub basin annual runoff as a percentage of total runoff from the Tárcoles compared to sub basin area shows that, prior to 1975, neither sub basin consistently contributes greater proportional runoff than the other. In all years, except two, after 1975 the Virilla contributes a greater proportion. Test reveal statistically significant changes in the counts above/below median annual flows pre- and post-1975 in both sub basins (Figure 4-4), although the pattern is less marked in the Virilla. Regression parameters (Figure 4-5) from the monthly time series indicate a statistically significant increase in percentage contribution from the Virilla from January to August.

Annual precipitation (Figure 4-6) display similar temporal patterns; however, no significant change in annual precipitation to the Grande de San Ramón was detected at all, the opposite to the significances observed in flows. Regression applied to the monthly precipitation time series (Figure 4-7) only yields significant linear trends in March and June. The former is

one of the driest months, and the trend in the latter in the opposite to that observed in flows Small changes in sub basin inputs appear to have produce disproportionate changes in flows.

SWAT Model

The principle purpose of the SWAT in this application is to determine the causes for observed changes in runoff rather than to focus on model construction performance; however its credibility in performing the former is predicated on the latter. Nash-Sutcliffe (NS) efficiency measures and bisector slope values (Table 4-2) suggest acceptable model fits after manual calibration. Measures of fit from validation trials should be equal to, or slightly less than, those from manual calibration as witnessed in for both sub-basins under 1986 land cover. However, validation of the Rio Virilla under 1975 land cover yields an extremely low NS and all validation measures for the Rio Grande de San Ramón under earlier land cover are higher than the respective values for the manual calibration.

The sensitivity analyses identified model parameters that affected the simulation response, particularly those that could be adjusted further to improve model performance. Runoff appears most sensitive (Table 4-1) to groundwater parameters, with the runoff curve number (RCN) and Manning's n for channel flow also rated highly.

Initial experimentation with autocalibration produced unsatisfactory NS values and bisector slopes. Although the variance about the bisector slope decreased considerably for the Grande de San Ramón under the 1975 land cover the NS value decreased substantially compared to the manual calibration (Table 4-2). Specifically, the autocalibration for the Grande de San Ramón under 1975 land cover performed worse than the manual calibration (Table 4-2) and there was a general lack of consistency in response of Grande de San Ramón to autocalibration. Further support for rejection of the autocalibrated models included increase in intercept (all

scenarios) and the bisector slope (Rio Virilla, 1975 land cover) although the variance about the bisector slope was reduced consistently for each simulation.

Computational demands of the PARASOL and SUNGLASSES processes permitted 2,000 trial simulations and led to an incomplete analysis of parameter and model uncertainties, as evidenced by the lack of sampling over the parameters range, especially for the baseflow alpha coefficient (Table 4-4). However, the results do provide insight into the ranges of uncertainty for more sensitive groundwater flow parameters. Others challenges of premature termination of optimizations and convergence of parameter populations may be corrected by increasing the number of optimization simulations ten-fold. This was not a feasible option during this study.

Simulations

Figures 4-8 and 4-9 show absolute differences between simulated runoffs under the different precipitation and land cover scenarios and can best be viewed as paired scenarios; that is, runoff differences (red and green bars) resulting from the land cover scenarios be paired together, and those from precipitation (blue and yellow) be viewed separately. Regardless of subbasin, land cover or precipitation regime, the null hypothesis of no change in runoff is rejected. Sensitivities of runoff (Figure 4-8) within the Grande de San Ramón follow the hydro-climatology regime of the region (Figure 4-1). Land cover dominates runoff in the drier months and precipitation in the wetter ones. Comparing the pre- and post-75 influences of precipitation and land cover on runoff differences, equal influence is implied during January-April; however land cover prevails at the beginning of the rainy season (May and June), when soil moisture storage is at a minimum. Reduced precipitation in July and August, the Veranillos, renders little difference between simulations, however, sensitivities switch to precipitation during the height of the rainy season (September-November). These observations are consistent with those of Bruijnzeel (2004) and Bonnell (2004).

The reversals of runoff sensitivities of changes between precipitation periods for the changing land cover and vice versa are perplexing. For example, the scenario combination 1/3, of pre-75 precipitation under changing land cover conditions from 1975 to 1986, produces sensitivity in runoff during the dry season (January to March), the Veranillos (July and August) and October and November, then reverses to scenario combination 2/4 for April to June, September, and December.. Over all the Virilla displays a greater sensitivity to changes in precipitation (scenarios 1/2 and 3/4), as expected given the more extensive urban cover which proportionally converts more rainfall to runoff than a vegetated surface. The trend of runoff sensitivities to changing precipitation persists throughout the year, except during June and July, when land cover exerts control over runoff. The change in runoff sensitivities during the dry season and the Veranillos is not apparent. However, similar to the Grande de San Ramon, a marked reversal is seen of runoff sensitivities to changing precipitation under the two land cover conditions, from scenario 1/2 in the drier months to 3/4 in the wetter months. Again the runoff sensitivity to scenario 3/4 is pronounced from June to September.

Climate Variability

Climate variability, specifically the combined effects of ENSO and the Atlantic sea surface temperature anomalies (SSTA), may explain precipitation trends highlighted by the statistical analyses. A global climate shift has been identified in the mid-1970s. In the time series available here the Southern Oscillation Index (SOI) indicates more warm phase events of ENSO (El Niños: droughts in the basins) than cold events (La Niñas: excess rainfall) after 1975. The Atlantic also shows a change about 1975, with predominately positive SSTAs earlier and negative SST anomalies post-1975. Coupling of SSTs in the two ocean basin have been shown to heavily influence precipitation inputs to the area (Poveda et al. 2006).

Standardized seasonal precipitation deviates from 1959-1986 (Figure 4-10) indicates low precipitation (negative deviate) in season 1 (JFMA) for the Rio Grande de San Ramon and slight positive deviate for the Virilla. The discharge record reflects the release of the groundwater and soil moisture stores during this period, and variability in seasonal precipitation has little impact on discharge. Season 2 (MJ) also experiences more negative deviates in precipitation due to the cold Atlantic-warm Pacific combination. Much of the precipitation normally replenishes subsurface water stores depleted in the previous season. The diminished precipitation in the Grande de San Ramon appears to have been amplified by basin characteristics (e.g. topographically-induced rain-shadow) producing even lower flows.

Season 3 (JA) encompassing the *veranillos,* has been shown to be particularly sensitive to the ENSO signal. Droughts associated with warm phases and cooler Atlantic SSTAs, are particularly apparent in the Grande de San Ramon. However, regardless of the diminished precipitation subsurface water stores are still filling in both seasons 2 and 3. Drought-like conditions persist during season 4 (SO) with an even greater deviations. Although the Grande de San Ramon shows a greater response than the Virilla, discharges do not reflect this as the subsurface water stores were full and both subbasins respond similarly (as evidenced by the non-linearity of basins responses). In season 5 (ND) the signal flips from the previous season and both subbasins show a positive response to the ENSO-Atlantic influence. In the Grande de San Ramon this was relatively unimportant since the rainy season was ending and discharge enters the recession stage. The Virilla has a higher deviate explainable by the gap over the Cerro Carpinteral near Cartago, which allows increased precipitation influenced by *nortes* (Waylen et al. 1998) coming down from the North American continent and interacting with the Northeast trades.

Discussion

Model Performance

Although this work expounds on mesoscale watershed modeling simulations in the tropics there are some shortcomings. The inability of SWAT to assign more than one rain gauge for each watershed diminishes the realistic spatial simulation of daily rainfall distribution over the watershed. The model fit during calibration may have been improved by the use of the complete set of the generated random rain gauge locations based on the interpolation of the actual daily gauges. This, combined with the low number, and intermittent nature, of available daily gauges, inevitably leads to an over-simplification in the representation of rainfall inputs.

The coarse scale of the atmospheric parameters available to simulate evapotranspiration is a potential limitation. The complex topography of the Tarcoles watershed (Figure 4-1) gives rise to great spatial variability in wind speeds, temperatures and humidity depending on spatial and topographic position, none of which was captured by the single value permitted for the calculation of evapotranspiration in the model.

Values of important soil hydraulic parameters were assigned using literature values related to soil group without field validation and verification. Although shown to have little significance during the sensitivity analysis, important model parameters such as saturated hydraulic conductivity and available water content can have a significant effect on model performance, and impact the resulting calibrations and simulations.

These modeling challenges and limitations are not unique to this study. Other researchers (Bonell 1999; Bruijnzeel 1990; Bruijnzeel 2004) have echoed the difficulties of conducting mesoscale watershed modeling efforts in the tropics due to the lack of field data, and model parameterization using literature or derived parameters. Surrogate parameters from secondary sources are inadequate to capture the complex, spatial heterogeneity of mesoscale watersheds.

Currently, however, there is a dearth of “sufficient” data for mesoscale studies. Methods need to be practical and operational to determine the appropriate scale of model parameters and to validate these data for real-world conditions, particularly in the tropics (Bonell 1999).

Non-Linear Nature of Sub-Basins

The observed changes in the Virilla (Figure 4-9) from rainfall dominated responses under 1975 land cover in seasons one and two to sensitivities under the 1986 land cover are physically reasonable as the "more" naturally vegetated conditions of 1975 produce a stronger response during drier conditions. Under wetter conditions, more disturbed land cover (e.g. urban and pasture) produces a greater proportional response in runoff. This sensitivity is most apparent after the soil and groundwater stores have been depleted during the dry season. In June sensitivities are almost equal, particularly in the simulation under pre 1975 rainfall and 1975 land cover. Although there appear to be no significant increases in rainfall, it does appear to dominate the differences in runoff in the simulation results. The Virilla sub-basin has complex rainfall climatology caused by the interaction of the Pacific influences and an incursion of Caribbean air to the southeast.

Observed annual precipitation and runoff in both basins are plotted against one another (Figure 4-11). The 1:1 line represents the special case of no evapotranspiration losses. An upper enveloping line represents the maximum expected runoff for a given annual precipitation. The difference between the enveloping line and the 1:1 line represents minimum possible evapotranspiration. As precipitation increases, the absolute value of evapotranspiration decreases and evapotranspiration as a percentage of precipitation declines even more markedly in both subbasins. In years of diminished rain a lower proportion of the input goes to runoff; while in rainy years the opposite is true.

With respect to this non-linear amplification of rainfall signal in runoff, there are two other notable aspects of land cover and the 1975 switch in runoff responses. The non-linearity is not as apparent in the Virilla. Being a more urban basin, more runoff goes directly rivers, by-passing potential sources for evapotranspiration in soil and groundwater stores. Observations of the Grande de San Ramon post-1975 clearly plot below those of pre-1975. So although rainfall has declined little since 1975 (Figure 4-6) evapotranspiration appears to have increased; an effect that is not as marked in the Virilla where the groundwater stores are by-passed.

Challenges of Mesoscale Modeling Studies

Some contemporary mesoscale watershed studies have shortcomings, including a lack of statistical rigor in testing and others which only incorporate implicitly land use/land cover. Costa et al. (2003) used parametric statistics without testing for normality of their hydro-climatic data while agricultural census data (from 1960 and 1995) and satellite data (from 1995) provided empirical observations of changes in agricultural lands. Neither land cover nor agricultural census data were included explicitly in the statistical analysis of the hydro-climatic data. Correct use of statistical methods and the explicit inclusion of land cover are needed to improve mesoscale watershed studies. A preferred approach is to use complementary statistical methods coupled with dynamic hydrologic modeling simulations such as Lorup et al. (1998).

Contradictory results as to the effects of land cover change on climatic and hydrologic responses are common in the literature. Wilk et al. (2001) reported that despite a greater than 50% reduction in forest from 1957 to 1995 no changes in seasonal or annual rainfall totals were detected. Lorup et al. (1998) found no indication of increased runoff or changes in land use although population increased significantly. In contrast to previous research (Bonell and Balek 1993; Bruijnzeel 1990) Costa et al. (2003) propose that alterations in hydrologic regime arising from land use changes would be more evident in the rainy season and that higher discharges

would be expected from more intense land use. Reduced infiltration, although insufficient to affect dry season flow, increased surface runoff during the rainy season, while associated reduced evapotranspiration increased discharge throughout the year (Costa et al. 2003).

As watershed size increases, traditional paired catchment studies become infeasible due to excessive cost of instrumentation and difficulty in controlling land cover treatments (Bosch and Hewlett 1982). Results from small watershed studies cannot be upscaled to larger watersheds (Bruijnzeel 2004; Wilk et al. 2001; Bonell and Balek 1993), in which it is difficult to separate the effects on river discharge from climate variability and anthropogenic land cover change. Additionally, large withdrawal of water for municipal, agricultural and industrial uses complicate hydrologic land cover analyses (Bruijnzeel 2004). A variety of biophysical and hydro-climatic factors complicate the analysis of hydrologic responses to land cover change in large watersheds.

Unlike well-instrumented experimental hillslopes and small catchments, the heterogeneity resulting from combinations of soils, geology, and spatial and temporal distribution of rainfall, makes detection of the effects of land cover change considerably more difficult. Hydrologic impacts may be muted by the heterogeneous watershed characteristics and mosaic of multiple land covers and varied land use practices, underlain by variability in soils, geology, and topography (Bruijnzeel 2004). Land use and land cover changes are spatially and temporally heterogeneous, and impede the detection of changes in discharge and other variables in the water balance (Wilk et al. 2001). Increased surface runoff may not be detectable in river discharge due to the spatial variability of rainfall. The effect of land cover fragmentation on altered hydrologic regimes is not well understood especially in large watersheds nor is the hydrologic connectivity between land cover fragments. As intensive and extensive hydro-climatic instrumentation in

large watersheds is unfeasible we must continue to refine similar analytical studies with improved hydrologic models and statistical methods.

Conclusions

Both sub-basins show a statistically significant decline in discharge at the annual time scale after 1975 – the Rio Virilla less so than the Rio Grande de San Ramon. Precipitation inputs however have not changed significantly. Basins characteristics, particularly land cover types, act to amplify and modify the conversion of precipitation to discharge. The non-linearity of response in the Rio Grande de San Ramon becomes evident through the analysis of simulation model results. The post-1975 decline may also result from to occurrence of warm phase ENSO (drought) conditions, whose effects are amplified by a persistently cooler Atlantic. Although the basins are contiguous, the historic data indicate slightly different responses to ENSO forcing, while varying land use land cover further enhance this, yielding the noted degrees of diminished discharges over the time period.

Changes in runoff stem from both land cover change and climate variability and are particularly pronounced at the monthly and seasonal scales. Following earlier literature, dry season flows are more affected by changes in land cover while precipitation exerts a greater control in the wet season. In climatically and hydrologically complex areas such as Costa Rica, it is very difficult to disentangle the effects of land cover change from climate variability on stream flow in larger scale (mesoscale) watersheds. The Rio Tarcoles watershed is complex, experiencing interplay between the Atlantic and Caribbean, and the Pacific and various time scales (5-7 years ENSO, several decades for Atlantic). Changes in the resultant climate variability need to be accounted for when seeking hydrologic consequences to changing land cover conditions. Further exploration of climate variability might include the division of the simulation periods conditioned upon ENSO phase and investigation of differences in the mean

monthly runoff. In addition to the standard precipitation deviates, the influences of ENSO and Atlantic SSTs can be controlled providing a description of the runoff responses most expected under different ENSO phases.

The application of the process-based simulation model SWAT in Costa Rica (a first) aims to resolve mesoscale watershed heterogeneity by identifying non-linear hydro-climatic responses in two sub-basins with differing dominant land cover characteristics. The impacts of long term climate variability on a 26 year historic hydro-climatic record are identified using the integrative approach of hydrologic modeling and statistical analyses focused on addressing changing discharge contributions from two tropical sub-basins. This research augments existing mesoscale watershed studies combining simulation modeling and statistical analysis to distinguish the hydrologic impacts from land cover from those due to climate variability on discharge contributions within a tropical watershed. This is currently an understudied area with potential impacts on water withdrawals for municipal and agricultural use not only in Costa Rica's central valley, but for other global metropolitan areas.

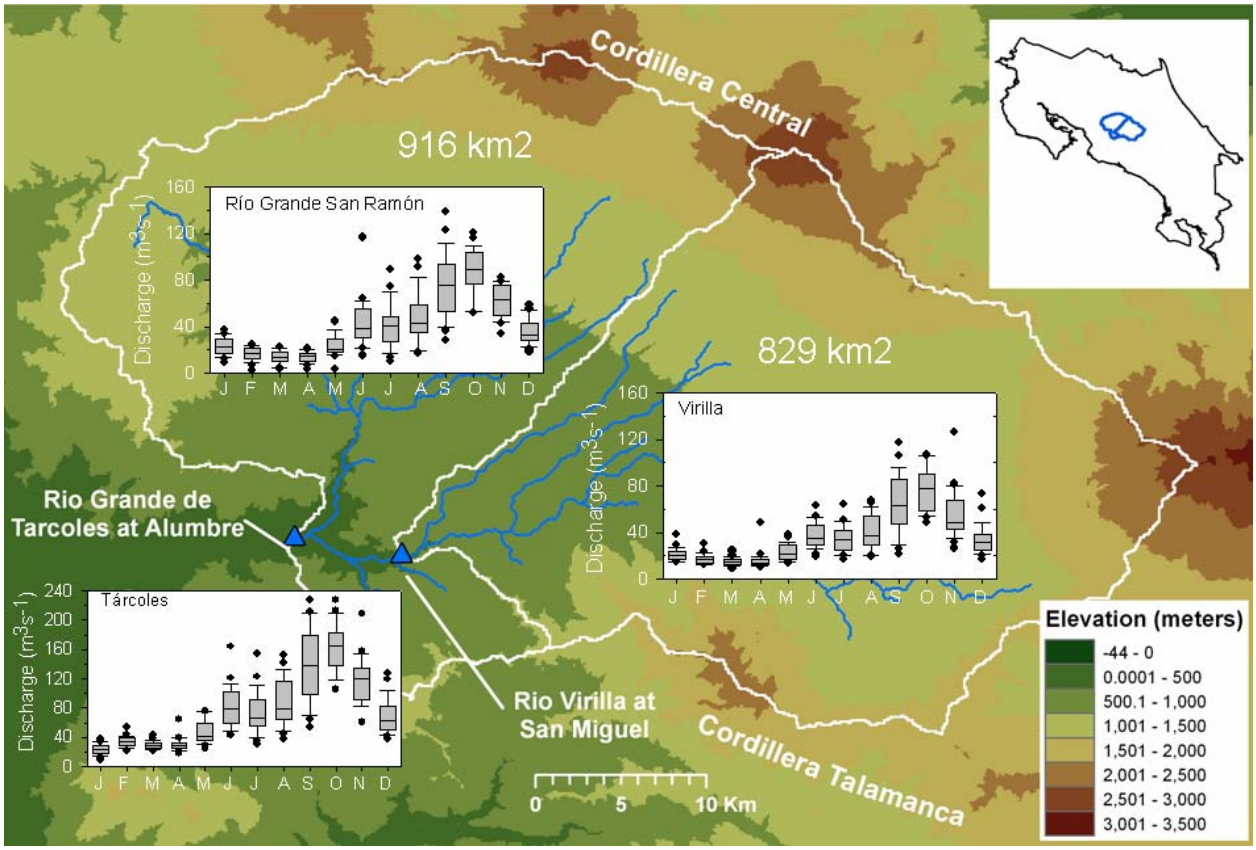

Figure 4- 1. Study area and monthly runoff regimes

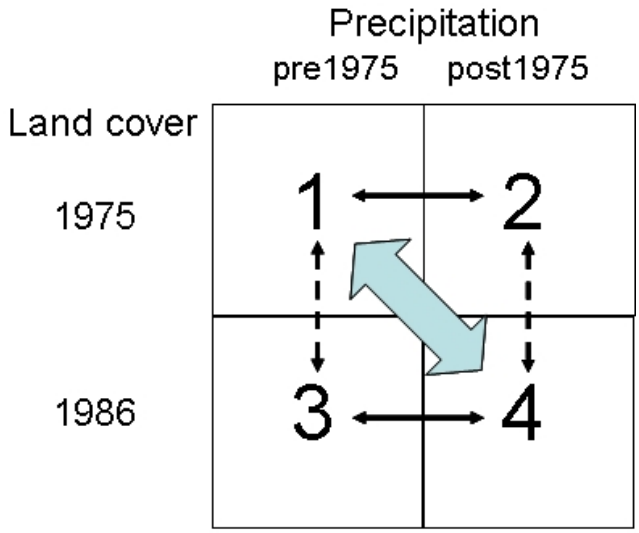

Figure 4- 2. Matrix of possible combinations under changing precipitation and land cover conditions for SWAT simulations

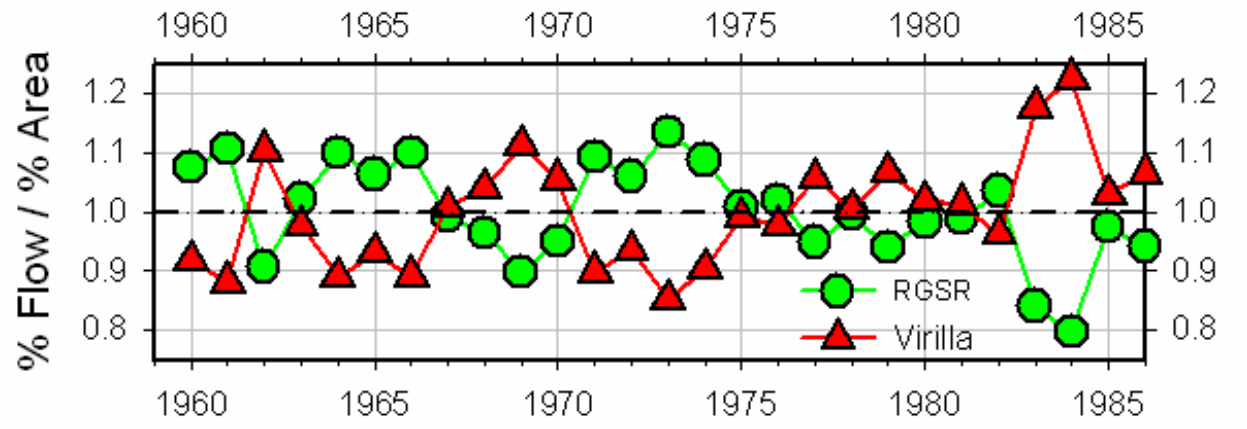

Figure 4- 3. Sub basin annual runoff as a percentage of confluence runoff compared to sub basin

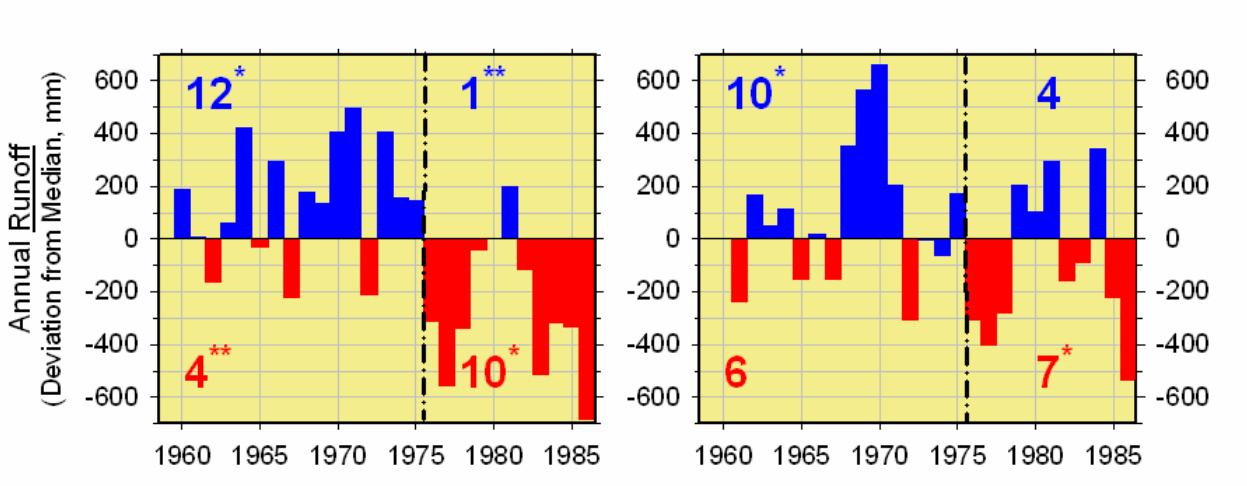

Figure 4- 4. Deviates from median annual runoff

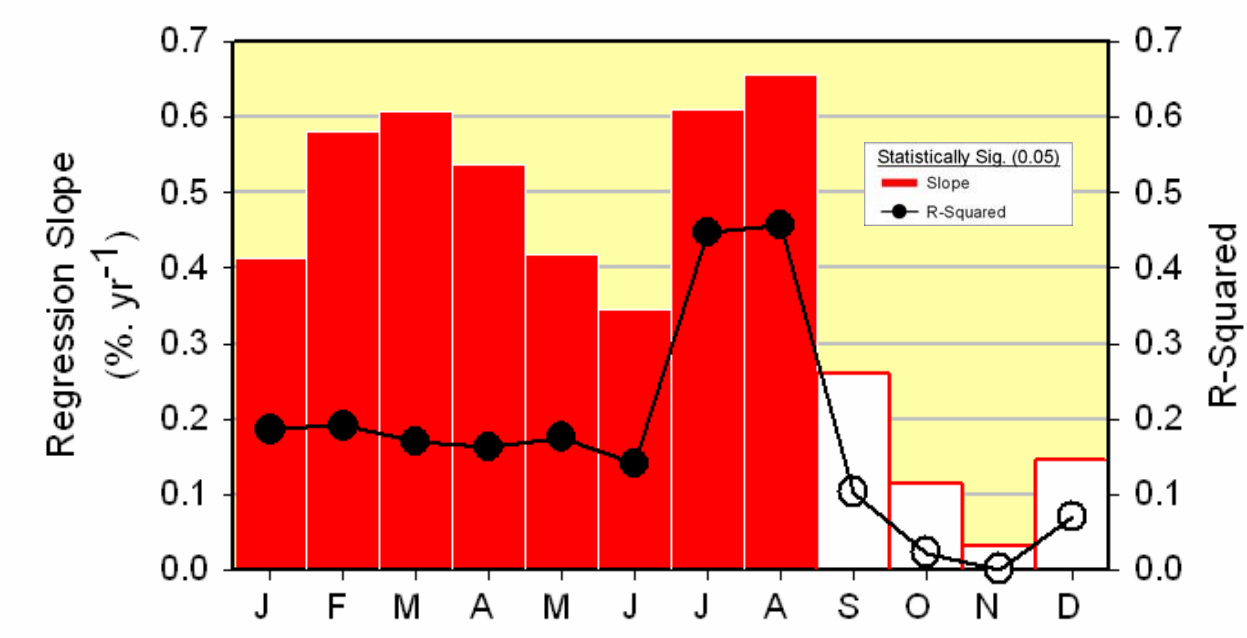

Figure 4- 5. Regression summaries of monthly runoff step plots

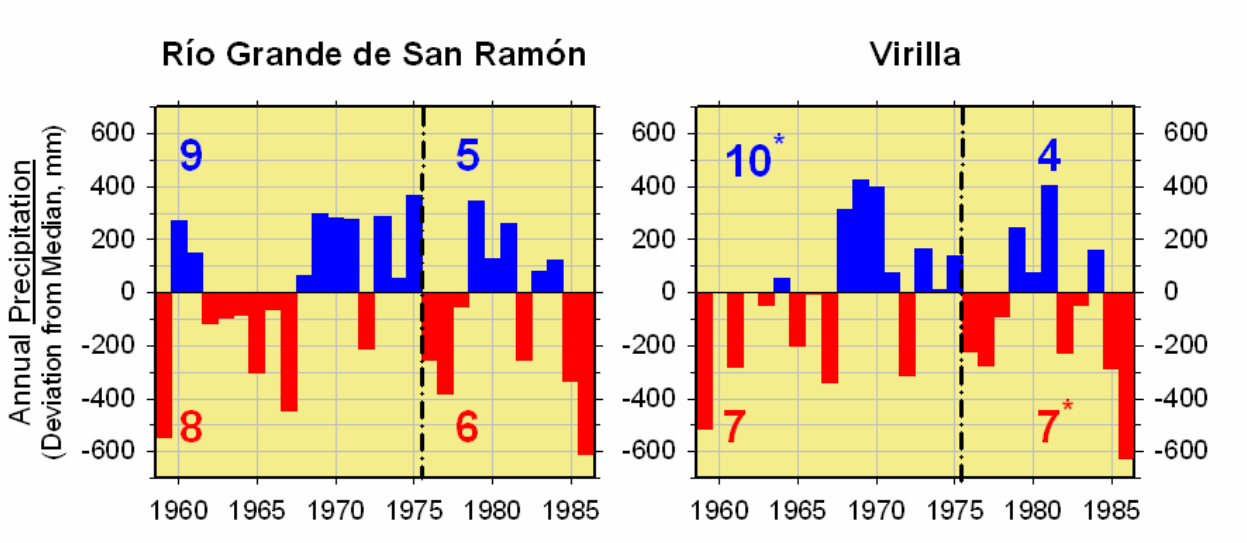

Figure 4- 6. Deviates from median annual precipitation

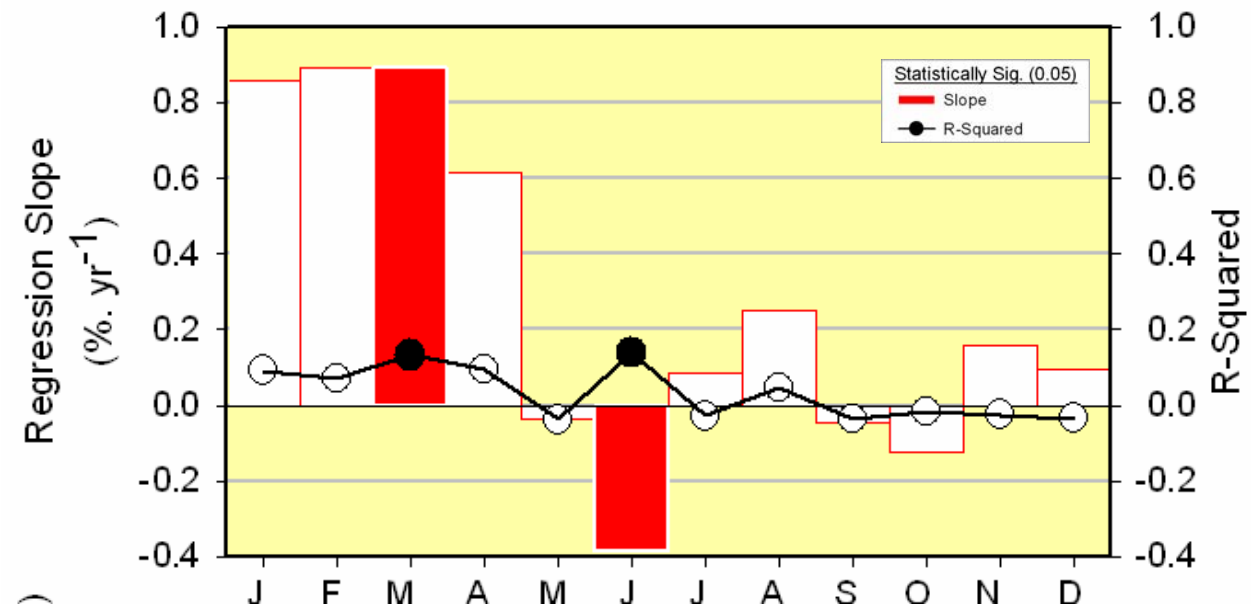

Figure 4- 7. Regression summaries of monthly precipitation step plots

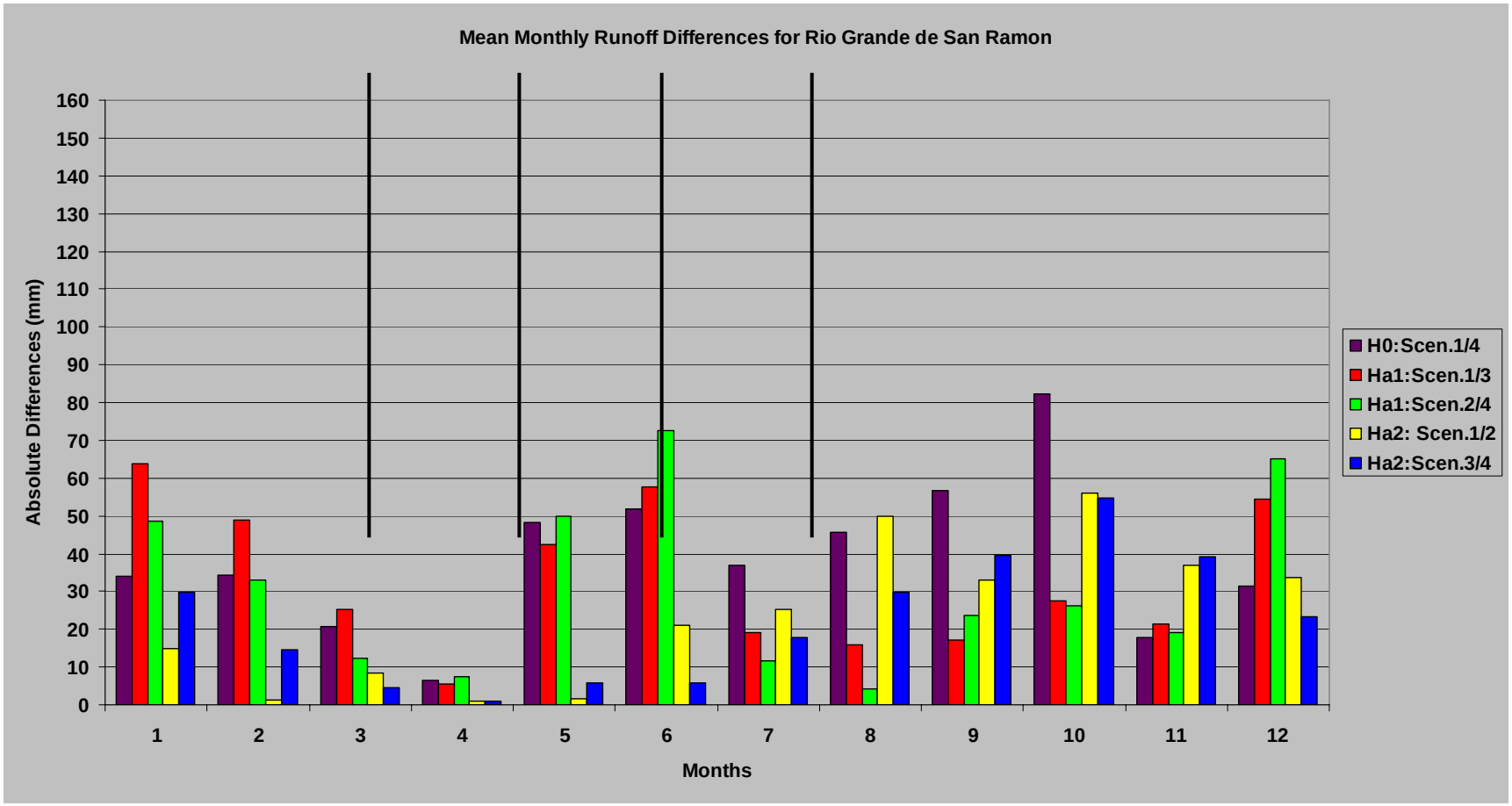

Figure 4- 8. Mean monthly runoff differences for the Rio Grande de San Ramon under various land cover and precipitation combinations

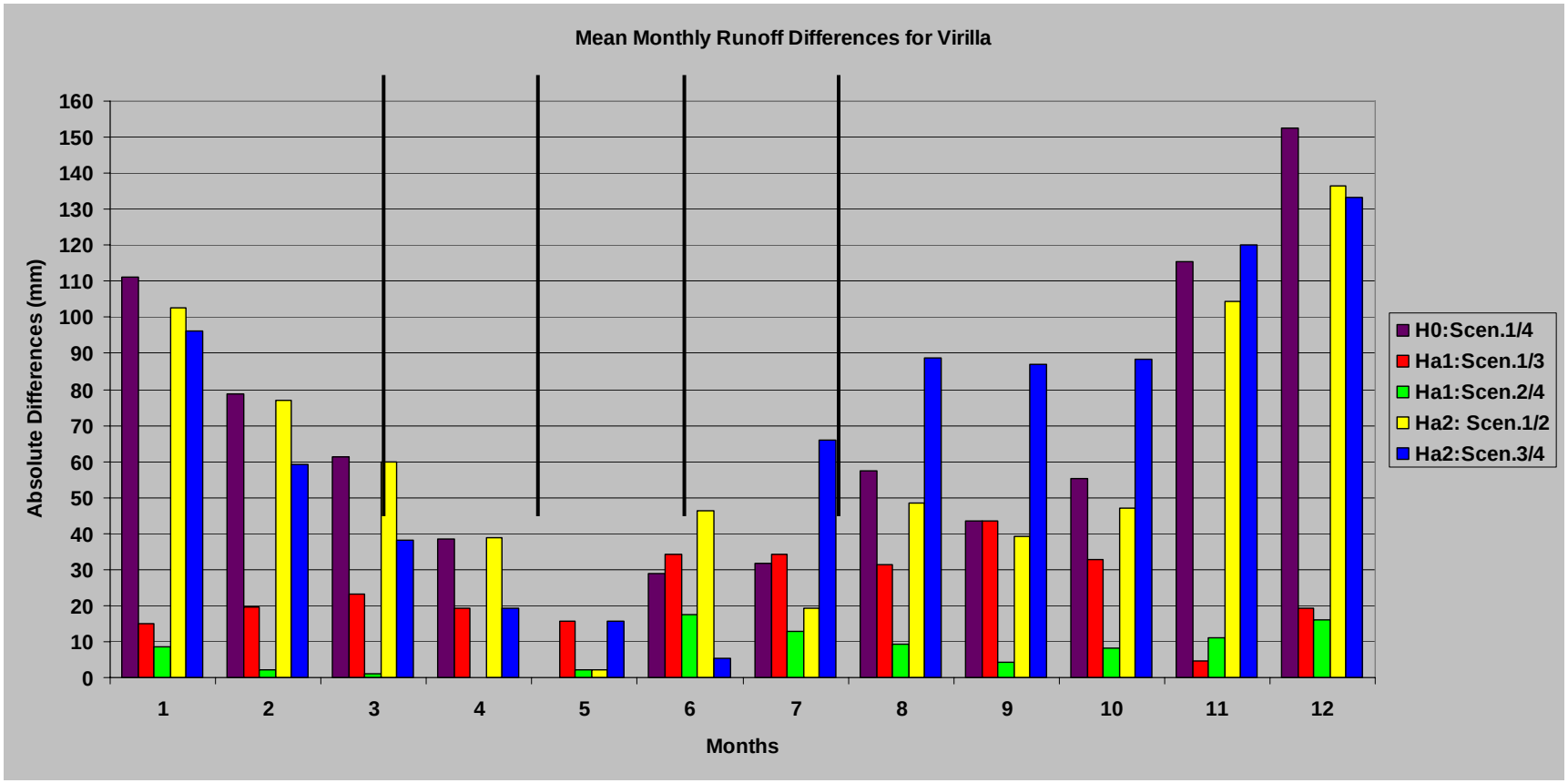

Figure 4- 9. Mean monthly runoff differences for the Virilla under various land cover and precipitation combinations

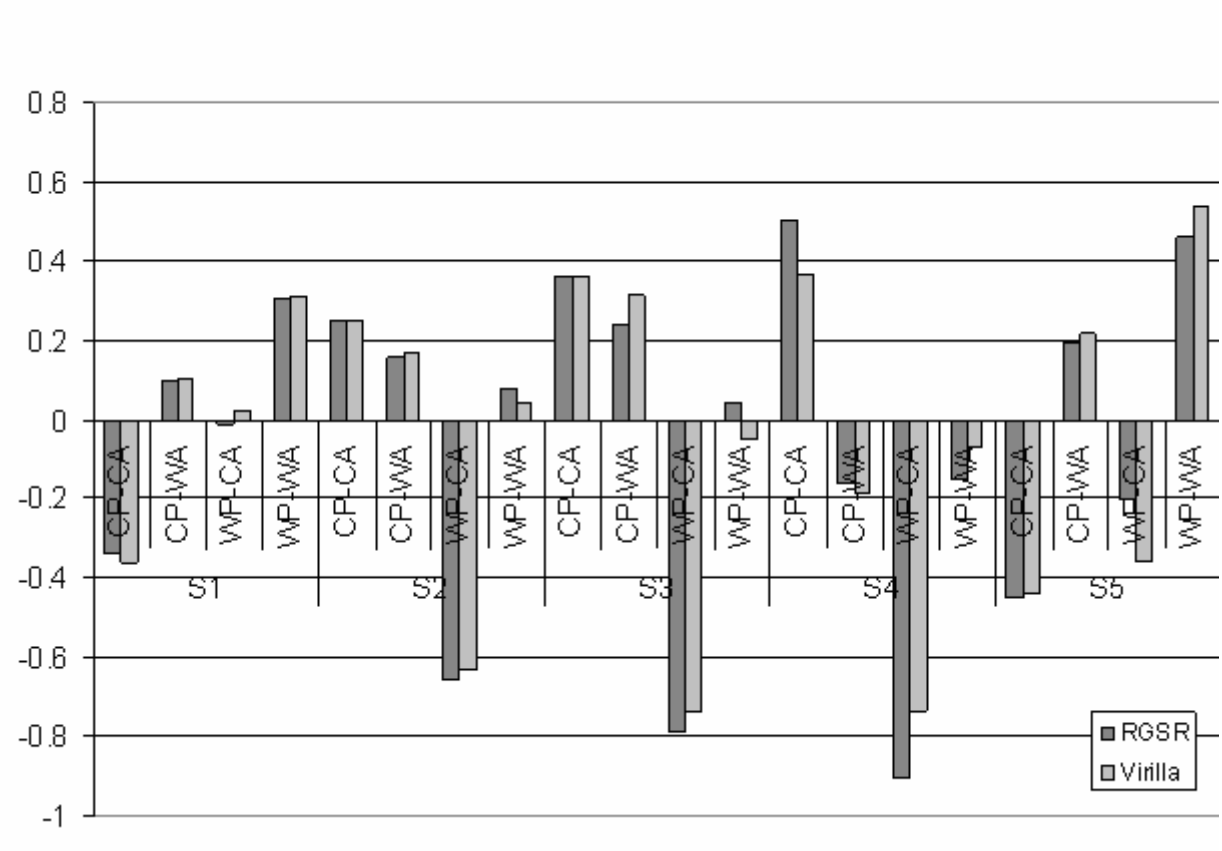

Figure 4- 10. Seasonal standardized precipitation deviates for the Rios Grande de San Ramon and Virilla

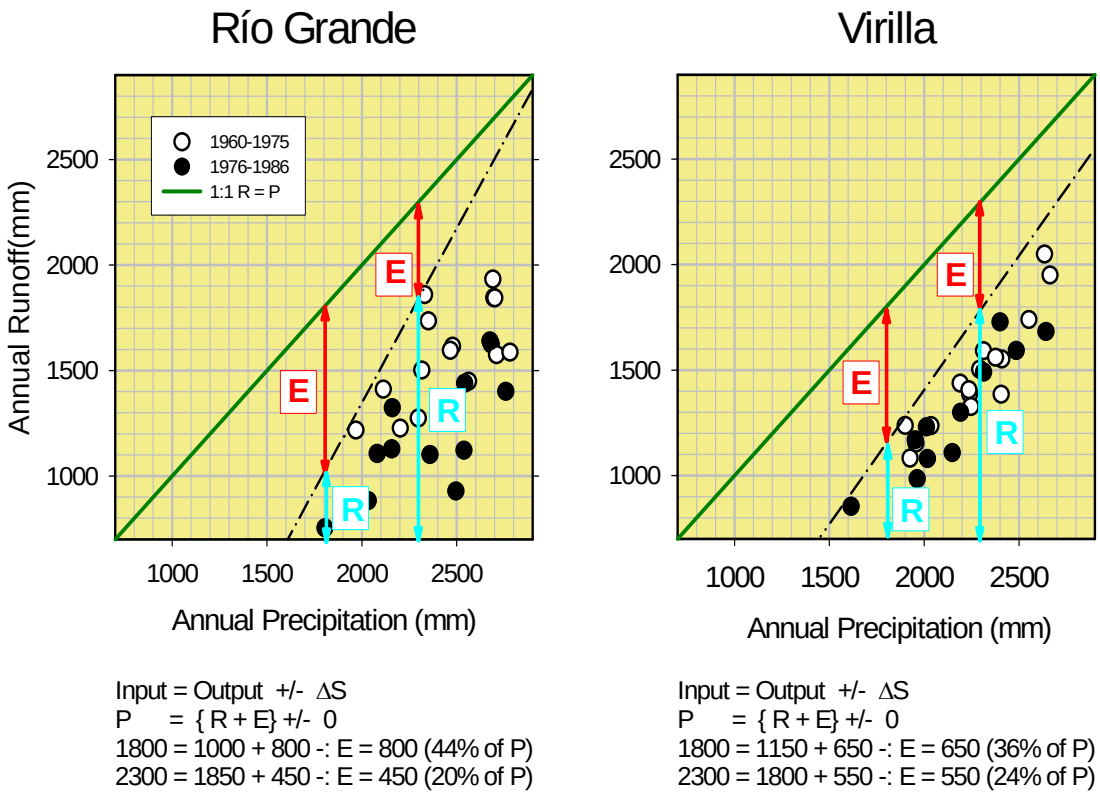

Input = Output +/- ΔS
P = { R + E} +/- 0
1800 = 1000 + 800 -: E = 800 (44% of P)
2300 = 1850 + 450 -: E = 450 (20% of P)

Input = Output +/- ΔS
P = { R + E} +/- 0
1800 = 1150 + 650 -: E = 650 (36% of P)
2300 = 1800 + 550 -: E = 550 (24% of P)

Figure 4- 11. Non-linearities in subbasin responses for runoff, precipitation, and evapotranspiration

Table 4-1. Model parameters adjusted during manual and automatic calibrations, and sensitivity and uncertainty analyses

Parameter	Variation method	Lower bound	Upper bound	Rio Grande de San Ramon		Rio Virilla	
				1975	1986	1975	1986
Baseflow alpha coefficient (days)	1	0	1	8	6	6	8
Manning's n for channel	1	0	1	7	8	7	7
Initial SCS CN II value	3	-25	25	3	3	3	3
Soil evaporation compensation factor	1	0	1	1	2	1	2
Groundwater delay time (days)	2	-10	10	6	7	8	6
Groundwater "revap" coefficient	2	-0.036	0.036	4	4	4	4
Threshold water depth in shallow aquifer for flow	2	-1000	1000	2	1	2	1
Threshold water depth in shallow aquifer for "revap"	2	-100	100	5	5	5	5
Average slope steepness	3	-25	25	10	10	10	11
Average slope length (m)	3	-25	25	11	11	11	10
Surface runoff lag	1	0	10	9	9	9	9

Table 4-2. Measures of model fit for manual calibration and validation

Year	Calibration	Slope	Slope theoretical	Variance of slope	Intercept	Nash-Sutcliffe efficiency
1975	Rio Grande de San Ramon	1.171	1.321	0.270	-27.041	0.5234
	Rio Virilla	1.121	1.229	0.092	11.492	0.4018
1986	Rio Grande de San Ramon	1.017	1.034	0.037	14.125	0.7055
	Rio Virilla	1.211	1.397	0.434	-29.584	0.5486

Year	Validation	Slope	Slope theoretical	Variance of slope	Intercept	Nash-Sutcliffe efficiency
1975	Rio Grande de San Ramon	1.035	1.068	0.084	-28.690	0.6477
	Rio Virilla	1.107	1.200	0.304	32.169	0.0768
1986	Rio Grande de San Ramon	0.984	0.968	0.131	35.335	0.6032
	Rio Virilla	1.259	1.482	0.815	-17.856	0.4357

Table 4-3. Measures of model fit for automatic calibration

Year	Calibration	Slope	Slope Theoretical	Variance of Slope	Intercept	Nash-Sutcliffe Efficiency
1975	Rio Grande de San Ramon	0.861	0.729	0.047	-28.495	0.0696
	Rio Virilla	1.120	1.227	0.091	11.648	0.4023
1986	Rio Grande de San Ramon	0.913	0.816	0.012	20.381	0.7207
	Rio Virilla	1.098	1.482	0.175	-22.010	0.6866

Table 4-4. Output SWAT parameter ranges and percentages of value range from PARASOL automatic calibration routine. Sub-basins are coded where RGSR is the Rio Grande de San Ramon and RV is the Rio Virilla.

	Parameter	Variation method	Minimum value (1975)	Maximum value (1975)	Percentage of range (1975)	Minimum value (1986)	Maximum value (1986)	Percentage of range (1986)
RGSR	Baseflow alpha coefficient (days)	1	0	2.594E-05	0.00	0.0081878	0.014919	0.67
	Soil evaporation compensation factor	1	0	0.44921	44.92	0	0.25236	25.24
	Groundwater delay time (days)	2	-10	10	100.00	-10	-1.8251	40.87
	Groundwater "revap" coefficient	2	-0.036	0.036	100.00	-0.036	-0.000518	49.28
	Threshold water depth in shallow aquifer for flow	2	-1000	1000	100.00	-1000	-110.13	44.49
	Threshold water depth in shallow aquifer for "revap"	2	-100	100	100.00	-39.632	100	69.82
RV	Baseflow alpha coefficient (days)	1	0.0037725	0.013649	0.99	0.0043699	0.013839	0.95
	Soil evaporation compensation factor	1	0	0.31192	31.19	0	0.42711	42.71
	Groundwater delay time (days)	2	-4.9694	10	74.85	-10	10	100.00
	Groundwater "revap" coefficient	2	-0.036	0.02832	89.33	-0.036	0.036	100.00
	Threshold water depth in shallow aquifer for flow	2	-1000	333.28	66.66	-1000	93.768	54.69
	Threshold water depth in shallow aquifer for "revap"	2	-100	100	100.00	-100	100	100.00

Table 4-5. Output SWAT parameter ranges and percentages of value range from SUNGLASSES uncertainty analysis routine. Sub-basins are coded where RGSR is the Rio Grande de San Ramon and RV is the Rio Virilla.

	Parameter	Variation method	Minimum value (1975)	Maximum value (1975)	Percentage of range (1975)	Minimum value (1986)	Maximum value (1986)	Percentage of range (1986)
RGSR	Baseflow alpha coefficient (days)	1	0	0	0.00	0	0	0.00
	Soil evaporation compensation factor	1	0	0.40532	40.53	0	0.35506	35.51
	Groundwater delay time (days)	2	-10	10	100.00	-10	10	100.00
	Groundwater "revap" coefficient	2	-0.036	0.036	100.00	-0.036	0.036	100.00
	Threshold water depth in shallow aquifer for flow	2	701.18	1000	14.94	-1000	1000	100.00
	Threshold water depth in shallow aquifer for "revap"	2	-100	100	100.00	-100	100	100.00
RV	Baseflow alpha coefficient (days)	1	0.0028127	0.0073213	0.45	0	0.038523	3.85
	Soil evaporation compensation factor	1	0	0.032286	3.23	0	0.93862	93.86
	Groundwater delay time (days)	2	5.728	10	21.36	-10	10	100.00
	Groundwater "revap" coefficient	2	-0.036	0.036	100.00	-0.036	0.036	100.00
	Threshold water depth in shallow aquifer for flow	2	-1000	354.51	67.73	-1000	1000	100.00
	Threshold water depth in shallow aquifer for "revap"	2	-100	100	100.00	-100	100	100.00

Table 4-6. Measures of fit for the PARASOL automatic calibration routine for each subbasin and land cover year

Results using Xi squared statistic	Rio Grande de San Ramon (1975)	Rio Grande de San Ramon (1986)	Rio Virilla (1975)	Rio Virilla (1986)
Minimum global objective function	410.0	877.5	1278.5	1096.0
Total number of runs	787	1001	1003	1000
Minimum objective functions	1826300	514320	2259100	1480300
Maximum objective functions	4262900	1046900	4322900	2860100
Minimum output values	33.944	27.856	32.485	25.749
Maximum output values	49.560	43.169	40.745	33.688
90% probability uncertainty analysis	**Rio Grande de San Ramon (1975)**	**Rio Grande de San Ramon (1986)**	**Rio Virilla (1975)**	**Rio Virilla (1986)**
Total number of observations	820.0	1755.0	2557.0	2192.0
Number of free parameters	6	6	6	6
Limit on global objective function	415.361732	882.840759	1283.83502	1101.33711
Number of selections	540	171	504	472
Minimum objective functions	1826300	514320	2259100	1480300
Maximum objective functions	1868200	522470	2290700	1502300
Minimum output values	33.944	39.837	37.540	31.092
Maximum output values	36.366	40.630	39.135	32.257
Percentage of range	15.510	5.179	19.310	14.674

Table 4-7. Measures of fit for the SUNGLASSES uncertainty analysis for each subbasin and land cover year

Results using Xi squared statistic	Rio Grande de San Ramon (1975)	Rio Grande de San Ramon (1986)	Rio Virilla (1975)	Rio Virilla (1986)
Minimum global objective function	2338.52368	1323.01172	2921.99438	2191.5
Total number of runs	710	703	2002	2000
Minimum objective functions	1928200	4792200	2875900	4885200
Maximum objective functions	7560100	6646900	7371500	8765300
Minimum output values	36.622	39	35.129	35.078
Maximum output values	43.803	48.439	39.305	40.413
90% probability uncertainty analysis	**Rio Grande de San Ramon (1975)**	**Rio Grande de San Ramon (1986)**	**Rio Virilla (1975)**	**Rio Virilla (1986)**
Total number of observations	4677	2646	5844	4383
Number of free parameters	6	6	6	6
Limit on global objective function	2343.85307	1328.34636	2927.32234	2416.9
Number of selections	349	400	332	1720
Minimum objective functions	1928200	4792200	2875900	4885200
Maximum objective functions	1949400	4859400	2909900	5427100
Minimum output values	36.622	39	37.04	35.078
Maximum output values	36.990	40.475	37.812	39.808
Percentage of range	5.12463	15.62666	18.48659	88.65979

Table 4-8. Percentages of land cover and land cover change per sub-basin

Sub-basin	Land cover class	1975 Area (%)	1986 Area (%)	Change from 1975 to 1986
Rio Grande de San Ramon	Agricultural Land-Row Crops	4.6	1.1	-3.5
	Forest-Deciduous	10.1	7.0	-3.1
	Pasture	14.2	27.3	13.1
	Range-Brush	19.6	13.2	-6.4
	Residential-Med/Low Density	0.9	0.9	0.0
Rio Virilla	Agricultural Land-Row Crops	4.2	1.4	-2.9
	Forest-Deciduous	10.5	8.1	-2.4
	Pasture	15.4	24.1	8.7
	Range-Brush	14.3	10.1	-4.1
	Residential-Med/Low Density	6.2	6.9	0.8
	Totals	100.0	100.0	

CHAPTER 5
CONCLUSIONS

I present interdisciplinary perspectives on spatial-temporal methods for land cover change from three interrelated sub-disciplines of physical geography –landscape ecology, remote sensing, and hillslope hydrology. By linking and analyzing space and time together, these methods can improve the understanding of the complexity and dynamics of land cover change in various geographic locations (Rindfuss et al. 2004). In this way, these methods can contribute to detecting and understanding linkages between patterns and processes of land cover change. Land change science (Gutman 2004), though currently in its infancy of development, could use generally accepted, mechanistic descriptions of the biophysical processes associated with land cover change as it develops into a science. The challenge lies in the vast number of ecosystem processes, each with distinct disciplinary representations, occurring at a range of scales.

Significance of Findings

The first study (Chapter 2) applies methods from remote sensing and GIScience with guidance of pattern-process linkages from landscape ecology. To better understand pattern-process interdependencies, we need to determine important scales of landscape heterogeneity, human activities, and ecosystem processes that most effectively explain heterogeneous spatial patterns (Southworth et al. 2006). The development of new methods, specifically of multiscalar analysis as applied to observed patterns captured by remotely sensed data, can yield appropriate temporal and spatial scale domains important for the applied study of linking landscape and ecological patterns and processes. The incorporation and scaling of spatial, temporal and spectral information into land cover change analyses greatly improves the amount of information obtained.

The second study (Chapter 3) draws on classic remote sensing change detection through trajectory analysis coupled with landscape level fragmentation analysis, which is common in landscape ecology. This approach, combined with remote sensing, categorizes land cover types and identifies land cover changes by linking temporal rates and spatial patterns of these changes with patch-level fragmentation indices at multiple scales. In this study, these changes are conditioned upon distance from population centers and a major road corridor. The trajectory analysis provides a baseline for tracking changes over time of an individual landscape patch between two dates, which with intermediate time steps can help identify the timings of important pattern forming processes (Crews-Meyer 2006).

The combined simulation modeling and statistical analysis conducted in the third study (Chapter 4) highlights the complexity of the climate and land cover change on hillslope hydrology and investigates aspects of spatial and temporal heterogeneity of a complex watershed. The SWAT hydrologic model is process driven, representing the major components in watershed hydrology. The continuous simulation capabilities under different land cover conditions enable the observation of the impacts on the surface hydrologic cycle due to land cover change. Given the difficulties of empirical monitoring for land cover change in large, regional scale (> 1000km^2) watersheds (Bonell 1999; Bruijnzeel 2004), watershed models do permit investigations into the spatial and temporal complexities of impacted hillslope hydrology.

The identification of disciplinary strengths from hillslope hydrology, remote sensing, and landscape ecology can lead to improved methods of spatial-temporal analyses of land cover change, and could improve the understanding of the complexity and potential outcomes on biophysical systems resulting from land cover change.

Identification of Disciplinary Strengths

Landscape ecology leads the way in spatial-temporal analysis methods (Turner et al. 1989) with many approaches for detecting landscape patterns (Dale et al. 2002) and does well at linking ecological pattern and process (Turner 1989). Remote sensing and field mapping provide the raw materials for discerning pertinent ecological patterns (Aplin 2005). Current challenges include observing long-term temporal changes, and linking satellite images and empirical field data due to scale and location dependence. Complexities of scale (Levin 1992; Turner et al. 1989) are dealt with practical implementation in the construction of sampling designs (Bellehumeur and Legendre 1998). With a strong foundation in the ecological tradition of empirical data collection, models analyze and predict observed patterns (Levin 1992) with a primary focus on how those linkages change with scale (Levin 1992; Wiens 1989).

Compared to ecology and landscape ecology, remote sensing is data and method driven and an application based 'science' (Aplin 2005). However, remote sensing has provided valuable information about the surface of the Earth (E.F.Lambin et al. 1999; Turner et al. 1995) with greater understanding of land cover patterns and changes through time (Lambin and Geist 2006), has amassed an incredible amount of data about the Earth's surface from many diverse platforms for quite an extensive period of time (Woodcock and Ozdogan 2004), and has been integrated easily into many disciplines. Remotely sensed data provide unbiased observations of land covers, and, in this way, comprise primary data sources in many types of interdisciplinary simulation models, especially those with an emphasis on land cover change. Since image analysis focuses on the detection of landscape patterns, it is reasonable that remote sensing researchers have adopted principles from landscape ecology (Crews-Meyer 2006) to analyze patterns of land cover change. Remote sensing, tied in with both landscape ecology and geography, has made

much progress in the past decade with developing spatial-temporal analyses (Petit and Lambin 2001; Mertens and Lambin 2000; Southworth et al. 2004; Southworth et al. 2006).

Hillslope hydrology has a lengthy history of collecting high-resolution temporal data (Bonell 1999) and uses process-specific simulation models (Beven et al. 1980; Beven et al. 1984; Beven et al. 1987) able to simulate streamflow production. In the 1960s and 1970s hydrology made great advances in understanding the spatial distributions of runoff generation on a hillslope (Dunne 1978) and throughout a watershed (Freeze 1972; Hewlett and Hibbert 1967). Since then, especially after the development of Freeze and Harlan's blueprint for a hydrologic simulation model (Freeze and Harlan 1969) more attention has been directed to the development of better and more detailed hydrologic models and to data collection at higher spatial and temporal resolutions (Schulz et al. 2006). Over the past decade, in response to the popularity and availability of GIS and remote sensing technologies, an interest has emerged in the spatial configurations of hydrologic patterns and their processes of formation (Grayson et al. 2002). Simulation and field hydrology has advanced primarily due to emerging new technologies capable of generating high resolution spatial and temporal data (McDonnell et al. 2007). Challenges arise from the lack of effective empirical monitoring of key hydrologic variables linked to dominant watershed processes at multiple scales. Much of the existing hydrologic knowledge stems from intensive field work in small, experimental watersheds, the increased use of remote sensing, simulation modeling, and spatial analyses can advance hydrology (Grayson and Bloschl 2001) by linking hydrologic pattern and process, particularly at regional scales, which would compliment current land cover change research agendas.

Recommendations

Conceptually speaking, landscape ecology has done well with analyzing spatial patterns with numerous methods, linking pattern and process, treatment of scale, and providing guiding

concepts and theories. Remote sensing offers 30 plus years of multi-scalar and multiple platform data for natural, “seamless” integration into many disciplines. Individual disciplinary studies that incorporate remotely sensed data use hypothesis testing based on comparisons between the imagery and the empirical data. Hydrology offers a history of process identification and the modeling of key watershed processes in a compartmentalized fashion by grouping core watershed processes that generate observable patterns. The goal here is to combine the strengths of each discipline to form intedisciplinary tenants for spatial-temporal analyses for land cover change. The primary question is this: *What can each discipline learn from each other?* The following are recommendations for the incorporation of current research directions for the development of robust methods to tackle the complexities of land cover change research.

- Landscape ecology should identify and compartmentalize key ecological process to continue pattern-process linkages across multiple scales.
- Remote sensing should continue to develop data products and refine analysis methods directed towards hydrology and other ‘subsurface’ disciplines.
- Spatial-temporal analyses of land cover and habitat change in both landscape ecology and remote sensing should use trajectory, or panel analysis methods to account for changes over time.
- Land cover change research using hydrologic models should incorporate spatial land cover data, either from remotely sensed imagery or existing spatial data.
- Hillslope hydrology needs to incorporate spatial structure, scale, dominant processes, connectivity and critical thresholds to help identify key watershed processes that are impacted by land cover change.
- Develop a classification system for cataloging of watershed patterns and hydrologic parameters controlled or produced by land cover change and develop hypotheses incorporating these field data testable by simulation models run at multiple scales.

A way forward for land cover change research is to inventory current research agendas and draw methodological strengths from complimentary disciplines. For example, the incorporation of remote sensing and field data, spatial analyses and simulation modeling for hydrologic studies

investigating land cover change at multiple scales to link pattern and process would yield an understanding of how changes in land cover within the watershed impact runoff and the resulting hydrologic responses. Interdisciplinary research, like land cover change, would be best served by complimentary methods of analysis and research agendas, and the incorporation and combination of theoretical concepts to better identify and understand the complex processes and outcomes of global change in human-environment systems. This research makes a good start along this approach and can be built upon in my future research and by other researchers who choose to use similar, interdisciplinary methods.

APPENDIX A
LANDSAT IMAGES USED IN LAND COVER CHANGE ANALYSIS FOR PANDO, BOLIVIA

Table A-1 Landsat image platform, path, row, and acquisition date information.

Platform	Path	Row	Year	Month	Day
TM	1	67	1986	7	30
TM	1	68	1986	7	30
TM	2	67	1986	8	6
TM	2	68	1986	8	6
TM	2	69	1986	9	7
TM	3	67	1986	7	28
TM	3	68	1986	7	12
TM	3	69	1986	7	12
TM	1	67	1991	7	28
TM	1	68	1991	7	28
TM	2	67	1991	7	27
TM	2	68	1991	7	27
TM	2	69	1991	7	27
TM	3	68	1991	10	14
TM	3	69	1991	10	14
TM	3	67	1992	6	18
TM	1	67	1996	7	25
TM	2	67	1996	8	1
TM	2	68	1996	7	16
TM	2	69	1996	8	17
TM	3	67	1996	7	23
TM	3	68	1996	7	23
TM	3	69	1996	7	23
TM	1	68	1997	9	14
ETM+	2	67	1999	8	2
ETM+	1	67	2000	7	28
ETM+	1	68	2000	8	13
TM	2	67	2000	7	27
ETM+	2	68	2000	11	24
TM	2	69	2000	7	27
ETM+	3	67	2000	5	23
ETM+	3	68	2000	7	26
ETM+	3	69	2000	5	23
TM	1	67	2005	6	16
TM	1	68	2005	8	3
TM	2	67	2005	8	10
TM	2	68	2005	6	7
TM	2	69	2005	8	10
TM	3	67	2005	6	30
TM	3	68	2005	9	18
TM	3	69	2005	9	18

APPENDIX B
ASTER IMAGES USED IN LAND COVER CHANGE ANALYSIS FOR PANDO, BOLIVIA

Table B-1. ASTER images used for classification and trajectory accuracy assessment.

GLOVIS L1A ID	Acquistion Date	Sun Azimuth	Sun Elevation	Scene Center Latitude	Scene Center Longitude	VNIR Look angle	TIR Look angle	SWIR Look angle	Cloud Condition
SC:AST_L1A.003:2003396555	6/29/2001	33.368	48.730	-11.209794	-67.211437	0.000	0.000	0.000	None
SC:AST_L1A.003:2003396560	6/29/2001	33.097	48.421	-11.744631	-67.328358	0.000	0.000	0.000	None
SC:AST_L1A.003:2003642025	7/29/2001	38.642	52.641	-10.738689	-69.746039	0.000	0.000	0.000	None
SC:AST_L1A.003:2003642028	7/29/2001	38.286	52.109	-11.273812	-69.861367	0.000	0.000	0.000	None
SC:AST_L1A.003:2003768861	8/7/2001	41.235	55.309	-9.710410	-67.680141	0.000	0.000	0.000	None
SC:AST_L1A.003:2003768862	8/7/2001	40.859	55.032	-10.245577	-67.794400	0.000	0.000	0.000	None
SC:AST_L1A.003:2003768864	8/7/2001	40.601	54.570	-10.780825	-67.908885	0.000	0.000	0.000	None
SC:AST_L1A.003:2003768865	8/7/2001	40.349	54.105	-11.315893	-68.023553	0.000	0.000	0.000	None
SC:AST_L1A.003:2004493410	9/17/2001	59.158	64.988	-11.242403	-66.987314	0.000	0.000	0.000	None
SC:AST_L1A.003:2004493415	9/17/2001	58.356	64.728	-11.777346	-67.103513	0.000	0.000	0.000	None
SC:AST_L1A.003:2009936839	8/20/2000	42.400	58.602	-11.272874	-68.322753	0.000	0.000	0.000	Some
SC:AST_L1A.003:2010879893	9/21/2000	60.067	68.409	-10.686346	-68.562147	0.000	0.000	0.000	Some
SC:AST_L1A.003:2010879953	9/21/2000	59.131	68.147	-11.221333	-68.678395	0.000	0.000	0.000	Few
SC:AST_L1A.003:2010879955	9/21/2000	58.222	67.712	-11.756269	-68.794933	0.000	0.000	0.000	Few
SC:AST_L1A.003:2010879956	9/21/2000	57.338	67.440	-12.291173	-68.911780	0.000	0.000	0.000	Few
SC:AST_L1A.003:2010879958	9/21/2000	56.480	67.164	-12.825864	-69.028914	0.000	0.000	0.000	Few
SC:AST_L1A.003:2018642412	9/5/2000	50.055	64.982	-9.750218	-67.401382	8.588	8.567	8.000	Few
SC:AST_L1A.003:2018642447	9/5/2000	48.023	63.859	-11.355908	-67.743708	8.588	8.567	8.000	None

Table B-1. Continued

GLOVIS L1A ID	Acquistion Date	Sun Azimuth	Sun Elevation	Scene Center Latitude	Scene Center Longitude	VNIR Look angle	TIR Look angle	SWIR Look angle	Cloud Condition
SC:AST_L1A.003:2018642453	9/5/2000	48.671	64.368	-10.820633	-67.629394	8.588	8.567	8.000	None
SC:AST_L1A.003:2018642458	9/5/2000	49.352	64.676	-10.285447	-67.515305	8.588	8.567	8.000	None
SC:AST_L1A.003:2018683275	9/12/2000	52.365	66.298	-10.821039	-69.172012	8.578	8.567	8.031	Some
SC:AST_L1A.003:2018683283	9/12/2000	50.041	65.165	-12.426434	-69.515532	8.578	8.567	8.031	Some
SC:AST_L1A.003:2018683286	9/12/2000	50.758	65.468	-11.891353	-69.400821	8.578	8.567	8.031	Some
SC:AST_L1A.003:2018683287	9/12/2000	51.496	65.768	-11.356222	-69.286320	8.578	8.567	8.031	Some
SC:AST_L1A.003:2018683295	9/12/2000	49.358	64.666	-12.961587	-69.630494	8.578	8.567	8.031	Some
SC:AST_L1A.003:2029535916	6/8/2005	34.646	48.435	-11.208756	-67.219635	-2.829	-2.853	-2.824	None
SC:AST_L1A.003:2029535919	6/8/2005	34.366	47.834	-11.743515	-67.337063	-2.829	-2.853	-2.824	None
SC:AST_L1A.003:2030305185	8/2/2005	40.864	50.068	-12.846886	-68.883442	-0.025	0.004	-0.006	None
SC:AST_L1A.003:2030653656	8/27/2005	52.149	57.363	-10.569448	-67.813325	-8.583	-8.558	-8.575	Some
SC:AST_L1A.003:2030653658	8/27/2005	51.595	56.850	-11.103915	-67.931617	-8.583	-8.558	-8.575	Few
SC:AST_L1A.003:2030653669	8/27/2005	51.063	56.573	-11.638459	-68.050323	-8.583	-8.558	-8.575	Few
SC:AST_L1A.003:2030807072	9/3/2005	55.504	60.762	-9.643626	-68.142435	0.016	0.005	-0.082	Haze
SC:AST_L1A.003:2030807073	9/3/2005	54.493	60.128	-10.178508	-68.258275	0.016	0.005	-0.082	Haze
SC:AST_L1A.003:2030807075	9/3/2005	53.861	59.856	-10.713612	-68.374434	0.016	0.005	-0.082	None
SC:AST_L1A.003:2030807077	9/3/2005	53.246	59.356	-11.248532	-68.490856	0.016	0.005	-0.082	None
SC:AST_L1A.003:2030807078	9/3/2005	52.643	59.080	-11.783402	-68.607585	0.016	0.005	-0.082	None

Table B-1. Continued

GLOVIS L1A ID	Acquistion Date	Sun Azimuth	Sun Elevation	Scene Center Latitude	Scene Center Longitude	VNIR Look angle	TIR Look angle	SWIR Look angle	Cloud Condition
SC:AST_L1A.003:2030807088	9/3/2005	52.054	58.802	-12.318226	-68.724621	0.016	0.005	-0.082	None
SC:AST_L1A.003:2034741183	6/25/2006	35.470	47.977	-10.708547	-69.953730	-0.017	0.004	-0.033	Few
SC:AST_L1A.003:2034741185	6/25/2006	35.181	47.679	-11.243494	-70.070299	-0.017	0.004	-0.033	Few
SC:AST_L1A.003:2034876294	7/4/2006	37.495	47.961	-10.565638	-69.383491	-8.578	-8.558	-8.509	None
SC:AST_L1A.003:2034876305	7/4/2006	37.189	47.370	-11.100249	-69.501921	-8.578	-8.558	-8.509	None
SC:AST_L1A.003:2034876310	7/4/2006	36.889	46.777	-11.634780	-69.620733	-8.578	-8.558	-8.509	None
SC:AST_L1A.003:2035845602	8/5/2006	43.593	52.296	-10.613081	-69.062602	-5.724	-5.700	-5.674	None
SC:AST_L1A.003:2035845603	8/5/2006	43.189	51.731	-11.147795	-69.180395	-5.724	-5.700	-5.674	Few
SC:AST_L1A.003:2035845656	8/5/2006	42.794	51.162	-11.682440	-69.298541	-5.724	-5.700	-5.674	None
SC:AST_L1A.003:2035845657	8/5/2006	42.417	50.871	-12.217016	-69.417054	-5.724	-5.700	-5.674	None
SC:AST_L1A.003:2035845659	8/5/2006	42.041	50.298	-12.751515	-69.535951	-5.724	-5.700	-5.674	None
SC:AST_L1A.003:2036830079	9/13/2006	57.381	63.627	-10.852487	-68.949709	8.580	8.567	8.492	Yes
SC:AST_L1A.003:2036830096	9/13/2006	55.903	62.886	-11.922671	-69.179032	8.580	8.567	8.492	Few
SC:AST_L1A.003:2036830098	9/13/2006	56.626	63.362	-11.387604	-69.064272	8.580	8.567	8.492	Yes
SC:AST_L1A.003:2036830102	9/13/2006	55.184	62.614	-12.457686	-69.294003	8.580	8.567	8.492	Few
SC:AST_L1A.003:2036896039	9/15/2006	59.572	63.142	-11.248567	-66.945133	-0.022	0.004	-0.011	Few
SC:AST_L1A.003:2036896072	9/15/2006	58.817	62.888	-11.783425	-67.061923	-0.022	0.004	-0.011	Few

APPENDIX C
TEST STATISTICS FOR FRAGMENTATION METRICS AT THE PANDO EXTENT

Table C-1. Kruskall-Wallis statistics for Mean Patch Size and Perimeter-Area Corrected metrics. Under the Bonferroni Test, to adjust for multiple tests, medians are significantly different if the z-value > 2.8070 as indicated in bold. Under the regular Z test medians are significantly different if the z-value > 1.9600. Metric types are defined where MPS is the mean patch size and PAC is the perimeter-area ratio- corrected.

Cover and metric	Year	1986	1991	1996	2000	2005
Forest MPS	1986	0.000				
	1991	1.270	0.000			
	1996	1.292	0.023	0.000		
	2000	0.721	0.549	0.572	0.000	
	2005	0.049	1.319	1.342	0.770	0.000
Non-forest MPS	1986	0.000				
	1991	0.767	0.000			
	1996	**3.647**	**4.414**	0.000		
	2000	2.637	1.870	**6.284**	0.000	
	2005	1.887	2.654	1.760	**4.524**	0.000
Forest PAC	1986	0.000				
	1991	1.447	0.000			
	1996	1.631	0.184	0.000		
	2000	**5.521**	**4.074**	**3.890**	0.000	
	2005	0.422	1.025	1.209	**5.099**	0.000
Non-forest PAC	1986	0.000				
	1991	0.860	0.000			
	1996	**3.012**	**3.872**	0.000		
	2000	**6.621**	**5.761**	**9.633**	0.000	
	2005	1.114	1.975	1.898	**7.735**	0.000

LIST OF REFERENCES

Alencar, A.A.C., L.A. Solorzano, and D.C. Nepstad. 2004. Modeling forest understory fires in an eastern Amazonian landscape. Ecological Applications 14(4):S139-S149.

Alvarado, A. and W. Forsythe. 2005. Densidad aparente en suelos de Costa Rica. *Agronomía Costarricense* 29(1):85-94.

Anderson, E.P., C.M. Pringle, and M. Rojas. 2006. Transforming tropical rivers: an environmental perspective on hydropower development in Costa Rica. *Aquatic Conservation-Marine and Freshwater Ecosystems* 16(7):679-693.

Aplin, P. 2005. Remote sensing: ecology. *Progress in Physical Geography* 29(1):104-113.

Arima, E.Y., R.T. Walker, S.G. Perz, and M. Caldas. 2005. Loggers and forest fragmentation: Behavioral models of road building in the Amazon basin. *Annals of the Association of American Geographers* 95(3):525-541.

Armenteras, D., G. Rudas, N. Rodriguez, S. Sua, and M. Romero. 2006. Patterns and causes of deforestation in the Colombian Amazon. *Ecological Indicators* 6(2):353-368.

Arnold, J.G. and N. Fohrer. 2005. SWAT2000: current capabilities and research opportunities in applied watershed modelling. *Hydrological Processes* 19(3):563-572.

Arnold, J.G., R. Srinivasan, R.S. Muttiah, and J.R. Williams. 1998. Large area hydrologic modeling and assessment - Part 1: Model development. *Journal of the American Water Resources Association* 34(1):73-89.

Asner, G.P., D.E. Knapp, E.N. Broadbent, P.J.C. Oliveira, M. Keller, and J.N. Silva. 2005. Selective logging in the Brazilian Amazon. *Science* 310(5747):480-482.

Ault, T.R. and C.R. Johnson. 1998. Spatially and temporally predictable fish communities on coral reefs. *Ecological Monographs* 68(1):25-50.

Bedient, P.B. and W.C. Huber. 1988. *Hydrology and floodplain analysis*. Addison-Wesley: Reading, Mass.

Bellehumeur, C. and P. Legendre. 1998. Multiscale sources of variation in ecological variables: modeling spatial dispersion, elaborating sampling designs. *Landscape Ecology* 13(1):15-25.

Beven, K., A. Calver, and E.M. Morris. 1987. The Institute of Hydrology Distributed Model. *Report - UK Institute of Hydrology* 98 (1987) p33p:33p.

Beven, K., R. Warren, J. Zaoui,) Danish Hydraulic Institute, and G. SOGREAH. 1980. SHE: towards a methodology for physically-based distributed forecasting in hydrology. *In Hydrological forecasting*, 133-7.

Beven, K.J., M.J. Kirkby, N. Schofield, and A.F. Tagg. 1984. Testing a physically-based flood forecasting model (TOPMODEL) for three UK catchments (Crimple Beck, Hodge Beck, Wye). *Journal of Hydrology* 69(1-4):119-143.

Blomquist, W.A., 1957-, A. William, and B. World. 2005. Institutional and policy analysis of river basin management the tarcoles river basin, Costa Rica /.

Bonell, M. 1998. Possible impacts of climate variability and change on tropical forest hydrology. *Climatic Change* 39(2-3):215-272.

Bonell, M. 1999. Tropical forest hydrology and the role of the UNESCO International Hydrological Programme. *Hydrology and Earth System Sciences* 3(4):451-461.

Bonell, M. and J. Balek. 1993. Recent scientific developments and research needs in hydrological processes of the humid tropics. *In Hydrology and water management in the humid tropics*, eds. M.Bonell, M.M.Hufschmidt, and J.S.Gladwell. 167-260. Cambridge University Press.

Borcard, D. and P. Legendre. 2002. All-scale spatial analysis of ecological data by means of principal coordinates of neighbour matrices. *Ecological Modelling* 153(1-2):51-68.

Bosch, J.M. and J.D. Hewlett. 1982. A Review of Catchment Experiments to Determine the Effect of Vegetation Changes on Water Yield and Evapo-Transpiration. *Journal of Hydrology* 55(1-4):3-23.

Boyd, D.S. and F.M. Danson. 2005. Satellite remote sensing of forest resources: three decades of research development. *Progress in Physical Geography* 29(1):1-26.

Boyd, D.S. and F. Petitcolin. 2004. Remote sensing of the terrestrial environment using middle infrared radiation (3.0-5.0 mu m). *International Journal of Remote Sensing* 25(17):3343-3368.

Breiman, L. 1984. Classification and regression trees /. Belmont, Calif. : Wadsworth International Group, Wadsworth International Group.

Brown, D.G., B.C. Pijanowski, and J.D. Duh. 2000. Modeling the relationships between land use and land cover on private lands in the Upper Midwest, USA. *Journal of Environmental Management* 59(4):247-263.

Bruijnzeel, L.A. 1990. *Hydrology of moist tropical forests and effects of conversion: a state of knowledge review*. Netherlands IHP Committee: Netherlands IHP Committee.

Bruijnzeel, L.A. 2004. Hydrological functions of tropical forests: not seeing the soil for the trees? *Agriculture Ecosystems & Environment* 104(1):185-228.

Butler, D.R., G.P. Malanson, and L.M. Resler. 2004. Turf-banked terrace treads and risers, turf exfoliation and possible relationships with advancing treeline. *Catena* 58(3):259-274.

Centro Científico Tropical (CCT). Tipo de Suelos en Costa Rica. Scale 1:200,000. 1989. Costa Rica.

Chan, J.C.W., N. Laporte, and R.S. Defries. 2003. Texture classification of logged forests in tropical Africa using machine-learning algorithms. *International Journal of Remote Sensing* 24(6):1401-1407.

Chen, K. 2002. An approach to linking remotely sensed data and areal census data. *International Journal of Remote Sensing* 23(1):37-48.

Chomitz, K.M. and D.A. Gray. 1996. Roads, land use, and deforestation: A spatial model applied to belize. *World Bank Economic Review* 10(3):487-512.

Cihlar, J. 2000. Land cover mapping of large areas from satellites: status and research priorities. *International Journal of Remote Sensing* 21(6-7):1093-1114.

Cohen, W.B. and C.O. Justice. 1999. Validating MODIS terrestrial ecology products: Linking in situ and satellite measurements. *Remote Sensing of Environment* 70(1):1-3.

Colby, J.D. 2001. Simulation of a Costa Rican watershed: Resolution effects and fractals. *Journal of Water Resources Planning and Management-Asce* 127(4):261-270.

Coops, N. and D. Culvenor. 2000. Utilizing local variance of simulated high spatial resolution imagery to predict spatial pattern of forest stands. *Remote Sensing of Environment* 71(3):248-260.

Coops, N.C. and P.C. Catling. 1997. Utilising airborne multispectral videography to predict habitat complexity in eucalypt forests for wildlife management. *Wildlife Research* 24(6):691-702.

Costa, M.H., A. Botta, and J.A. Cardille. 2003. Effects of large-scale changes in land cover on the discharge of the Tocantins River, Southeastern Amazonia. *Journal of Hydrology* 283(1-4):206-217.

Coxhead, I., A. Rola, and K. Kim. 2001. How do national markets and price policies affect land use at the forest margin? Evidence from the Philippines. *Land Economics* 77:250-267.

Crews-Meyer, K. 2006. Temporal Extensions of Landscape Ecology Theory and Practice: Examples from the Peruvian Amazon. *Professional Geographer* 58(4):421-435.

CUMAT. Desbosque de la Amazonia Boliviana. 1992. La Paz, Bolivia, Centro de Investigaciones de la Capacidad de Uso Mayor de la Tierra.

Cumming, G.S. 2003. Measures of "eroading" ecology. *Frontiers in Ecology and the Environment* 1(5):233.

Currie, J. 1981. *The Economic Theory of Agricultural Land Tenure*. Cambridge University Press: Cambridge.

Dale, M.R.T., P. Dixon, M.J. Fortin, P. Legendre, D.E. Myers, and M.S. Rosenberg. 2002. Conceptual and mathematical relationships among methods for spatial analysis. *Ecography* 25(5):558-577.

Dingman, S.L. 2002. *Physical hydrology*. Prentice Hall, Upper Saddle River, NJ.

Droogers, P. and G. Kite. 2002. Remotely sensed data used for modelling at different hydrological scales. *Hydrological Processes* 16(8):1543-1556.

Duncan, B.W., S. Bolye, D.R. Breininger, and P.A. Schmalzer. 1999. Coupling past management practice and historic landscape change on John F. Kennedy Space Center, Florida. *Landscape Ecology* 14:291-309.

Dunne, T. 1978. Field studies of hillslope processes. *In Hillslope Hydrology,* ed. M.J.Kirkby. 227-94. John Wiley and Sons: Chichester.

Dykes, A.P. and J.B. Thornes. 2000. Hillslope hydrology in tropical rainforest steeplands in Brunei. *Hydrological Processes* 14(2):215-235.

Elsenbeer, H. 2001. Hydrologic flowpaths in tropical rainforest soilscapes - a review. *Hydrological Processes* 15(10):1751-1759.

Elsenbeer, H. and D.K. Cassel. 1991. The mechanisms of overland flow generation in a small catchment in wetsern Amazonia. *In Water Management of the Amazon Basin Symposium: Proceedings of Manaus Symposium August 1990,* eds. B.P.F.Braga and C.A.Fernandez-Jauregui. 275-88. UNESCO: Montevideo, Uruguay.

Elsenbeer, H., K. Cassel, and J. Castro. 1992. Spatial-Analysis of Soil Hydraulic Conductivity in A Tropical Rain-Forest Catchment. *Water Resources Research* 28(12):3201-3214.

Elsenbeer, H., B.E. Newton, T. Dunne, and J.M. de Moraes. 1999. Soil hydraulic conductivities of latosols under pasture, forest and teak in Rondonia, Brazil. *Hydrological Processes* 13(9):1417-1422.

Etter, A., C. McAlpine, K. Wilson, S. Phinn, and H. Possingham. 2006. Regional patterns of agricultural land use and deforestation in Colombia. *Agriculture Ecosystems & Environment* 114(2-4):369-386.

Evans, T.P., G.M. Green, and L.A. Carlson. 2001. Multi-scale analysis of landcover composition and landscape management of public and private lands in Indiana. *In GIS and Remote Sensing Applications in Biogeography and Ecology,* eds. A.C.Millington, S.J.Walsh, and P.E.Osborne. 271-87. Kluwer Academic Publications: Boston, MA.

Fearnside, P.M. 2002. Avanca Brasil: Environmental and social consequences of Brazil's planned infrastructure in Amazonia. *Environmental Management* 30(6):735-747.

Foley, J.A., G.P. Asner, M.H. Costa, M.T. Coe, R. Defries, H.K. Gibbs, E.A. Howard, S. Olson, J. Patz, N. Ramankutty, and P. Snyder. 2007. Amazonia revealed: forest degradation and loss of ecosystem goods and services in the Amazon Basin. *Frontiers in Ecology and the Environment* 5(1):25-32.

Freeze, R.A. 1972. Role of Subsurface Flow in Generating Surface Runoff .2. Upstream Source Areas. *Water Resources Research* 8(5):1272-&.

Freeze, R.A. and R.L. Harlan. 1969. Blueprint for a physically-based, digitally-simulated hydrologic response model. *Journal of Hydrology* 9(3):237-258.

Gehlke, C.E. and K. Biel. 1934. Certain effects of grouping upon the size of the correlation coefficient in census tract material. *Journal of the American Statistical Association* 29(185A):169-170.

Giambelluca, T.W. 2002. Hydrology of altered tropical forest. *Hydrological Processes* 16(8):1665-1669.

Goodchild, M.E. 2004. GIScience, geography, form, and process. *Annals of the Association of American Geographers* 94(4):709-714.

Grayson, R.B., G. Bloschl, A.W. Western, and T.A. McMahon. 2002. Advances in the use of observed spatial patterns of catchment hydrological response. *Advances in Water Resources* 25(8-12):1313-1334.

Green, C.H. and A. van Griensven. 2008. Autocalibration in hydrologic modeling: Using SWAT2005 in small-scale watersheds. *Environmental Modelling & Software* 23:422-434.

Green, G., C. Schweik, M. Hanson, L. Weber, C. Agarwal, G. Bullman, L. Carlson, M. Reisinger, S. Shields, J. Hanson, A.C. Barros, and B. Davis. Radiometric Calibration for Landsat 5 TM scenes (Equation 6) Version 1.0. 1999. Bloomington, IN, CIPEC: Center for the Study of Institutions, Population, and Envronmental Change, Indiana University. Ref Type: Data File

Green, G., C. Schweik, M. Hanson, L. Weber, C. Agarwal, G. Bullman, L. Carlson, M. Reisinger, S. Shields, J. Hanson, A.C. Barros, and B. Davis. Radiometric Calibration for Landsat 7 ETM+ scene using CPF (Equation 8) V. 1. 2001. Bloomington, IN, CIPEC: Center for the Study of Institutions, Population, and Envronmental Change, Indiana University.

Gustafson, E.J. 1998. Quantifying landscape spatial pattern: What is the state of the art? *Ecosystems* 1(2):143-156.

Gutman, G. 2004. Land change science : observing, monitoring and understanding trajectories of change on the Earth's surface /. Dordrecht: Kluwer Academic Publishers.

Habeeb, R.L., J. Trebilco, S. Wotherspoon, and C.R. Johnson. 2005. Determining natural scales of ecological systems. *Ecological Monographs* 75(4):467-487.

Hamilton, D. 2006. Interoceanic highway: The road to riches, the road to ruin. 26-32. www.geographical.co.uk Date last accessed: January 3, 2008.

Hastenrath, S. 2002. The Intertropical Convergence Zone of the eastern Pacific revisited. *International Journal of Climatology* 22(3):347-356.

He, H.S., S.J. Ventura, and D.J. Mladenoff. 2002. Effects of spatial aggregation approaches on classified satellite imagery. *International Journal of Geographical Information Science* 16(1):93-109.

Herbert, M.E. and F.P. Gelwick. 2003. Spatial variation of headwater fish assemblages explained by hydrologic variability and upstream effects of impoundment. *Copeia*(2):273-284.

Hewlett, J.D. and A.R. Hibbert. 1967. Factors affecting the the response of smalll watersheds to precipitation in humid areas. *In Forest Hydrology*, eds. W.E.Sopper and H.W.Lull. 275-90. Pergamon Press: Oxford, New York.

Hill, M.F., J.D. Witman, and H. Caswell. 2002. Spatio-temporal variation in Markov chain models of subtidal community succession. *Ecology Letters* 5(5):665-675.

Horton, R.E. 1933. The role of infiltration in the hydrologic cycle. *Transactions of the American Geophysical Union* 14:446-460.

Houghton, R.A. 1994. The Worldwide Extent of Land-Use Change. *Bioscience* 44(5):305-313.

Imbernon, J. and A. Branthomme. 2001. Characterization of landscape patterns of deforestation in tropical rain forests. *International Journal of Remote Sensing* 22(9):1753-1765.

INPE. Monitoramento da Floresta Amazônica Brasileira por Satélite. 2008. Instituto Nacional de Pesquisas Espaciais. Projeto PRODES. Instituto de Pesquisa Espaciais.

Isobe, T., E.D. Feigelson, M.G. Akritas, and G.J. Babu. 1990. Linear-Regression in Astronomy .1. *Astrophysical Journal* 364(1):104-113.

Jensen, J.R. 2005. *Introductory digital image processing : a remote sensing perspective*. Prentice Hall, Upper Saddle River, N.J.

Kaimowitz, D., G. Thiele, and P. Pacheco. 1999. The effects of structural adjustment on deforestation and forest degradation in lowland Bolivia. *World Development* 27(3):505-520.

Kaimowitz, D., A. Angelsen, and Center for International Forestry Research. 1998. *Economic models of tropical deforestation : a review*. CIFOR, Bogor, Indonesia.

Kalnay, E., M. Kanamitsu, R. Kistler, W. Collins, D. Deaven, L. Gandin, M. Iredell, S. Saha, G. White, J. Woollen, Y. Zhu, M. Chelliah, W. Ebisuzaki, W. Higgins, J. Janowiak, K.C. Mo, C. Ropelewski, J. Wang, A. Leetmaa, R. Reynolds, R. Jenne, and D. Joseph. 1996. The NCEP/NCAR 40-year reanalysis project. *Bulletin of the American Meteorological Society* 77(3):437-471.

Kauth, R.J., B.J.S.C. Lyndon, Earth Observation Division., and Environmental Research Institute of Michigan. 1976. System for analysis of Landsat agricultural data : automatic computer-assisted proportion estimation of local areas : final report /. Ann Arbor, Mich. : Environmental Research Institute of Michigan, Environmental Research Institute of Michigan.

Killeen, T.J., V. Calderon, L. Soria, B. Quezada, M.K. Steininger, G. Harper, L.A. Solorzano, and C.J. Tucker. 2007. Thirty years of land-cover change in Bolivia. *Ambio* 36(7):600-606.

Krishnaswamy, J., P.N. Halpin, and D.D. Richter. 2001. Dynamics of sediment discharge in relation to land-use and hydro-climatology in a humid tropical watershed in Costa Rica. *Journal of Hydrology* 253(1-4):91-109.

Lambin, E.F. 1999. Monitoring forest degradation in tropical regions by remote sensing: some methodological issues. *Global Ecology and Biogeography* 8(3-4):191-198.

Lambin, E.F. 1997. Modelling and monitoring land-cover change processes in tropical regions. *Progress in Physical Geography* 21(3):375-393.

Lambin, E.F., H.J. Geist, and E. Lepers. 2003. Dynamics of land-use and land-cover change in tropical regions. *Annual Review of Environment and Resources* 28:205-241.

Lambin, E.F. and A.H. Strahler. 1994. Indicators of Land-Cover Change for Change-Vector Analysis in Multitemporal Space at Coarse Spatial Scales. *International Journal of Remote Sensing* 15(10):2099-2119.

Lambin, E.F. and H.J. Geist. 2006. Land-use and land-cover change : local processes and global impacts. Berlin: Springer.

Lambin, E.F., X.Baulies, N.Bockstael, G.Fischer, T.Krug, R.Leemans, E.F.Moran, R.R.Rindfuss, Y.Sato, D.Skole, B.L.Turner II, and C.Vogel. 1999. Land-Use and Land-Cover Change (LUCC) : implementation strategy /. Stockholm : International Geosphere-Biosphere Programme, International Geosphere-Biosphere Programme.

Laurance, W.F., A.K.M. Albernaz, P.M. Fearnside, H.L. Vasconcelos, and L.V. Ferreira. 2004. Deforestation in Amazonia. *Science* 304(5674):1109.

Legendre, P. and E.D. Gallagher. 2001. Ecologically meaningful transformations for ordination of species data. *Oecologia* 129(2):271-280.

Legendre, P. and J. Legendre. 1998. *Numerical ecology*. Elsevier, Amsterdam ; New York.

Lehner, B., K. Verdin, and A. Jarvis. HydroSHEDS Technical Documentation Version 1.0. 2006.

Levin, S.A. 1992. The Problem of Pattern and Scale in Ecology. *Ecology* 73(6):1943-1967.

Loehle, C. and B.L. Li. 1996. Statistical properties of ecological and geologic fractals. *Ecological Modelling* 85(2-3):271-284.

Loh, W.Y. and Y.S. Shih. 1997. Split selection methods for classification trees. *Statistica Sinica* 7(4):815-840.

Lorup, J.K., J.C. Refsgaard, and D. Mazvimavi. 1998. Assessing the effect of land use change on catchment runoff by combined use of statistical tests and hydrological modelling: Case studies from Zimbabwe. *Journal of Hydrology* 205(3-4):147-163.

Lu, D., A. Batistella, P. Mausel, and E. Moran. 2007. Mapping and monitoring land degradation risks in the Western Brazilian Amazon using multitemporal landsat TM/ETM plus images. *Land Degradation & Development* 18(1):41-54.

Lu, D.S., P. Mausel, M. Batistella, and E. Moran. 2004. Comparison of land-cover classification methods in the Brazilian Amazon Basin. *Photogrammetric Engineering and Remote Sensing* 70(6):723-731.

Magana, V., J.A. Amador, and S. Medina. 1999. The midsummer drought over Mexico and Central America. *Journal of Climate* 12(6):1577-1588.

Malanson, G.P., D.R. Butler, D.M. Cairns, T.E. Welsh, and L.M. Resler. 2002. Variability in an edaphic indicator in alpine tundra. *Catena* 49(3):203-215.

Marceau, D.J. 1999. The scale issue in social and natural sciences. *Canadian Journal of Remote Sensing* 25(4):347.

Marshall, E. and T. Randhir. 2008. Spatial modeling of land cover change and watershed response using Markovian cellular automata and simulation. *Water Resources Research* 44(4):W04423.

Marsik, M. and P. Waylen. 2006. An application of the distributed hydrologic model CASC2D to a tropical montane watershed. *Journal of Hydrology* 330(3-4):481-495.

McDonnell, J.J., M. Sivapalan, K. Vache, S. Dunn, G. Grant, R. Haggerty, C. Hinz, R. Hooper, J. Kirchner, M.L. Roderick, J. Selker, and M. Weiler. 2007. Moving beyond heterogeneity and process complexity: A new vision for watershed hydrology. *Water Resources Research* 43(7).

Mertens, B. and E.F. Lambin. 2000. Land-cover-change trajectories in southern Cameroon. *Annals of the Association of American Geographers* 90(3):467-494.

Ministerio de Agricultura y Ganadería (MAG). Uso de la Tierra en Costa Rica en 1992. Landsat image (30m x 30m). 1992.

Ministerio de Recursos Naturales, E.y.M. Instituto Meterológico Nacional Año del Centenario 1888-1988: Catastrode las Series de Precipitaciones Medidas en Costa Rica. 1-361. 1988. San José, Costa Rica, MINAE.

Mladenoff, D.J. and B. DeZonia. APACK 2.14 Users Guide. 2000. Madison, WI, Department of Forest Ecology and Management, University of Wisconsin.

Moody, A. and C.E. Woodcock. 1995. The influence of scale and the spatial characteristics of landscapes on land-cover mapping using remote sensing. *Landscape Ecology* 10(6):363-379.

Moran, E., E. Ostrom, and J.C. Randolph. A Multilevel Approach to Studying Global Environmental Change in Forest Ecosystems. 1-26. 1998. Bloomington, IN, Center for the Study of Institutions, Population, and Environmental Change.

Moran, E.F. 1993. Deforestation and Land-Use in the Brazilian Amazon. *Human Ecology* 21(1):1-21.

Mostacedo, B., J. Balcazar, and J.C. Montero. 2006. Tipos de bosque, diversidad y composición florística en la Amazonia sudoeste de Bolivia. *Ecología en Bolivia* 41(2):99-116.

Munroe, D.K., J. Southworth, and C.M. Tucker. 2004. Modeling spatially and temporally complex land-cover change: The case of western Honduras. *Professional Geographer* 56(4):544-559.

Myers, R.L. 1990. *Ecosystems of Florida*. University of Central Florida Press, Orlando.

Nagendra, H., J. Southworth, and C. Tucker. 2003. Accessibility as a determinant of landscape transformation in western Honduras: linking pattern and process. *Landscape Ecology* 18(2):141-158.

Nash, J.E. and J.V. Sutcliffe. 1970. River flow forecasting through conceptual models part I -- A discussion of principles. *Journal of Hydrology* 10(3):282-290.

Naughton-Treves, L. 2004. Deforestation and carbon emissions at tropical frontiers: A case study from the Peruvian Amazon. *World Development* 32(1):173-190.

Neitsch, S.L., J.G. Arnold, J.R. Kinry, and J.R. Williams. Soil and Water Assessment Tool. Version 2000. Theoretical Documentation. TWRI Report TR-192, 1-412. 2002. Texas Water Resources Institute, College Station, Texas.

Nelson, G.C. and D. Hellerstein. 1997. Do roads cause deforestation? Using satellite images in econometric analysis of land use. *American Journal of Agricultural Economics* 79(1):80-88.

Nepstad, D., G. Carvalho, A.C. Barros, A. Alencar, J.P. Capobianco, J. Bishop, P. Moutinho, P. Lefebvre, U.L. Silva, and E. Prins. 2001. Road paving, fire regime feedbacks, and the future of Amazon forests. *Forest Ecology and Management* 154(3):395-407.

Nortcliff, S. and J.B. Thornes. 1981. Seasonal Variations in the Hydrology of a Small Forested Catchment near Manaus, Amazonas, and the Implications for its Management. *In Tropical Agricultural Hydrology*, eds. R.Lal and E.W.Russell. 37-57. John Wiley & Sons Ltd.: Chichester, U.K.

O'Neill, R.V., C.T. Hunsaker, S.P. Timmins, B.L. Jackson, K.B. Jones, K.H. Riitters, and J.D. Wickham. 1996. Scale problems in reporting landscape pattern at the regional scale. *Landscape Ecology* 11(3):169-180.

O'Neill, R.V. and A.W. King. 1998. Homage to St. Michael: Or why are there so many books on scale? *In Ecological Scale, Theory and Applications.,* eds. D.L.Peterson and V.T.Parker. 3-15. Columbia University Press: New York, NY.

Ojima, D.S., K.A. Galvin, and B.L. Turner. 1994. The Global Impact of Land-Use Change. *Bioscience* 44(5):300-304.

Oliveira, P.J.C., G.P. Asner, D.E. Knapp, A. Almeyda, R. Galvan-Gildemeister, S. Keene, R.F. Raybin, and R.C. Smith. 2007. Land-use allocation protects the Peruvian Amazon. *Science* 317(5842):1233-1236.

Oliveira Filho, F. and J. Metzger. 2006. Thresholds in landscape structure for three common deforestation patterns in the Brazilian Amazon. *Landscape Ecology* 21(7):1061-1073.

Openshaw, S. The Modifiable Areal Unit Problem. Concepts and Techniques in Modern Geography. 38, 1. 1984. Norwich, UK., Geobooks.

Openshaw, S. 1977. Geographical Solution to Scale and Aggregation Problems in Region-Building, Partitioning and Spatial Modeling. *Transactions of the Institute of British Geographers* 2(4):459-472.

Openshaw, S. 1978. Empirical-Study of Some Zone-Design Criteria. *Environment and Planning A* 10(7):781-794.

Panayotou, P. and S. Sungsuwan. 1994. An econometric analysis of the causes of tropical deforestation: the case of Northeast Thailand. *In The Causes of Tropical Deforestation,* eds. K.Brown and D.W.Pearce. 192-207. University of British Columbia Press: Vancouver, British Columbia.

Pearson, D.M. 2002. The application of local measures of spatial autocorrelation for describing pattern in north Australian landscapes. *Journal of Environmental Management* 64(1):85-95.

Perz, S., S. Brilhante, F. Brown, M. Caldas, S. Ikeda, E. Mendoza, C. Overdevest, V. Reis, J.F. Reyes, D. Rojas, M. Schmink, C. Souza, and R. Walker. 2008. Road building, land use and climate change: prospects for environmental governance in the Amazon. *Philosophical Transactions of the Royal Society B-Biological Sciences* 363(1498):1889-1895.

Petit, C.C., T. Scudder, and E.F. Lambin. 2001. Integration of multi-source remote sensing data for land cover change detection. *International Journal of Geographical Information Science* 15(8):785-803.

Poveda, G., P. Waylen, and R. Pulwarty. 2006. Annual and Interannual Variability of Present Climate in Northern South America and Southern Mesoamerica. *Paleogeography, Paleoclimatology, Paleoecology* 234:3-27.

Qi, Y. and J.G. Wu. 1996. Effects of changing spatial resolution on the results of landscape pattern analysis using spatial autocorrelation indices. *Landscape Ecology* 11(1):39-49.

Quattrochi, D.A. and M.F. Goodchild. 1997. *Scale in remote sensing and GIS*. Lewis Publishers, Boca Raton, Fla.

Refsgaard, J.C., International Hydrological Program, and Unesco. 1989. Methodology for distinguishing between man's influence and climatic effects on the hydrological cycle. Paris : Unesco, Unesco.

República de Bolivia. Ley del Servicio Nacional de Reforma Agraria. Ley no. 1715. 10-18-1996. La Paz, Bolivia.

Riitters, K.H., R.V. Oneill, C.T. Hunsaker, J.D. Wickham, D.H. Yankee, S.P. Timmins, K.B. Jones, and B.L. Jackson. 1995. A Factor-Analysis of Landscape Pattern and Structure Metrics. *Landscape Ecology* 10(1):23-39.

Rindfuss, R.R., S.J. Walsh, B.L. Turner, J. Fox, and V. Mishra. 2004. Developing a science of land change: Challenges and methodological issues. *Proceedings of the National Academy of Sciences of the United States of America* 101(39):13976-13981.

Roberts, D.A., M. Keller, and J.V. Soares. 2003. Studies of land-cover, land-use, and biophysical properties of vegetation in the Large Scale Biosphere Atmosphere experiment in Amazonia. *Remote Sensing of Environment* 87(4):377-388.

Rogers, P. 1994. Hydrology and water quality. *In Changes in land use and land cover : a global perspective*, ed. William B.Meyer and B.L.Turner II. 231-57. Cambridge University Press: New York, NY.

Rojas, D.M., I. Martínez, W. Cordero, and F. Contreras. Tasa de Deforestación de Bolivia 1993-2000. 2003. Santa Cruz, Bolivia, BOLFOR; Superintendencia Forestal.

Rundle, H.D. and D.A. Jackson. 1996. Spatial and temporal variation in littoral-zone fish communities: A new statistical approach. *Canadian Journal of Fisheries and Aquatic Sciences* 53(10):2167-2176.

Schaap, M.G., F.J. Leij, and M.T. van Genuchten. 2001. ROSETTA: a computer program for estimating soil hydraulic parameters with hierarchical pedotransfer functions. *Journal of Hydrology* 251(3-4):163-176.

Schroder, B. and R. Seppelt. 2006. Analysis of pattern-process interactions based on landscape models-Overview, general concepts, and methodological issues. *Ecological Modelling* 199:505-516.

Schulz, K., R. Seppelt, E. Zehe, H.J. Vogel, and S. Attinger. 2006. Importance of spatial structures in advancing hydrological sciences. *Water Resources Research* 42(3).

Siriwardena, L., B.L. Finlayson, and T.A. McMahon. 2006. The impact of land use change on catchment hydrology in large catchments: The Comet River, Central Queensland, Australia. *Journal of Hydrology* 326(1-4):199-214.

Skole, D., W.H. Chomentowski, W.A. Salas, and A.D. Nobre. 1994. Physical and human dimensions of deforestation in Amazonia. *Bioscience* 44(5):314-322.

Soares, B.S., D.C. Nepstad, L.M. Curran, G.C. Cerqueira, R.A. Garcia, C.A. Ramos, E. Voll, A. McDonald, P. Lefebvre, and P. Schlesinger. 2006. Modelling conservation in the Amazon basin. *Nature* 440(7083):520-523.

Southworth, J., D. Munroe, and H. Nagendra. 2004a. Land cover change and landscape fragmentation - comparing the utility of continuous and discrete analyses for a western Honduras region. *Agriculture Ecosystems & Environment* 101(2-3):185-205.

Southworth, J., H. Nagendra, L.A. Carlson, and C. Tucker. 2004b. Assessing the impact of Celaque National Park on forest fragmentation in western Honduras. *Applied Geography* 24(4):303-322.

Southworth, J., H. Nagendra, and C. Tucker. 2002. Fragmentation of a landscape: incorporating landscape metrics into satellite analyses of land cover change. *Landscape Research* 27(3):253-269.

Southworth, J., G.S. Cumming, M. Marsik, and M.W. Binford. 2006. Linking Spatial and Temporal Variation at Multiple Scales in a Heterogeneous Landscape. *The Professional Geographer* 58(4):406-420.

Steininger, M.K., C.J. Tucker, J.R.G. Townshend, T.J. Killeen, A. Desch, V. Bell, and P. Ersts. 2001. Tropical deforestation in the Bolivian Amazon. *Environmental Conservation* 28(2):127-134.

Turner, B.L., D. Skole, G. Sanderson, G. Fischer, L.O. Fresco, and R. Leemans. Land-Use and Land-Cover Change Science/Research Plan. 1-132. 1995. Stockholm and Geneva, The International Geosphere-Biosphere Programme: A Study of Global Change (IGBP) of the International Council of Scientific Unions (ICSU) and the Human Dimensions of Global Environmental Change Programme (HDP) of the International Social Science Council (ISSC).

Turner, M.G. 2005. Landscape ecology: What is the state of the science? *Annual Review of Ecology Evolution and Systematics* 36:319-344.

Turner, M.G. 1989. Landscape Ecology - the Effect of Pattern on Process. *Annual Review of Ecology and Systematics* 20:171-197.

Turner, M.G. 1990. Spatial and temporal analysis of landscape patterns. *Landscape Ecology* 4(1):21-30.

Turner, M.G., V.H. Dale, and R.H. Gardner. 1989. Predicting across scales: theory development and testing. *Landscape Ecology* 3(3-4):245-252.

van Griensven, A. and T. Meixner. Dealing with unidentifiable sources of uncertainty within environmental models. Pahl-Wostl, Claudia, Schmidt, Sonja, Rizzoli, A. E., and Jakeman, A. J. 2[1], 1045-1052. 2004. University of Osnabrück, Germany. Complexity and Integrated Resources Management Transactions of the 2nd Biennial Meeting of the International Environmental Modelling and Software Society. 6-14-2004.

van Loon, E.E. and P.A. Troch. 2002. Tikhonov regularization as a tool for assimilating soil moisture data in distributed hydrological models. *Hydrological Processes* 16(2):531-556.

Varlyguin, D.L., R.K. Wright, S.J. Goetz, and S.D. Prince. Advances in land cover classification for applications research: a case study from the Mid-Atlantic RESAC. 2001. St. Louis, MO. Proceedings, ASPRS 2001: Gateway to the New Millennium. 2001.

Vasquez, A. Metodologia para la determinacion de la capacidad de uso de la tierra. 1-60. 1980. San Jose, Costa Rica., Direccion de Investigaciones Agricolas, Ministerio de Agricultura y Ganaderia.

Vitousek, P.M. 1994. Beyond global warming: Ecology and global change. *Ecology* 75:1861-1876.

Wachholtz, R., J.L. Artola, R. Carmargo, and D. Yurca. Avance de la deforestación mecanizada en Bolivia: Tasa anual de deforestación mecanizada en los años 2004 y 2005. 2006. Santa Cruz de la Sierra, Bolivia, Superintendencia Forestal, República de Bolivia.

Walker, R. 2004. Theorizing land-cover and land-use change: The case of tropical deforestation. *International Regional Science Review* 27(3):247-270.

Walsh, S.J. and K.A. Crews-Meyer. 2002. *Linking people, place, and policy : a GIScience approach*. Kluwer Academic Publishers ; Norwell, MA : Distributors for North, Central and South America, Kluwer Academic Publishers, Boston.

Ware, S., C. Frost, and P. Doerr. 1989. Southern mixed hardwood forest: the former longleaf pine forest. *In Biodiversity of the southeastern United States: Lowland terrestrial communities.,* eds. W.H.Martin, S.G.Boyce, and A.C.Echternacht. 447-93. John Wiley & Sons, Inc: New York, NY.

Waylen, P. and M.E. Quesada. 2002. The Effect of Atlantic and Pacific Sea Surface Temperatures on the Mid-Summer Drought of Costa Rica. *In Environmental Change and Water Sustainability*, eds. J.M.Garcia-Ruiz, A.A.Jones, and J.Arnáez. 197-209. Instituto Pirenaico de Ecología, Consejo Superior de Investigaciones Científicas.: Zaragoza, Spain.

Waylen, P., M. Quesada, C. Caviedes, G. Poveda, and O. Mesa. 1998. Rainfall distribution and regime in Costa Rica and its response to the El Nino-Southern Oscillation. *Conference of Latin Americanist Geographers Yearbook* 24 (1998) p75-84:75-84.

Western, A.W., G. Bloschl, and R.B. Grayson. 2001. Toward capturing hydrologically significant connectivity in spatial patterns. *Water Resources Research* 37(1):83-97.

Western, A.W., T.A. McMahon, R.B. Grayson, G. Bloschl, and G.R. Willgoose. 1999. Observed spatial organization of soil moisture and its relation to terrain indices. *Water Resources Research* 35(3):797-810.

Western, A.W., S.L. Zhou, R.B. Grayson, T.A. McMahon, G. Bloschl, and D.J. Wilson. 2004. Spatial correlation of soil moisture in small catchments and its relationship to dominant spatial hydrological processes. *Journal of Hydrology* 286(1-4):113-134.

Wiens, J.A. 1989. Spatial scaling in ecology. *Functional Ecology* 3:385-397.

Wilk, J., L. Andersson, and V. Plermkamon. 2001. Hydrological impacts of forest conversion to agriculture in a large river basin in northeast Thailand. *Hydrological Processes* 15(14):2729-2748.

Williams, J.B. 1982. Temporal and Spatial Patterns of Abundance of the Chydoridae (Cladocera) in Lake Itasca, Minnesota. *Ecology* 63(2):345-353.

Winchell, M., R. Srinivasan, M. Di Luzio, and J.G. Arnold. ArcSWAT interface for SWAT2005 – User's Guide. 1-431. 2007. Temple, Texas., Blackland Research Center, Texas Agricultural Experiment Station and Grassland, Soil and Water Research Laboratory, USDA Agricultural Research Service.

Woodcock, C.E. and S. Gopal. 2000. Fuzzy set theory and thematic maps: Accuracy assessment and area estimation. *International Journal of Geographical Information Systems* 14(2):153-172.

Woodcock, C.E. and M. Ozdogan. 2004. Trends in Land Cover Mapping and Monitoring. *In Land Change Science: Observing, Monitoring and Understanding Trajectories of Change on the Earth's Surface.*, ed. G.Gutman. 367-77.

Woodcock, C.E. and A.H. Strahler. 1987. The Factor of Scale in Remote-Sensing. *Remote Sensing of Environment* 21(3):311-332.

Woods, C.H. and D. Skole. 1998. Linking satellite, census, and survey data to study deforestation in the Brazilian Amazon. *In People and Pixels: Linking remote sensing and social science*, eds. D.M.Liverman, E.Moran, E.F.Rindfuss, and P.C.Stern. 70-93. National Academy Press: Washington, D.C.

Wu, J., D.E.Jelinski, M.Luck, and P.T.Tueller. 2000. Multiscale analysis of landscape heterogeneity: Scalevariance and pattern metrics. *Geographic Information Sciences* 6(1):6-19.

Wu, J.G. and J.L. David. 2002. A spatially explicit hierarchical approach to modeling complex ecological systems: theory and applications. *Ecological Modelling* 153(1-2):7-26.

Wu, W., C.A.S. Hall, and F.N. Scatena. 2007. Modelling the impact of recent land-cover changes on the 25 stream flows in northeastern Puerto Rico. *Hydrological Processes* 21(21):2944-2956.

Ziegler, A.D., T.W. Giambelluca, L.T. Tran, T.T. Vana, M.A. Nullet, J. Fox, T.D. Vien, J. Pinthong, J.F. Maxwell, and S. Evett. 2004. Hydrological consequences of landscape fragmentation in mountainous northern Vietnam: evidence of accelerated overland flow generation. *Journal of Hydrology* 287(1-4):124-146.

ZONISIG. Zonifícación Agroecológica y Socioeconómica y Perfíl Ambiental del Departamento de Pando. 1997. La Paz, Bolivia, Proyecto de Zonifíficación Agroecológica y Establecimiento de Una Base de Datos y Red de Sistema de Información Geográfica en Bolivia.

BIOGRAPHICAL SKETCH

Matt Marsik earned an Associate in Arts degree in December 1997 from Valencia Community College, Orlando, Florida, and received a Bachelor of Science degree with high honors in December 2000 from the Department of Geological Sciences, University of Florida. His master's work, from January 2001 to May 2003, focused on the consequences of 30 years of land cover change on stream flow in a small watershed in San Ramón, Costa Rica. While maintaining interests in watershed hydrology and land cover change, his PhD work expanded to incorporate remote sensing and landscape ecology to develop and apply methods toward improved spatial and temporal analyses of land cover change. Focused on intedisciplinary applications of land cover change, Matt has free range to pursue a career either in agency, non-governmental, consulting firms, or academics, or any combination of the previous.